Title
Live Imaging of Myocardial Development in the Zebrafish

Permalink
https://escholarship.org/uc/item/58m0w0sh

Author
Staudt, David Wells

Publication Date
2013

Supplemental Material
https://escholarship.org/uc/item/58m0w0sh#supplemental

Peer reviewed|Thesis/dissertation

Live Imaging of Myocardial Development in the Zebrafish

by

David Wells Staudt

DISSERTATION

Submitted in partial satisfaction of the requirements for the degree of

DOCTOR OF PHILOSOPHY

in

Biomedical Sciences

in the

GRADUATE DIVISION

of the

UNIVERSITY OF CALIFORNIA, SAN FRANCISCO

Dedication

This thesis is dedicated to all my family and friends who have helped me along this journey so far.

Acknowledgements

I would first like to thank Didier Stainier for being a terrific thesis advisor. Over the course of my PhD, Didier provided the perfect mix of intellectual freedom that allowed this fairly risky project to move forward, mixed with just enough focused direction that kept me from veering wildly off course in many different directions. He also gave me the opportunity to experience many different parts of a life in science, from writing a review to applying for a grant, not to mention trying multiple projects with varying degrees of success and failure. I truly appreciate his dedication to my training, and feel lucky to have found him as a mentor. I would also like to thank the members of my thesis and qualification exam committees: Jeremy Reiter, Takashi Mikawa, Shaun Coughlin, and Orion Weiner. I have enjoyed our scientific discussions, and have greatly appreciated your support and guidance.

In addition to being a great mentor for my PhD, Didier also put together a wonderful lab environment. I have benefitted greatly from the incredibly intelligent, friendly, and helpful members of the Stainier lab, all of whom have helped me along the path to a PhD and have made these past few years fun and intellectually stimulating. I would especially like to thank Jiandong Liu for setting me on the path to study cardiac trabeculation and for teaching me much of what I know about using zebrafish to study the heart. I would also like to thank Sven Reischauer, Kim Evason, Benoit Vanhollebeke, Rima Arnaout, Stephanie Woo, Anna Reade, and Philipp Gut for many helpful and interesting

Live Imaging of Myocardial Development in the Zebrafish

By

David Staudt

Abstract

Despite extensive research on cardiovascular development, much remains to be learned about the molecular and cellular mechanisms that give rise to the fully formed 3D structure of the heart. Though genetic studies have identified genes necessary for proper cardiac morphogenesis, our understanding of how these genes impact myocardial cell biology is limited. In this thesis, I use 4D microscopy of zebrafish embryos coupled with computational pos-processing to study how individual cells contribute to the formation of the ventricular trabeculae, and I identify a subpopulation of cardiomyocytes that can be marked by their activation of Notch signaling which go on to form the cortical myocardial layer of the adult zebrafish heart.

The wall of the developing ventricle is covered by a network of sheet-like muscular structures termed the cardiac trabeculae. Though a number of mutants have been identified that lack trabeculae, little is known about how cardiomyocytes interact to form these sheets. Previous work from our lab had suggested that cardiomyocytes migrate from the outer, compact layer of the heart towards the lumen to form these sheets. However, how exactly they migrated was unknown. I found that cardiomyocytes form the trabecular layer first by extending long processes over their neighbors, then by constricting their abluminal surfaces to move their cell bodies into the forming sheets. I

further found that two mutations that disrupt trabeculation affect the initial processes differently. While *erbb2* mutant cells form normal, stable processes, cells in embryos with non-contractile hearts extend processes that collapse quickly. This finding sheds new light on how different mutations can differentially inhibit trabecular development.

While examining the formation of the trabecular network, **we** identified a subset of cells in the compact layer that activated the Notch signaling pathway. These cells were found in stripes along the outer curvature of the heart, mirroring the pattern of trabecular development. Through lineage tracing analysis, we determine that these migrate to the trabecular layer by juvenile stages, and proceed to contribute to the outermost cortical layer of cardiomyocytes in the adult heart. Thus, we identify an interesting subpopulation of cardiomyocytes with roles in later stages of development.

Table of Contents

Chapter 1: Uncovering the Molecular and Cellular Mechanisms of Heart

Development using the Zebrafish

The content of this chapter was modified from the following publication:

<u>Abstract</u>

Over the past 20 years, the zebrafish has emerged as a powerful model organism for studying cardiac development. Its ability to survive without an active circulation and amenability to forward genetics has led to the identification of numerous mutants whose study has helped elucidate new mechanisms in cardiac development. Furthermore, its transparent, externally developing embryos have allowed detailed cellular analyses of heart development. In this review, we discuss the molecular and cellular processes involved in zebrafish heart development from progenitor specification to development of the valve and conductive tissue. We focus on imaging studies that have uncovered cellular bases of heart development, and on zebrafish mutants with cardiac abnormalities whose study has revealed novel molecular pathways in cardiac cell specification and tissue morphogenesis.

Introduction

During development, the embryonic heart undergoes a series of complex morphogenetic

and differentiation processes to form the mature cardiac structures (Auman and Yelon,

2004; Bakkers et al., 2009; Christoffels et al., 2000; Srivastava, 2006). Problems with

these processes can lead to congenital heart defects. Understanding the mechanisms that

form the heart is a difficult challenge, as early heart defects causes lethality in most

vertebrates. One notable exception is the zebrafish, which develops a functional heart

within 24 hours post fertilization (hpf), but can survive through the first week of

development without a functioning cardiovascular system. Taking advantage of this

property, along with the external development of the zebrafish embryo, fast generation

time and high number of offspring, a number of forward genetic screens have been

performed and identified dozens of mutants with defects in cardiac structure or function

(Alexander et al., 1998; Beis et al., 2005; Chen et al., 1996; Chi et al., 2008a; Stainier et

al., 1996). Complementary to forward genetic approaches, a number of tools and

techniques allow disruption of specific genes of interest. Morpholino antisense

oligonucleotides allow for rapid disruption of genes of interest (Eisen and Smith, 2008),

but often cause non-specific effects, particularly in the cardiovascular system. Emerging

technologies such as zinc finger nucleases (Ekker, 2008), TAL effector nucleases

(TALENs) (Huang et al., 2011; Sander et al., 2011), and TILLING (Moens et al., 2008)

enable generation or identification of mutations in genes of interest, and do not suffer

from the same off-target effects as morpholinos. Recently, powerful transgenic tools

have allowed spatial and temporal manipulation of gene expression, and advances in

microscopy have utilized the transparency of zebrafish embryos and larvae to monitor complex developmental processes *in vivo* (Forouhar et al., 2006; Ohn et al., 2009; Scherz et al., 2008; Schoenebeck and Yelon, 2007). Furthermore, many small molecules enter zebrafish after addition to the water, which, along with the ability to raise embryos and larvae in multi-well plates, allows for rapid *in vivo* screening of chemical libraries (Baker, 2011). Automated screening technologies continue to improve, and platforms capable of performing high-throughput confocal imaging with cellular resolution have been recently described (Pardo-Martin et al., 2010).

Remarkably, the zebrafish heart also shows high regenerative capacity, and can re-form a fully functional heart even after substantial damage (Chablais et al., 2011; González-Rosa et al., 2011; Jopling et al., 2010; Kikuchi et al., 2010; Poss, 2007; Poss et al., 2002; Schnabel et al., 2011; Wang et al., 2011). Since the regenerative process seems to reactivate developmental pathways (Kikuchi et al., 2010), understanding zebrafish heart development also helps us understand the remarkable cardiac regenerative potential of this model organism.

Despite being a two-chambered organ, the zebrafish heart exhibits many similarities to the amniote heart, and cellular and molecular studies clearly illustrate the common evolutionary origin of these structures. For this reason, many scientists who have traditionally used the mouse to study heart development have now fully embraced the zebrafish model system. Here, we present an overview of the processes involved in cell differentiation, morphogenesis, and physiology during zebrafish heart development, with

particular emphasis on findings made possible by the unique properties of this powerful model system.

<u>Early Cardiac Progenitors</u>

Cardiac progenitors can first be identified at the blastula stage. Fate mapping places myocardial progenitors close to the embryonic margin in lateral fields on either side of the embryo (Keegan et al., 2004; Stainier et al., 1993). Even at this early stage, atrial and ventricular progenitors are segregated, with ventricular progenitors occupying a position closer to the margin and more dorsal than their atrial counterparts. Meanwhile, endocardial progenitors occupy a similar area of the margin (Lee et al., 1994), but do not appear to be organized by chamber (Keegan et al., 2004). Myocardial progenitors retain their relative positions through gastrulation and by the 6-9 somite stages are found within the posterior half of the anterior lateral plate mesoderm (ALPM) (Fig 1A). This territory expresses the transcription factor genes *hand2* and *gata4* (Schoenebeck et al., 2007; Yelon et al., 2000). Ventricular progenitors are enriched in the medial aspect of this region, which expresses the transcription factor gene *nkx2.5*, while atrial progenitors are enriched laterally. Progenitors are commonly visualized by the expression of *nkx2.5* and the cardiac regulatory myosin light chain gene *myl7* (previously *cmlc2*) (Glickman and Yelon, 2002). Ventricular progenitors remain medial to the atrial progenitors, and these two populations can be distinguished by their expression of ventricular myosin heavy chain (*vmhc*) and atrial myosin heavy chain (*amhc/myh6*), respectively (Yelon et al., 1999).

Several signaling pathways have been shown to regulate the number of myocardial progenitors including retinoic acid (RA) (Keegan et al., 2005; Stainier and Fishman, 1992; Waxman et al., 2008), Wnt (Ueno et al., 2007), Hedgehog (Hh) (Thomas et al., 2008), Fgf (Marques et al., 2008), Bmp (Marques and Yelon, 2009; Reiter et al., 2001), and Nodal (Keegan et al., 2004; Reiter et al., 2001). While hedgehog signaling seems to be important for establishing progenitors for both chambers (Thomas et al., 2008), bmp inhibition greatly decreases atrial progenitor specification (Marques and Yelon, 2009). In contrast, decreasing Nodal or Fgf signaling suppresses both atrial and ventricular specification, but with a greater effect on ventricular progenitors (Keegan et al., 2004; Marques et al., 2008; Reiter et al., 2001). Meanwhile, although inhibition of RA signaling increases both atrial and ventricular populations to the same degree, it appears to accomplish this effect through different mechanisms (Waxman et al., 2008). While ventricular populations increase due to an increased number of ventricular progenitors within the blastula, atrial populations seem to increase due to an increase in the number of progeny per early progenitor. Other studies have revealed interesting temporal roles for these signaling pathways. For example, activation of Wnt signaling at pre-gastrulation stages increases progenitor numbers, whereas activation an hour after the onset of gastrulation significantly decreases numbers, possibly through induction of programmed cell death in cardiac progenitors (Dohn and Waxman, 2012; Ueno et al., 2007). Though the heat-shock inducible transgenic animals used in these studies allowed for temporal analysis of Wnt signaling in cardiac specification, genetic loss-of-function studies are needed to dissect the role of this pathway in this process. Looking forward,

though many pathways have been identified to contribute to cardiac progenitor specification, how these different pathways interact to produce the correct number and distribution of progenitors remains an open question, as does the elucidation of the gene regulatory networks downstream of these signaling pathways. Importantly, it is very likely that the role of these pathways and their effectors in cardiac cell specification is conserved throughout evolution and thus that the zebrafish model will continue to contribute significantly to these studies.

Once progenitors are specified, they migrate to the correct location within the ALPM where they further differentiate. Two studies have implicated G-protein coupled receptors (GPCRs) in this migration (Scott et al., 2007; Zeng et al., 2007). The *grinch* mutant has greatly diminished heart fields and, occasionally, a completely absent heart (Scott et al., 2007). This mutation maps to *agtrl1b*, a GPCR for the signaling peptide Apelin. Cell transplantation data using morpholino knockdown of *agtr1b* suggest that the receptor works cell-autonomously to limit both cardiac potential and cell movement during gastrulation. Surprisingly, transgenic overexpression of *apelin* before gastrulation, but not during, also inhibits heart formation. Hence, these data support a model where localized Apelin/Agtr1b signaling directs the movement of myocardial progenitors to the correct location within the ALPM, where they can receive myocardial differentiation signals.

Once in the ALPM, interactions with other tissues influence cardiac cell differentiation. Within the ALPM, vascular and hematopoietic precursors neighbor the heart field

anteriorly and pectoral fin precursors posteriorly. The absence of vascular and

hematopoietic precursors in the *cloche* (*clo*) mutant leads to the expansion of *hand2*

expression and ectopic cardiomyocyte differentiation in the anterior ALPM, which leads

to an increase in atrial cell number (Schoenebeck et al., 2007). Conversely, expansion of

vascular and hematopoietic progenitors by injection of *scl* and *etsrp* RNA reduces the

size of the heart field. Interestingly, knocking down *etsrp* in an *etsrp:GFP* BAC

transgenic line that marks vascular and hematopoietic progenitors revealed that

etsrp:GFP positive cells became myocardium, suggesting that Etsrp functions in vascular

progenitors at least in part to prevent myocardial differentiation (Palencia-Desai et al.,

2011). On the posterior side, RA signaling is required cell-autonomously in the forelimb

field for its specification (Waxman et al., 2008). RA signaling inhibition also leads to a

posterior expansion of Fgf signaling, which also represses forelimb specification (Sorrell

and Waxman, 2011). Suppression of differentiation of the forelimb field allows the heart

field to expand posteriorly. The RA downstream target gene *hoxb5b* is expressed in the

forelimb field territory, and morpholino knockdown of this gene allows the expansion of

atrial progenitors into the forelimb field, indicating that *hoxb5b* regulates an unknown

signal that limits atrial progenitor expansion (Waxman et al., 2008).

A network of transcription factors controls myocardial differentiation. As in amniotes, a

combination of the GATA factors Gata4, Gata5, and Gata6 regulates heart formation

(Holtzinger and Evans, 2007; Peterkin et al., 2007; Reiter et al., 1999, 2001; Trinh et al.,

2005). *faust* mutants, which carry a mutation in *gata5*, show a variable decrease in

cardiac progenitors, and *gata5* overexpression is sufficient to produce ectopic beating

tissue (Reiter et al., 1999, 2001). The variability of the *faust* phenotype may suggest that other GATA factors are compensating for loss of Gata5 function. In support of this, combinatorial morpholino-mediated knockdown of *gata5* and *gata6* results in a complete absence of *nkx2.5* positive cardiac progenitors (Holtzinger and Evans, 2007; Peterkin et al., 2007). Analysis of null alleles of these genes is needed to confirm this result. Recent work suggests that GATA factors work with the BAF chromatin remodeling complex to promote cardiac specification (Lou et al., 2011; Takeuchi et al., 2011), and overexpression of *gata5* and the BAF component *smarcd3b* dramatically increases cardiac progenitor specification cell-autonomously (Lou et al., 2011). Intriguingly, these two factors also cell-autonomously drive overexpressing cells to migrate to the cardiogenic regions of the ALPM, even from neurogenic regions, and dramatically increases cardiac incorporation in transplant experiments. This finding opens up a number of interesting questions about what drives this induced migratory behavior, and what it can tell us about heart development.

Another major player in cardiac specification is the HAND transcription factor Hand2. It is expressed in all myocardial progenitors, and functions to increase their number, particularly ventricular progenitors (Schoenebeck et al., 2007; Yelon et al., 2000). Hand2 is also necessary for maintenance of the expression of *tbx5*, a T-box transcription factor gene mutated in Holt-Oram syndrome and necessary for heart and pectoral fin development in fish (Garrity et al., 2002; Yelon et al., 2000). *nkx2.5* expression is not abolished in *hand2* mutants, but rather a population of *nkx2.5* positive, *myl7* negative cells can be found adjacent to the population of *nkx2.5* positive, *myl7* positive cells,

suggesting that *hand2* is also necessary for differentiation of *nkx2.5* expressing cells (Schoenebeck et al., 2007). Morpholino knockdown experiments suggest that Nkx2.5 itself is not critical for progenitor specification within the ALPM, but that instead it plays a redundant role with the closely related Nkx2.7 to promote heart tube extension (Targoff et al., 2008; Tu et al., 2009). Nkx2.5 and Nkx2.7 seem to regulate the size of the two chambers, as combinatorial knockdown of both genes increases the number of atrial cardiomyocytes during heart tube stages, while diminishing the number of ventricular cells produced by 52 hpf. Further analysis of the downstream targets of these and other transcription factors will be necessary to understand how the gene regulatory network correctly specifies cardiac progenitors.

Midline Migration

As they differentiate, the bilateral populations of myocardial progenitors, sandwiched between the overlying anterior endoderm and underlying yolk syncytial layer (YSL), migrate towards the embryonic midline. The populations make contact with each other by 18 hpf, first posteriorly, then anteriorly. They then merge, forming a shallow cone with ventricular progenitors at its dorsal apex (Fig 1B) (Stainier et al., 1993). A number of mutations have been identified that perturb this process, leading to cardia bifida, where two hearts form in lateral positions. Mutants with defects in endoderm formation display cardia bifida, revealing that the endoderm plays a role in cardiac migration (Alexander et al., 1999; Glickman and Yelon, 2002; Kikuchi et al., 2000; Reiter et al., 1999). Although this role for the endoderm was shown more than a decade ago, the underlying

mechanisms remain unknown. Another series of mutants have revealed a role for sphingolipid signaling in midline migration. The *miles apart* (*mil*) mutant displays cardia bifida and is caused by mutations in the sphingosine-1-phosphate (S1P) receptor *s1p2* (Kupperman et al., 2000). *mil/s1p2* appears to act cell non-autonomously in midline migration of the cardiac progenitors, and probably acts within the endoderm, as complete replacement of the anterior endoderm of *mil* mutants with WT endoderm can rescue the phenotype (Osborne et al., 2008). Meanwhile, mutations in *spinster homolog 2* (*spns2*), a gene of previously unknown function, exhibit a phenotype similar to *mil* (Kawahara et al., 2009; Osborne et al., 2008). Biochemical studies reveal that *spns2* can function as an S1P transporter (Kawahara et al., 2009). Targeted re-expression of *spns2* within the YSL rescues the mutant phenotype, suggesting that *spns2* functions in the YSL and most likely provides a source of S1P during midline migration (Kawahara et al., 2009). Despite these advances, the precise role of S1P in midline migration remains elusive.

One way the endoderm and YSL may be regulating midline migration is through the extracellular matrix (ECM). Fibronectin, an important ECM protein also required for mouse heart development (George et al., 1993), surrounds migrating myocardial precursors during midline migration, and the *natter* (*nat*) mutation in fibronectin causes cardia bifida (Trinh and Stainier, 2004). Recently, both the YSL and the myocardial precursors themselves have been implicated in regulating fibronectin deposition. Disruption of the transcription factor Mtx1 specifically in the YSL using targeted morpholino injections leads to cardia bifida accompanied by a profound reduction in fibronectin expression (Arrington and Yost, 2009; Sakaguchi et al., 2006). Additionally,

disruption of the proteoglycan gene *syndecan 2* (*sdc2*) in the YSL causes cardia bifida associated with normal expression of *fibronectin*, but undetectable fibronectin fibrillogenesis (Arrington and Yost, 2009). Interestingly, this phenotype can be rescued by injection of *sdc2* RNA into the YSL, but not into the whole embryo, suggesting that *sdc2* in the YSL is necessary to provide a substrate for fibronectin fibrillogenesis. Finally, the myocardial precursors themselves were recently found to regulate fibronectin deposition. *hand2* mutants have reduced numbers of myocardial precursors and a defect in midline migration (Yelon et al., 2000). Transplant experiments show that the defect in precursor production is cell-autonomous, but the defect in midline migration is cell non-autonomous (Garavito-Aguilar et al., 2010). Interestingly, *hand2* mutants express increased levels of Fibronectin, and the *hand2* midline migration defect can be ameliorated by heterozygosity of the *nat*^{tl43c} allele. These data suggest that expression of *hand2* within cells of the ALPM, possibly within the myocardial precursors themselves, limits excessive fibronectin deposition that itself can prevent midline migration. These studies suggest that a precise level of ECM components is necessary for midline migration, but do not reveal precisely how fibronectin influences cell behavior, a fundamental question zebrafish studies should help resolve.

Close examination of *fibronectin* mutants suggest that they may be acting through regulation of myocardial epithelial organization. During their migration to the midline, myocardial precursors maintain a polarized epithelial organization (Trinh and Stainier, 2004). *fibronectin* mutants exhibit defects in the organization and polarization of this epithelium, with some cells even losing coherence with the rest of the monolayer and

migrating separately. Though this phenotype suggests that epithelial organization is

necessary for midline migration, cardiomyocytes in mutants that disrupt epithelial

polarity eventually do migrate to the midline (Horne-Badovinac et al., 2001; Jensen and

Westerfield, 2004; Munson et al., 2008; Omori and Malicki, 2006; Peterson et al., 2001;

Wei and Malicki, 2002). The possibility remains that maternal contribution of these

epithelial polarity proteins plays a role in midline migration. The analysis of maternal

zygotic epithelial polarity mutants is necessary to resolve whether maternal polarity

factors are required for midline migration, as one might expect.

Endocardial Migration

In order to form a functional heart, the endocardium must also incorporate into the

developing structure. While the myocardium is migrating towards the midline,

endocardial progenitors, located more anteriorly in the ALPM (Fig 1A) (Schoenebeck et

al., 2007), stream medially and posteriorly, where they proceed to coat the interior of the

forming heart cone (Fig 1B) (Bussmann et al., 2007). This process requires the basic

helix-loop-helix (bHLH) transcription factor Scl/Tal1. A truncating mutation removing

the bHLH domain leads to defective posterior migration of endocardial precursors, which

in turn delays the anterior merging of the bilateral myocardial populations, resulting in a

delay in cardiac cone formation and clustering of endocardial cells at the arterial pole,

leading to a non-functional heart. Recent work has also shown that endocardial migration

requires Vegf signaling, which is regulated in a complex, dose-dependent manner by

Slit2 signaling through the Robo1 receptor (Fish et al., 2011). The balance of

Slit2/Robo1 signaling is in turn tuned by the microRNA mir-218, which lies within an intron of *slit2* and targets Robo receptors. Much work remains to determine how these and other as yet unidentified factors direct endocardial midline migration, as well as to understand how this process occurs in amniotes.

Recent data suggests that myocardial factors also play a role in endocardial midline migration. Maternal zygotic (MZ) mutants of *tmem2*, a transmembrane protein of unknown function, exhibit midline migration defects of both the endocardium and myocardium (Totong et al., 2011). Interestingly, transgenic re-expression of tmem2 in the myocardium of these animals rescues both myocardial and endocardial midline migration, while re-expression in the endocardium rescues neither, illustrating how myocardial factors are necessary for endocardial midline migration.

Reciprocally, the endocardium may also play a role in fine-tuning the migration of myocardial precursors. Myocardial precursor movements during midline migration can be separated into two types: a linear midline migration and a curved movement that closes the cardiac cone (Holtzman et al., 2007). In the absence of endocardium in *cloche* mutants, this second movement does not occur, leading to a dysmorphic cardiac cone. Interestingly, in *mil/s1p2* cardia bifida mutants, this second curving movement still occurs in the absence of midline migration. Removing the endocardium from this background by creating *mil*;*clo* double mutants abrogates this curving movement, revealing that the endocardium can direct this fine-tuning movement of myocardial precursors independent of medial migration. The signals that direct this curving

movement remain to be elucidated. In addition, the isolation and further analysis of the *cloche* gene will be necessary to confirm this model. Myocardial-endocardial interactions are a constant theme during heart formation and function and will remain a rich avenue of investigation.

<u>Heart Tube Assembly</u>

After endocardial and myocardial progenitors come together to form the cardiac cone, they migrate asymmetrically to form the linear heart tube (Fig 1C). Although cardiac progenitors migrate to the midline in epithelial polarity mutants, *has/prkci* mutant embryos fail to assemble a linear heart tube (Horne-Badovinac et al., 2001; Peterson et al., 2001), and detailed analysis of embryos injected with morpholinos targeting either *has/prkci* or *nok/mpp5a* showed that knockdown of these genes causes defects in the formation and tilting of the cardiac cone and heart tube elongation (Rohr, 2006). Time-lapse imaging has shown that, to transition from a cone to a linear tube, myocardial cells undergo an asymmetric involution, whereby cells on the right side of the cone move ventrally and medially (Rohr et al., 2008; Smith et al., 2008). The direction of this involution is controlled by global left/right signaling pathways. In order to accomplish this rearrangement, the cardiomyocytes must migrate as a cohesive epithelial sheet, and disruption of this epithelium in *has* and *nok* morphants leads to uncoordinated, non-directed migration and failure to create the heart tube (Rohr et al., 2008). This migration also requires the action of hyaluronan synthase, which is expressed in the migrating myocardium and produces the ECM molecule hyaluronic acid (Smith et al., 2008). Thus,

epithelial coherence and polarity, as well as correct ECM composition, are necessary to create the linear heart tube.

Looping and Ballooning

After its initial formation at 24 hpf, the heart tube gradually extends and undergoes a series of morphogenetic changes leading to the emergence of an anterior, right-sided ventricle and a more posterior, left-sided atrium separated by a constricted region called the atrioventricular canal (AVC). In order to form this asymmetrically positioned heart, the cardiomyocytes undergo a number of asymmetric movements, eventually culminating in rightward looping of the heart tube. Possible cellular mechanisms underlying these asymmetric movements have been reviewed elsewhere (Bakkers, 2011; Bakkers et al., 2009). As the heart loops, the chambers form as bulges in the heart tube in a process called ballooning. This bulging creates two distinct surfaces within the chambers: the concave inner curvature (IC) and the convex outer curvature (OC) (Fig 1D). In the ventricle, this morphogenetic change is accomplished by differential shape changes within the IC and the OC (Auman et al., 2007; Deacon et al., 2010). Measurements of individual cell shapes reveal that, while the surface area of both IC and OC cells increase relative to cells in the linear heart tube, OC cells, but not IC cells, increase in length, measured by a decrease in circularity. Failure of these cells to elongate leads to a smaller, rounder ventricle.

These shape changes seem to depend on cardiac function. In the *weak atrium* (*wea/myh6*) mutant, which lacks atrial contraction due to defects in atrial sarcomere formation, ventricular cells fail to increase their surface area, and fail to elongate (Auman et al., 2007). Transplantation of *wea* mutant cells into wild-type embryos revealed that this effect is cell non-autonomous, as *wea* mutant ventricular cardiomyocytes within otherwise wild-type hearts elongate normally. In contrast, *half-hearted* (*haf/vmhc*) mutants, which fail to form sarcomeres in the ventricle, develop enlarged ventricles with individual cells increasing their surface area and elongating more than in wild-type. This effect is eliminated in *wea;haf* double mutants, as well as in *silent heart* (*sih*) mutants, which lack sarcomeres in both chambers due to a mutation in *cardiac troponin T2a* (*tnnt2a*) (Auman et al., 2007; Sehnert et al., 2002). Taken together, these data suggest that sensing fluid flow and/or myocardial stretch increases myocardial surface area and causes OC cell elongation, while ventricular contractility modulates the extent of these shape changes.

In addition to forces, electrical conduction also appears to be required for OC morphogenesis. The *dococ* (*dco*) mutant exhibits uncoordinated conduction and contraction within the ventricle, caused by a mutation in the connexin gene *gap junction protein alpha 3* (*gja3*) (Chi et al., 2010). This mutation also causes defects in heart morphogenesis, namely a lack of constriction of the AV canal and a smaller, rounder ventricle. These defects are not secondary to disrupted flow as *sih/dco* OC cells are significantly less elongated than *sih* OC cells, even though the beat is completely disrupted in both settings. A similar flow-independent defect in elongation was also seen

17

in *sih;dco* AV myocardial cells. This study provides the first example of conduction affecting cardiomyocyte morphogenesis independently of contractility. Though still in its early stages, zebrafish research on structure/function relationships in the ballooning myocardium offers a powerful and highly relevant *in vivo* view of how forces and electrical signals shape cardiac morphogenesis.

Proliferation and Growth

In addition to undergoing morphogenetic cell movements, the developing heart must also increase its myocardial mass. This increase can happen through addition of differentiating cells from outside the forming heart, or by proliferation of cardiomyocytes. During heart tube stages, the main mode of cardiac growth is through differentiation rather than proliferation. Populations of cells at the arterial and venous poles contribute to myocardial growth by late addition of cells at either end (Hami et al., 2011; Lazic and Scott, 2011; de Pater et al., 2009; Zhou et al., 2011). The population contributing to the arterial pole shares many characteristics with the secondary heart field (SHF) seen in amniotes. These cells are marked by the expression of *latent TGF-β binding protein 3* (*ltbp3*), and contribute to myocardial, endothelial, and smooth muscle cells of the outflow tract. Late addition by these cells requires FGF (de Pater et al., 2009) TGF-β (Zhou et al., 2011), BMP and Hedgehog signaling (Hami et al., 2011). Interestingly, though *islet-1*, a transcription factor gene important in the SHF in mouse, can be detected in some cells that contribute to the arterial pole up through 48 hpf, its mutation does not disrupt late addition to the arterial pole, but does disrupt late addition

to the venous pole. SHF development is a very active area of investigation in amniotes and it will be interesting to see whether zebrafish studies will contribute novel concepts to this field.

After 48 hpf, cardiomyocyte proliferation progressively increases (Liu et al., 2010). Mutant studies have revealed some of the molecular determinants of cardiomyocyte proliferation in zebrafish. A mutation in a subunit of the cardiac L-type calcium channel results in a silent ventricle with greatly reduced numbers of cardiomyocytes at 72 hpf despite normal expression patterns of myofibrillar components and cardiac transcription factor genes up to 48 hpf (Rottbauer et al., 2001). This effect implicates calcium signaling and/or cardiac function in the control of late increases in cardiomyocyte number. Embryos harboring a mutation in *erbb2*, an EGFR family member tyrosine kinase receptor, exhibit a complete lack of myocardial proliferation between 3-5 dpf, even though the heart continues contracting (Liu et al., 2010). In contrast, an activating mutation in the DNA-stimulated ATPase Reptin in the *liebeskummer* (*lik*) mutant results in a dramatic cell-autonomous increase in ventricular myocyte proliferation between 48 and 72 hpf, and this can be phenocopied by morpholino-mediated knockdown of Pontin, another DNA-stimulated ATPase which is known to be a Reptin antagonist in other contexts (Rottbauer et al., 2002). The ability to manipulate and visualize single cardiomyocytes should make the zebrafish particularly well suited to gaining a better understanding of the mechanisms that control cardiomyocyte proliferation *in vivo*.

A complex of endocardial proteins plays a role in regulating the overall size of the heart, seemingly independent of proliferation (Mably et al., 2003, 2006). The zebrafish mutants *heart of glass* (*heg*), *santa* (*san*), and *valentine* (*vtn*) share a similar phenotype, namely a lack of circulation at 28-30 hpf and an enlarged, thin-walled heart by 48 hpf. *san* and *vtn* encode Krit (Ccm1) and Ccm2, respectively, proteins previously associated with familial cerebral cavernous malformations (CCMs) in humans (Labauge et al., 2007), while *heg* encodes a previously unidentified large transmembrane protein expressed in the endocardium (Mably et al., 2003). Combinatorial injection of low doses of morpholinos targeting *san*, *vtn*, and *heg* recapitulate the enlarged heart phenotype, suggesting that *heg* acts within the same pathway as *san* and *vtn* (Mably et al., 2006), and recently Ccm1, Ccm2, and Heg were shown to form a complex *in vitro*, further suggesting that Heg serves as a novel member of the Ccm pathway (Kleaveland et al., 2009). A third member of this complex, Ccm3, has been reported to cause a similar cardiac phenotype as in *san, val*, and *heg* mutants (Voss et al., 2009; Zheng et al., 2010), but more recent work has challenged those findings, indicating that morpholinos targeting Ccm3 disrupt cardiac morphology, but do not result in grossly dilated hearts (Yoruk et al., 2011). Genetic loss-of-function studies are needed to resolve this discrepancy. Importantly, comparison of *sih* to *heg*;*sih* double mutants reveals that *heg*;*sih* hearts are enlarged relative to *sih* hearts, indicating that the enlarged heart phenotype is not secondary to the lack of flow or dependent on contractility, at least in *heg* mutants. The number of endocardial and myocardial cells was unchanged in *heg* mutants at 72 hpf, or in 48 hpf embryos injected with morpholinos targeting *krit1* or *ccm2*. Thus, some other mechanism must explain the enlarged hearts. It was initially suggested that wild-type hearts underwent concentric

growth to create a multilayered myocardium, while these mutants arranged the same number of cells in a monolayer, resulting in an enlarged heart. In keeping with this explanation, fixed sections through wild-type hearts at 72 hpf appeared to have a multi-layered myocardium, while mutant hearts appeared to remain single-layered. However, embryonic heart morphology is not well maintained in fixed tissues, and recent confocal studies on live embryos have revealed that the wild-type myocardium is single-layered until the start of trabeculation around 60 hpf, well after the large-heart phenotype emerges (Arrenberg et al., 2010; Auman et al., 2007; Peshkovsky et al., 2011). Many questions remain regarding the etiology of CCMs, and continued studies in zebrafish should help address them.

FORMATION OF INTERNAL CARDIAC STRUCTURES

In order to function properly, the heart must form a number of internal structures. In the next section, we focus on two of these structures: the atrioventricular valve and the electrical conduction system. For the purposes of this review, two other important structures, the epicardium and coronary vessels, are not discussed, as they have been reviewed elsewhere (Bakkers, 2011).

<u>**Atrioventricular Canal and Valve Development**</u>

The valve structures in the AVC are crucial for maintaining unidirectional blood flow in the heart. The first sign of AVC differentiation occurs at 37 hpf, when a constriction

between the forming atrium and ventricle forms, and *bmp4* and *versican*, previously expressed in the whole heart tube, become restricted to the forming AVC myocardium (Beis et al., 2005; Walsh and Stainier, 2001). Similarly, *notch1b*, expressed in the entire ventricular endocardium at 36 hpf, becomes restricted to the AVC endocardium by 45 hpf. By 48 hpf the endocardial ring, a noticeable thickening of the AVC endocardium, has formed and the AVC prevents retrograde blood flow to some extent. The AVC becomes progressively more efficient at blocking retrograde flow over developmental time, completely blocking retrograde flow by 72 hpf (Scherz et al., 2008). Analysis of valve formation has been complicated by dramatic changes to the morphology of the valve upon fixation. Care must be taken in analyzing cellular architecture in fixed preparations. On a cellular level, the first noticeable event is the emergence at the AV boundary of cuboidal endocardial cells that express the cell adhesion molecule Alcama. By 55 hpf, a single layer of polarized cuboidal endocardial cells that stain strongly for Alcama has emerged at both the superior and inferior portions of the AVC. By 60 hpf, endocardial cells in the superior AVC send projections into the ECM between the AVC endocardium and myocardium. Cells in the inferior aspect do the same at 80 hpf. By 76 hpf, live imaging reveals a primitive valve leaflet two cells thick on the superior aspect of the AVC, which becomes readily apparent by 85 hpf (Scherz et al., 2008). The inferior valve leaflet becomes apparent by 102 hpf. The cells of the two sides of the valve leaflets assume different morphologies, with the side closest to the AVC remaining cuboidal and the side closest to the myocardium assuming a rounded shape. Importantly, live imaging suggests that, unlike in amniotes, this leaflet appears to form without a complete endothelial-mesenchymal transition (EMT), but rather through a direct invagination of

AVC endocardial cells (Fig 2). By 7 dpf, the two leaflets are clearly formed and are connected to the myocardial trabeculae.

A number of signaling pathways have been implicated in AVC development in zebrafish, many of which show parallels in amniotes. Detailed analyses have revealed the function of many of these pathways both at a cellular and molecular level. Notch signaling, known to be important for promoting EMT in mouse endocardium (Timmerman et al., 2004), seems to play multiple roles in zebrafish AVC development. First, inhibition of Notch signaling starting at 24 hpf results in the appearance at 60 hpf of ectopic cuboidal, Alcama positive endocardial cells in the ventricle, and constitutive activation of Notch in the endocardium eliminated the differentiation of cuboidal endocardial cells in the valve, suggesting that Notch activity restricts AVC differentiation in the ventricle (Beis et al., 2005). Second, inhibition of Notch signaling starting at 36 hpf resulted in a disorganized AVC endocardium with reduced Alcama expression, suggesting a later role in maintaining AVC identity. Calcineurin signaling has also been implicated in two stages in mouse AVC development, first for endocardial EMT and then for remodeling (Chang et al., 2004). In fish, inhibition of calcineurin from the one cell stage blocked AVC differentiation, while inhibition starting at 48 hpf caused a disorganized AVC endocardium (Beis et al., 2005). Combining inhibitor treatments with live imaging approaches allows for the identification of how different signaling pathways contribute to valve function. Inhibition of ErbB/Neuregulin, TGF-β, or prostaglandin signaling results in different degrees of retrograde flow at 72 hpf, occurring through three different mechanisms (Scherz et al., 2008). ErbB inhibition interferes with valve geometry,

leading to an open valve during atrial relaxation, TGF-β inhibition creates incompressible valve cells that do not seal the AVC, and inhibition of prostaglandin signaling changes myocardial structures, shifting the superior valve surface and preventing it from maintaining a seal. These functional readouts provide a new level of detail of how different signaling pathways contribute to valve formation.

Several mutants have revealed other signaling pathways involved in valvulogenesis. In wild-type embryos, Wnt activity can be strongly detected in the developing valve at 72 hpf (Hurlstone et al., 2003). This activation is associated with proliferation of the valvular endocardium. Constitutive activation of the Wnt pathway by mutations in *apc* leads to proliferation throughout the endocardium and diffuse expression of AVC markers such as *notch1b*, *bmp4*, *versican*, and *has2*. Interestingly, global inhibition of Wnt signaling by *dkk1* RNA injection can also cause a failure of AVC differentiation with regurgitation of blood from ventricle to atrium, suggesting that precise spatiotemporal control of Wnt signaling is necessary for valve formation. *bungee* mutants fail to form a valve, and show a redistribution of *notch1b* expression throughout the ventricular endocardium, as well as a lack of *spp1* staining, which normally marks endocardial cells undergoing EMT (Just et al., 2011). The mutation was mapped to a point mutation in *protein kinase D2* (*pkd2*) that inhibits kinase activity. Unlike the wild-type version, this mutant PKD2 cannot phosphorylate and prevent the nuclear localization of Histone Deacetylase 5 (HDAC5) *in vitro*, and morpholinos against HDAC5 rescue the *bungee* valve phenotype in some embryos. Interestingly, HDAC5 is known to repress *klf2a*, which has previously been shown to be important for zebrafish valve development

(Vermot et al., 2009), suggesting a PKD2/HDAC5/Klf signaling axis may be important for valve development. It remains to be determined what pathways activate PKD2 in the valvular endocardium.

Another series of mutants recently revealed a role for the transmembrane protein Tmem2 in valvulogenesis (Smith et al., 2011; Totong et al., 2011). Embryos harboring mutations in this gene exhibit expanded AV marker expression into the ventricular endocardium. Rescue experiments suggest both cell-autonomous and non-cell-autonomous roles for Tmem2 in the endocardium, as aberrant Alcama expression can be rescued by re-expression of Tmem2 in endocardial cells (Totong et al., 2011) and by morpholino knockdown of *bmp4*, which is expressed in the myocardium (Smith et al., 2011). As this gene has no known function, it represents an exciting avenue for future research.

Extracellular matrix proteins also play a role in AVC differentiation. As mentioned previously, two of the best markers for AVC differentiation are the ECM genes *cspg2* (versican) and *hyaluronan synthase 2* (*has2*), which become restricted to the AVC endocardium by 48 hpf (Hurlstone et al., 2003; Walsh and Stainier, 2001). One of the earliest zebrafish heart mutants cloned was *jekyll*, which shows toggling of blood between the two heart chambers. The *jekyll* mutation affects the UDP-glucose dehydrogenase (*ugdh*) gene, which encodes a critical enzyme in the synthesis of hyaluronic acid, heparan sulfate, and chondroitin sulfate glycosaminoglycans. Additionally, a recent morpholino study implicated nephronectin, an ECM protein previously uncharacterized in heart development, as acting through BMP signaling and

has2 production to ensure proper AVC differentiation (Patra et al., 2011). It is currently

unknown exactly how these ECM proteins influence valve formation, but it will be

interesting to study how they interact with and influence molecular and mechanical

signals necessary for valve development.

One of the most interesting observations in AVC development has been that fluid forces

play a role in valve formation. Mutants defective in cardiac contraction exhibit impaired

valve formation: for example, AVC endocardial cells in *sih* mutants fail to undergo

cuboidal morphogenesis and do not express Alcama (Bartman et al., 2004; Beis et al.,

2005). Furthermore, chemical inhibition of contraction results in a dose-dependent

decrease in endocardial ring formation. This failure of differentiation is most likely due to

lack of fluid flow, as physical occlusion of either the inflow or outflow tracts with 50 μm

glass beads inserted at 37 hpf resulted in a failure of valve formation, along with failure

of looping and multiple other cardiac defects (Hove et al., 2003). Recently, high-speed

observations of blood flow have allowed for measurement of wall shear stress (WSS) in

live 48 hpf zebrafish embryos over the course of each heart beat (Vermot et al., 2009).

Manipulations that changed flow patterns, ranging from genetic manipulation of cardiac

contractility to morpholino-based manipulation of blood viscosity, revealed that valve

defects correlated not with the magnitude of WSS, but with the degree of retrograde flow

during each beat. Increases in valve defects correlated with a significant reduction in the

expression of the known oscillatory flow-sensitive gene *klf2a*, and knockdown of *klf2a*,

while not changing retrograde flow, led to failed valve formation and a decrease in valve

marker expression. Though separating the role of oscillatory flow from other flow

parameters is difficult, these data suggest that Klf2a activity downstream of oscillatory flow plays a role in valve formation. More studies will be necessary to identify the molecular pathway upstream of *klf2a* responsible for sensing fluid forces, as well as the effector genes downstream of Klf2a. Since it can survive dramatic changes in blood flow, the zebrafish constitutes a powerful system for understanding the interactions between these myriad players in valve development. Furthermore, while zebrafish cardiac valves are structurally smaller and simpler than those in amniotes, it has become clear that the mechanisms underlying their formation are highly conserved. Thus, the zebrafish should continue to provide a fertile ground of research to address the formation of the cardiac valves, which are often affected in CHD.

Conduction System

In order to generate a coordinated beat, the heart relies on a specialized network of cardiomyocytes termed the cardiac conduction system (CCS). In vertebrates, the electrical signal initiates in the sinoatrial node, travels through the atrium/atria until it reaches specialized tissue called the atrioventricular (AV) node, where it slows dramatically. It then enters the ventricular fast conduction system, which rapidly conducts the signal to the apex of the heart, and then spreads from the apex to the rest of the ventricle (Fishman, 2005). As a result, this conduction pattern allows the apex-to-base contraction necessary to eject blood from the ventricle. Such a conduction path has been observed in both larval and adult zebrafish (Chi et al., 2008a; Hu et al., 2000; Sedmera et al., 2003). Interestingly, many of the electrical properties of the zebrafish

heart resemble those of the human heart (Kopp et al., 2005; Milan et al., 2006a; Sedmera et al., 2003; Zhang et al., 2010). Recently, the physiological development of the CCS in zebrafish has been traced using calcium-sensitive dyes, as well as a transgenic line that expresses a genetically encoded calcium-sensitive fluorescent protein (Chi et al., 2008a; Milan et al., 2006b). Coordinated, regular conduction develops as soon as the heart starts beating at 24 hpf, indicating the presence of pacemaker tissue. However, AV conduction delay between the forming chambers is not observed until 40 hpf (Milan et al., 2006b). By 48 hpf, both calcium imaging and patch clamp experiments confirm that atrial, ventricular, and AV myocardial cells have developed distinct electrical properties. Additionally, functional experiments using optogenetics have revealed that pacemaker activity starts out diffusely localized to the venous pole, but becomes restricted to a small area on the dorsal right quadrant of the sinoatrial ring by 3 dpf (Arrenberg et al., 2010). This gradual right-sided restriction is consistent with previous mapping in developing chick hearts (Kamino et al., 1981).

Maturation of ventricular conduction patterns begins at 72 hpf, when high-speed imaging of membrane potentials reveals that the conduction velocity in the outer curvature becomes markedly faster than that seen in the inner curvature (Panáková et al., 2010). Also around this time, myocardial sheets known as trabeculae begin to form in the developing ventricle (Liu et al., 2010; Peshkovsky et al., 2011). In other species, the fast conduction system is thought to form initially within these trabeculae (Rentschler et al., 2001; Sedmera et al., 2004). In the zebrafish, by 96 hpf conduction waves clearly pass from the AVC to the trabeculae before entering the rest of the ventricular myocardium

(Chi et al., 2008a). By 21 dpf, apex-to-base conduction can be seen. In the adult, the electrical impulse passes from the AVC into the trabecular network at two clearly defined points, propagates to the apex and then travels to the base of the heart (Sedmera et al., 2003). Severing the two connection points results in complete AV block. Thus, the trabeculae appear to serve as the fast conduction system in embryonic and adult zebrafish.

Only recently have studies begun to provide insight into the molecular mechanisms underlying the development of the different components of the CCS. The initial difference in conduction velocity observed between the inner and outer curvatures appears to be dependent on Wnt11 signaling, which may act at least in part by inhibiting L-type calcium channels, thereby decreasing calcium conductance (Panáková et al., 2010). The conduction properties of the AV canal, meanwhile, are dependent on a network of transcription factors. Foxn4 in AVC myocytes directly activates *tbx2b* in cooperation with Tbx5, resulting in AVC differentiation (Chi et al., 2008b). Additionally, in a recent forward genetic screen, a mutant in *tcf2* was identified that lacks AV delay (Chi et al., 2008a). Signals from the endocardium are also important for AV conduction tissue development, as *cloche* mutants fail to develop AV conduction delay (Milan et al., 2006b). In support of this idea, *neuregulin* and *notch1b* are both expressed in the AV endocardium, and morpholino knockdown of either of these genes inhibits AV delay. Trabecular formation is also dependent on the presence of endocardium, and requires signaling through the neuregulin co-receptor ErbB2 cell-autonomously within the myocardium, demonstrating that some ventricular conduction components rely on

similar signals as the AVC myocardium (Liu et al., 2010; Peshkovsky et al., 2011). Interestingly, different components of the conduction system respond differently to cardiac function. *sih* mutants completely lack trabeculae and *amhc* mutants show a variable decrease in trabecular formation (Chi et al., 2008a; Peshkovsky et al., 2011), while neither AV conduction (Chi et al., 2008a; Milan et al., 2006b) or the OC/IC conduction ratio (Panáková et al., 2010) are affected in contractile mutants. While a clear demonstration of Purkinje-like cells in the zebrafish heart remains a major question, the data so far point to the existence of a specialized conduction system. Given the importance of this tissue in heart function, and our limited understanding of its formation, one should approach it using a variety of model systems.

CARDIAC PHYSIOLOGY

Establishment and Maintenance of Cardiac Contractility

In order to pump blood effectively, the heart must not only form the correct morphology, but must also form contractile sarcomeres and regulate their contractility. Because the zebrafish can develop in the first week without a functional heart, it is an excellent *in vivo* model for studying proteins involved in sarcomerogenesis and cardiac contractility. Large-scale genetic screens have identified many mutations that cause defects in sarcomere assembly and contractility. These have included some mutations that completely disrupt sarcomere assembly in one or both chambers, including mutations in

sarcomeric genes (*titin, myl7, tnnt2, vmhc, amhc*) (Auman et al., 2007; Berdougo et al.,

2003; Rottbauer et al., 2006; Sehnert et al., 2002; Xu et al., 2002). These screens have

also identified mutants with impaired contractility but intact sarcomeres, which have

illuminated new mechanisms for maintaining cardiac contractility. A truncating mutation

in the essential cardiac myosin light chain gene (*cmlc1*) surprisingly does not affect

sarcomeres (Meder et al., 2009), in stark contrast to the absence of sarcomeres observed

in a morpholino knockdown of the same gene (Chen et al., 2008; Meder et al., 2009).

Examination of the carboxyl-terminus of Cmlc1 deleted in the mutant led to the

identification of a highly conserved serine residue that might constitute a previously

unknown post-translational modification site. Myocyte-specific expression of wild-type

cmlc1 rescues myocyte contractility in the mutant, while a version in which this serine

amino acid is mutated to an alanine cannot. Although the precise role of this serine is

unknown, this mutant reveals a novel sarcomeric modification site that contributes to

contractility.

Two mutants in combination helped to shed light on how cardiomyocytes sense stretch.

First, a nonsense mutation in *phospholipase C γ1* (*plcγ1*) leads to progressive loss of

ventricular contractility starting at 48 hpf, leading to a silent ventricle by 60 hpf

(Rottbauer et al., 2005). Sarcomeric structure remains normal in these mutants. Further

analysis indicates that PLCγ1 functions downstream of Vegf signaling through the

receptor Flt-1 to increase calcium transients in cardiomyocytes, leading to increased

contractility. Second, *main squeeze* (*msq*) mutants, which carry a mutation in the

integrin-linked kinase gene (*ilk*), exhibit a progressive loss of ventricular contractility

with seemingly normal sarcomeric structure (Bendig et al., 2006). ILK co-localizes with alpha-actinin at Z disks, but also binds β-parvin, which in turn binds integrins, providing a link between the ECM and the sarcomere. In keeping with this model, embryos carrying one copy of a separately isolated nonsense allele of *ilk*, termed *lost contact (loc)* are sensitized to morpholino knockdown of the ECM component laminin alpha 4, suggesting that ILK's function may depend on integrin-mediated interactions with laminins (Knöll et al., 2007). The *msq* mutation decreases kinase activity and ILK's affinity for β-parvin, and while expression of wild-type ILK can rescue *msq* mutant embryos, known mutants which lack either kinase activity or the ability to bind to β-parvin cannot. Additionally, *msq* mutants can be rescued by injection of RNA encoding activated, membrane-associated protein kinase B (PKB) or VEGF. Overall, analysis of these two mutants suggests a stretch response pathway, where ILK serves as a link between the costamere and the ECM through β-parvin and integrins. In this model, stretch along the costamere/ECM axis leads to ILK activation. Kinase activation in turn activates PKB, leading to expression of VEGF, which activates PLCγ1 downstream of Flt-1, increasing calcium transients, and thus increasing contractility upon increased stretch. Though this pathway needs further confirmation in other systems, it is an attractive model for how force sensing may connect to increased contractility and, possibly, contraction-dependent differentiation, as seen in the ventricular trabeculae.

HUMAN DISEASE

Insights into Human Disease

The zebrafish has emerged as a unique model for studying human disease. The combination of forward and reverse genetic techniques available in the zebrafish, coupled with the possibility of performing *in vivo* drug screens (Baker, 2011) allows a number of different approaches for dissecting human diseases. The similarity between the electrical properties of zebrafish and human hearts (Sedmera et al., 2003; Zhang et al., 2010) makes the fish particularly useful for modeling conduction defects. Mutations in the zebrafish homolog of the hERG potassium channel gene have led to models of short QT syndrome and long QT syndrome, which had been difficult to generate in murine systems, probably due to inherent differences in the channels used for conduction in mice and humans (Arnaout et al., 2007; Hassel et al., 2008). Meanwhile, morpholino technology has been used to model Barth syndrome (Khuchua et al., 2006), and dilated cardiomyopathy (Vogel et al., 2009). The ease of manipulation of the zebrafish embryo can also facilitate identification of the function of human mutations. One study identified mutant forms of the BMP receptor ALK2 in patients with atrioventricular septal (AVS) defects. Injection of RNA for the mutant receptors into zebrafish embryos led to the discovery of a dominant-negative form of the receptor associated with AVS defects (Smith et al., 2009). The zebrafish can also be used to validate new human heart disease genes. A search through publicly available microarray data identified *nexilin* as a gene of unknown function enriched in the heart (Hassel et al., 2009). Nexilin was found to be a component of sarcomeric Z-disks, and morpholino-based inhibition led to enlarged ventricles and decreased fractional shortening reminiscent of dilated cardiomyopathy (DCM). Given the DCM phenotype of the *nexilin* knockdown, a cohort of DCM patients was sequenced,

33

and three heterozygous mutations from 9 patients were identified. RNA injection of the mutant forms of nexilin into zebrafish embryos confirmed that these mutations led to dominant negative forms of the protein that disrupted heart function, providing support for a causative role of these mutations in DCM. Finally, using the forward genetic potential of zebrafish can identify new genetic modifiers of heart disease. One study used an intriguing approach to screen for modulators of cardiac repolarization. Treating embryos with inhibitors of zERG causes 2:1 heart block. By treating embryos from a library of mutant fish with zERG inhibitors and screening for enhancement or repression of the heart block phenotype led to the identification of a number of modifiers of repolarization (Milan et al., 2009). Cross-referencing the identified genes with human genome-wide association studies looking at altered cardiac repolarization revealed that one gene, GINS3, was in a region highly associated with human QT interval defects. These studies highlight the multiple advantages of the zebrafish system for examining human heart disease, and pave the way for continued contributions from this model system.

Summary:

1. With a large number of cardiac mutants already identified and analyzed, the zebrafish provides a unique genetic model for studying heart development.

2. Advances in imaging and transgenesis combined with the transparency of the zebrafish embryo and larvae allow for analysis of cellular behaviors during heart formation.

3. Mechanical forces and electrical signals contribute substantially to heart development and morphogenesis.

4. Large-scale screening approaches available in zebrafish make it a powerful platform for uncovering novel mechanisms of human disease.
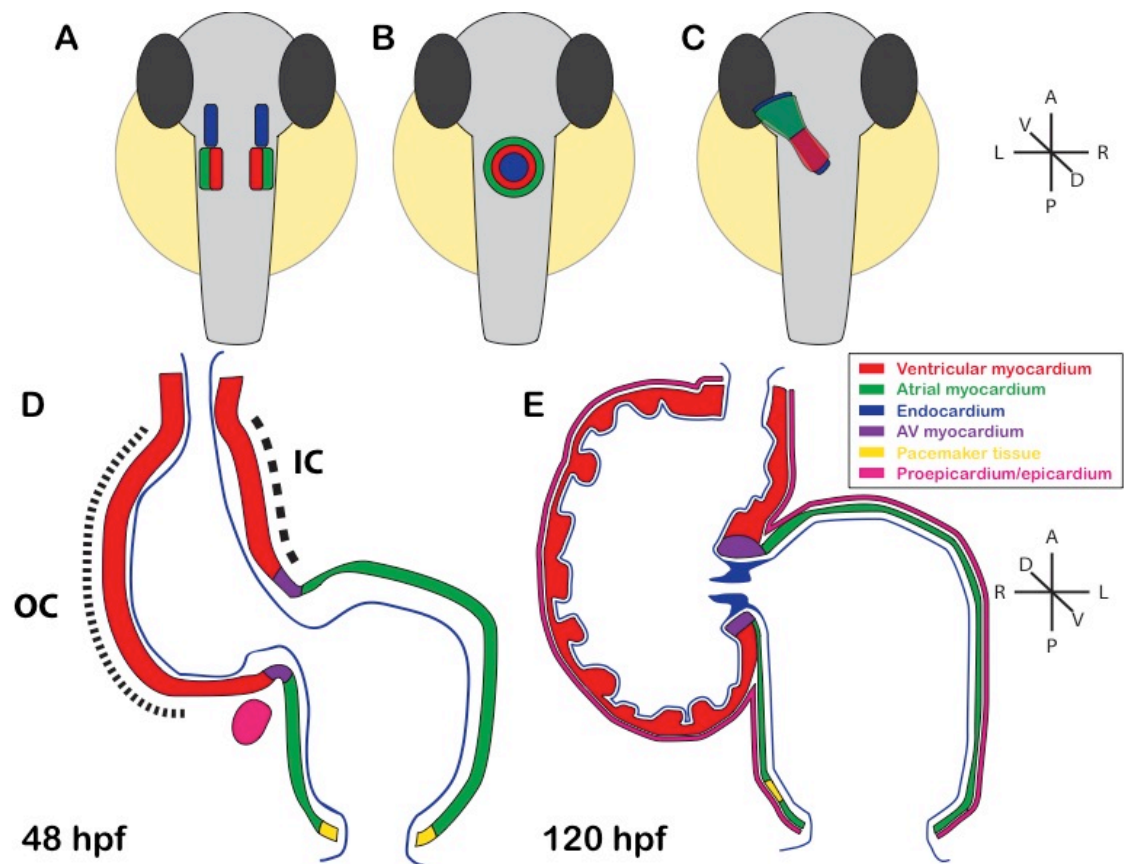
Figure 1: Overview of zebrafish heart development

Figure 1: Overview of zebrafish heart development (A-C) Heart development before

looping. Embryos are shown in a dorsal view. (A) At 12 hpf (15 somites), myocardial

progenitors are found in the ALPM, with ventricular progenitors more medial than atrial

progenitors. Endocardial progenitors lie anterior in the ALPM. (B) Myocardial and

endocardial progenitors migrate to the midline and fuse by 19 hpf (20 somites) to create

the cardiac cone. (C) Through a process of involution, the myocardium rearranges to

surround the endocardium and form the linear heart tube by 24 hpf. (D-E) Later heart

development. Heart sections are shown from a ventral view. (D) By 48 hpf, the heart has

looped to form a right-sided ventricle and left-sided atrium. Distinct outer and inner

curvatures have formed, and the ventricular OC has started to balloon. AV myocardium

has functionally differentiated to create a delay, and pacemaker activity has become

restricted to the sinoatrial ring. The proepicardial organ has coalesced near the AVC. (E)

By 120 hpf, the OC has fully ballooned, and trabecular ridges have formed. The AV

valve leaflets are well formed and prevent retrograde flow. The epicardium has expanded

over the entire exterior surface of the myocardium. The SA nodal tissue has restricted to

a few cells on the right side of the atrium several cell diameters from the sinoatrial ring.

E

Cells Per Beat

12
10
8
6
4
2
0

55h 63h 72h 86h 96h 102h

Modified from Scherz et. al. 2008

A

55 hpf

B

60 hpf

C

72 hpf

D

96 hpf
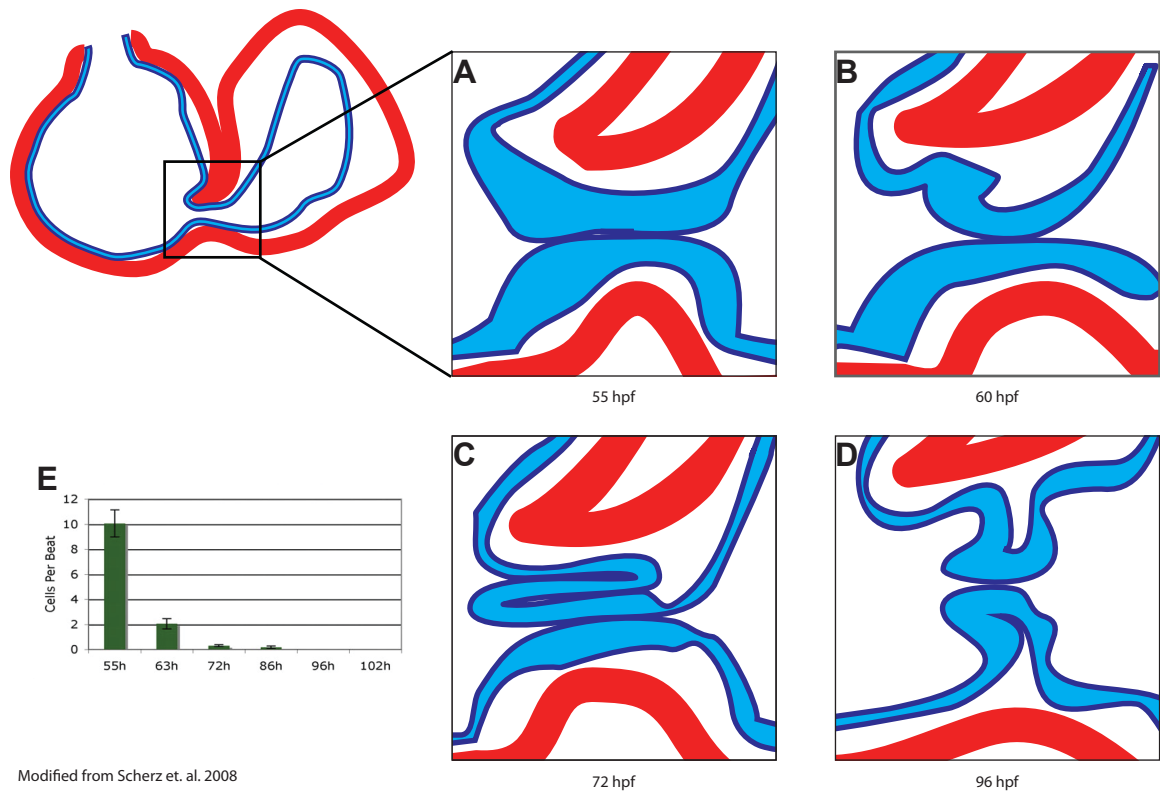
Figure 2: Zebrafish Valve Development

Figure 2: Zebrafish Valve Development (A) By 55 hpf, the AV endocardium forms a thick monolayer. (B) by 60 hpf, the endocardial layer shows signs of involution. (C) By 72 hpf, a superior leaflet has formed through the involution of the AV endocardium. (D) At 96 hpf, both superior and inferior leaflets have formed. (E) Retrograde flow of blood cells observed over developmental time. By 72 hpf, retrograde flow has essentially ceased.

References

Alexander, J., Stainier, D.Y., and Yelon, D. (1998). Screening mosaic F1 females for mutations affecting zebrafish heart induction and patterning. Dev. Genet *22*, 288–299.

Alexander, J., Rothenberg, M., Henry, G.L., and Stainier, D.Y. (1999). casanova plays an early and essential role in endoderm formation in zebrafish. Dev. Biol *215*, 343–357.

Arnaout, R., Ferrer, T., Huisken, J., Spitzer, K., Stainier, D.Y.R., Tristani-Firouzi, M., and Chi, N.C. (2007). Zebrafish model for human long QT syndrome. Proc. Natl. Acad. Sci. U.S.A *104*, 11316–11321.

Arrenberg, A.B., Stainier, D.Y.R., Baier, H., and Huisken, J. (2010). Optogenetic control of cardiac function. Science *330*, 971–974.

Arrington, C.B., and Yost, H.J. (2009). Extra-embryonic syndecan 2 regulates organ primordia migration and fibrillogenesis throughout the zebrafish embryo. Development *136*, 3143–3152.

Auman, H.J., and Yelon, D. (2004). Vertebrate organogenesis: getting the heart into shape. Curr. Biol *14*, R152–153.

Auman, H.J., Coleman, H., Riley, H.E., Olale, F., Tsai, H.J., and Yelon, D. (2007). Functional modulation of cardiac form through regionally confined cell shape changes. PLoS Biol *5*, e53.

Baker, M. (2011). Screening: the age of fishes. Nat Meth *8*, 47–51.

Bakkers, J. (2011). Zebrafish as a model to study cardiac development and human cardiac disease. Cardiovasc. Res. *91*, 279–288.

Bakkers, J., Verhoeven, M.C., and Abdelilah-Seyfried, S. (2009). Shaping the zebrafish

heart: from left-right axis specification to epithelial tissue morphogenesis. Dev. Biol

330, 213–220.

Bartman, T., Walsh, E.C., Wen, K.K., McKane, M., Ren, J., Alexander, J., Rubenstein,

P.A., and Stainier, D.Y.R. (2004). Early myocardial function affects endocardial

cushion development in zebrafish. PLoS Biology *2*, 673–681.

Beis, D., Bartman, T., Jin, S.-W., Scott, I.C., D'Amico, L.A., Ober, E.A., Verkade, H.,

Frantsve, J., Field, H.A., Wehman, A., et al. (2005). Genetic and cellular analyses of

zebrafish atrioventricular cushion and valve development. Development *132*, 4193–

4204.

Bendig, G., Grimmler, M., Huttner, I.G., Wessels, G., Dahme, T., Just, S., Trano, N.,

Katus, H.A., Fishman, M.C., and Rottbauer, W. (2006). Integrin-linked kinase, a

novel component of the cardiac mechanical stretch sensor, controls contractility in the

zebrafish heart. Genes & Development *20*, 2361–2372.

Berdougo, E., Coleman, H., Lee, D.H., Stainier, D.Y.R., and Yelon, D. (2003). Mutation

of weak atrium/atrial myosin heavy chain disrupts atrial function and influences

ventricular morphogenesis in zebrafish. Development *130*, 6121–6129.

Bertrand, J.Y., Chi, N.C., Santoso, B., Teng, S., Stainier, D.Y.R., and Traver, D. (2010).

Haematopoietic stem cells derive directly from aortic endothelium during

development. Nature *464*, 108–111.

Bussmann, J., Bakkers, J., and Schulte-Merker, S. (2007). Early Endocardial

Morphogenesis Requires Scl/Tal1. PLoS Genet *3*, e140.

Chablais, F., Veit, J., Rainer, G., and Jaźwińska, A. (2011). The zebrafish heart regenerates after cryoinjury-induced myocardial infarction. BMC Dev. Biol. *11*, 21.

Chang, C.-P., Neilson, J.R., Bayle, J.H., Gestwicki, J.E., Kuo, A., Stankunas, K., Graef, I.A., and Crabtree, G.R. (2004). A field of myocardial-endocardial NFAT signaling underlies heart valve morphogenesis. Cell *118*, 649–663.

Chen, J.N., Haffter, P., Odenthal, J., Vogelsang, E., Brand, M., van Eeden, F.J., Furutani-Seiki, M., Granato, M., Hammerschmidt, M., Heisenberg, C.P., et al. (1996). Mutations affecting the cardiovascular system and other internal organs in zebrafish. Development *123*, 293–302.

Chen, Z., Huang, W., Dahme, T., Rottbauer, W., Ackerman, M.J., and Xu, X. (2008). Depletion of zebrafish essential and regulatory myosin light chains reduces cardiac function through distinct mechanisms. Cardiovasc Res *79*, 97–108.

Chi, N.C., Shaw, R.M., Jungblut, B., Huisken, J., Ferrer, T., Arnaout, R., Scott, I., Beis, D., Xiao, T., Baier, H., et al. (2008a). Genetic and Physiologic Dissection of the Vertebrate Cardiac Conduction System. PLoS Biol *6*, e109.

Chi, N.C., Shaw, R.M., De Val, S., Kang, G., Jan, L.Y., Black, B.L., and Stainier, D.Y.R. (2008b). Foxn4 directly regulates tbx2b expression and atrioventricular canal formation. Genes & Development *22*, 734–739.

Chi, N.C., Bussen, M., Brand-Arzamendi, K., Ding, C., Olgin, J.E., Shaw, R.M., Martin, G.R., and Stainier, D.Y.R. (2010). Cardiac conduction is required to preserve cardiac chamber morphology. Proc. Natl. Acad. Sci. U.S.A *107*, 14662–14667.

Christoffels, V.M., Habets, P.E.M.H., Franco, D., Campione, M., de Jong, F., Lamers, W.H., Bao, Z.-Z., Palmer, S., Biben, C., Harvey, R.P., et al. (2000). Chamber

Formation and Morphogenesis in the Developing Mammalian Heart. Developmental Biology *223*, 266–278.

Curado, S., Anderson, R.M., Jungblut, B., Mumm, J., Schroeter, E., and Stainier, D.Y.R. (2007). Conditional targeted cell ablation in zebrafish: a new tool for regeneration studies. Dev. Dyn. *236*, 1025–1035.

Curado, S., Stainier, D.Y.R., and Anderson, R.M. (2008). Nitroreductase-mediated cell/tissue ablation in zebrafish: a spatially and temporally controlled ablation method with applications in developmental and regeneration studies. Nat Protoc *3*, 948–954.

Deacon, D.C., Nevis, K.R., Cashman, T.J., Zhou, Y., Zhao, L., Washko, D., Guner-Ataman, B., Burns, C.G., and Burns, C.E. (2010). The miR-143-adducin3 pathway is essential for cardiac chamber morphogenesis. Development *137*, 1887 –1896.

Dohn, T.E., and Waxman, J.S. (2012). Distinct phases of Wnt/β-catenin signaling direct cardiomyocyte formation in zebrafish. Dev. Biol. *361*, 364–376.

Eisen, J.S., and Smith, J.C. (2008). Controlling morpholino experiments: don't stop making antisense. Development *135*, 1735 –1743.

Ekker, S.C. (2008). Zinc finger-based knockout punches for zebrafish genes. Zebrafish *5*, 121–123.

Fish, J.E., Wythe, J.D., Xiao, T., Bruneau, B.G., Stainier, D.Y.R., Srivastava, D., and Woo, S. (2011). A Slit/miR-218/Robo regulatory loop is required during heart tube formation in zebrafish. Development *138*, 1409 –1419.

Fishman, G.I. (2005). Understanding Conduction System Development: A Hop, Skip and Jump Away? Circ Res *96*, 809–811.

Forouhar, A.S., Liebling, M., Hickerson, A., Nasiraei-Moghaddam, A., Tsai, H.-J., Hove, J.R., Fraser, S.E., Dickinson, M.E., and Gharib, M. (2006). The embryonic vertebrate heart tube is a dynamic suction pump. Science *312*, 751–753.

Garavito-Aguilar, Z.V., Riley, H.E., and Yelon, D. (2010). Hand2 ensures an appropriate environment for cardiac fusion by limiting Fibronectin function. Development *137*, 3215–3220.

Garrity, D.M., Childs, S., and Fishman, M.C. (2002). The heartstrings mutation in zebrafish causes heart/fin Tbx5 deficiency syndrome. Development *129*, 4635–4645.

George, E.L., Georges-Labouesse, E.N., Patel-King, R.S., Rayburn, H., and Hynes, R.O. (1993). Defects in mesoderm, neural tube and vascular development in mouse embryos lacking fibronectin. Development *119*, 1079–1091.

Glickman, N.S., and Yelon, D. (2002). Cardiac development in zebrafish: coordination of form and function. Semin. Cell Dev. Biol *13*, 507–513.

González-Rosa, J.M., Martín, V., Peralta, M., Torres, M., and Mercader, N. (2011). Extensive scar formation and regression during heart regeneration after cryoinjury in zebrafish. Development *138*, 1663–1674.

Hami, D., Grimes, A.C., Tsai, H.-J., and Kirby, M.L. (2011). Zebrafish cardiac development requires a conserved secondary heart field. Development *138*, 2389–2398.

Hassel, D., Scholz, E.P., Trano, N., Friedrich, O., Just, S., Meder, B., Weiss, D.L., Zitron, E., Marquart, S., Vogel, B., et al. (2008). Deficient zebrafish ether-à-go-go-related gene channel gating causes short-QT syndrome in zebrafish reggae mutants. Circulation *117*, 866–875.

Hassel, D., Dahme, T., Erdmann, J., Meder, B., Huge, A., Stoll, M., Just, S., Hess, A., Ehlermann, P., Weichenhan, D., et al. (2009). Nexilin mutations destabilize cardiac Z-disks and lead to dilated cardiomyopathy. Nat Med *15*, 1281–1288.

Holtzinger, A., and Evans, T. (2007). Gata5 and Gata6 are functionally redundant in zebrafish for specification of cardiomyocytes. Dev. Biol *312*, 613–622.

Holtzman, N.G., Schoenebeck, J.J., Tsai, H.-J., and Yelon, D. (2007). Endocardium is necessary for cardiomyocyte movement during heart tube assembly. Development *134*, 2379–2386.

Horne-Badovinac, S., Lin, D., Waldron, S., Schwarz, M., Mbamalu, G., Pawson, T., Jan, Y., Stainier, D.Y., and Abdelilah-Seyfried, S. (2001). Positional cloning of heart and soul reveals multiple roles for PKC lambda in zebrafish organogenesis. Curr. Biol *11*, 1492–1502.

Hove, J.R., Koster, R.W., Forouhar, A.S., Acevedo-Bolton, G., Fraser, S.E., and Gharib, M. (2003). Intracardiac fluid forces are an essential epigenetic factor for embryonic cardiogenesis. Nature *421*, 172–177.

Hu, N., Sedmera, D., Yost, H.J., and Clark, E.B. (2000). Structure and function of the developing zebrafish heart. Anat. Rec *260*, 148–157.

Huang, C.-J., Tu, C.-T., Hsiao, C.-D., Hsieh, F.-J., and Tsai, H.-J. (2003). Germ-line transmission of a myocardium-specific GFP transgene reveals critical regulatory elements in the cardiac myosin light chain 2 promoter of zebrafish. Developmental Dynamics *228*, 30–40.

Huang, P., Xiao, A., Zhou, M., Zhu, Z., Lin, S., and Zhang, B. (2011). Heritable gene targeting in zebrafish using customized TALENs. Nat Biotech *29*, 699–700.

Hurlstone, A.F.L., Haramis, A.-P.G., Wienholds, E., Begthel, H., Korving, J., Van Eeden, F., Cuppen, E., Zivkovic, D., Plasterk, R.H.A., and Clevers, H. (2003). The Wnt/beta-catenin pathway regulates cardiac valve formation. Nature *425*, 633–637.

Jensen, A.M., and Westerfield, M. (2004). Zebrafish mosaic eyes is a novel FERM protein required for retinal lamination and retinal pigmented epithelial tight junction formation. Current Biology *14*, 711–717.

Jopling, C., Sleep, E., Raya, M., Martí, M., Raya, A., and Belmonte, J.C.I. (2010). Zebrafish heart regeneration occurs by cardiomyocyte dedifferentiation and proliferation. Nature *464*, 606–609.

Just, S., Berger, I.M., Meder, B., Backs, J., Keller, A., Marquart, S., Frese, K., Patzel, E., Rauch, G.-J., Katus, H.A., et al. (2011). Protein kinase D2 controls cardiac valve formation in zebrafish by regulating histone deacetylase 5 activity. Circulation *124*, 324–334.

Kamino, K., Hirota, A., and Fujii, S. (1981). Localization of pacemaking activity in early embryonic heart monitored using voltage-sensitive dye. Nature *290*, 595–597.

Kawahara, A., Nishi, T., Hisano, Y., Fukui, H., Yamaguchi, A., and Mochizuki, N. (2009). The sphingolipid transporter spns2 functions in migration of zebrafish myocardial precursors. Science *323*, 524–527.

Keegan, B.R., Meyer, D., and Yelon, D. (2004). Organization of cardiac chamber progenitors in the zebrafish blastula. Development *131*, 3081–3091.

Keegan, B.R., Feldman, J.L., Begemann, G., Ingham, P.W., and Yelon, D. (2005). Retinoic acid signaling restricts the cardiac progenitor pool. Science *307*, 247–249.

Khuchua, Z., Yue, Z., Batts, L., and Strauss, A.W. (2006). A Zebrafish Model of Human Barth Syndrome Reveals the Essential Role of Tafazzin in Cardiac Development and Function. Circ Res *99*, 201–208.

Kikuchi, K., Holdway, J.E., Werdich, A.A., Anderson, R.M., Fang, Y., Egnaczyk, G.F., Evans, T., Macrae, C.A., Stainier, D.Y.R., and Poss, K.D. (2010). Primary contribution to zebrafish heart regeneration by gata4(+) cardiomyocytes. Nature *464*, 601–605.

Kikuchi, K., Gupta, V., Wang, J., Holdway, J.E., Wills, A.A., Fang, Y., and Poss, K.D. (2011). tcf21+ epicardial cells adopt non-myocardial fates during zebrafish heart development and regeneration. Development *138*, 2895–2902.

Kikuchi, Y., Trinh, L.A., Reiter, J.F., Alexander, J., Yelon, D., and Stainier, D.Y.. (2000). The zebrafish bonnie and clyde gene encodes a Mix family homeodomain protein that regulates the generation of endodermal precursors. Genes & Development *14*, 1279.

Kleaveland, B., Zheng, X., Liu, J.J., Blum, Y., Tung, J.J., Zou, Z., Sweeney, S.M., Chen, M., Guo, L., Lu, M., et al. (2009). Regulation of cardiovascular development and integrity by the heart of glass-cerebral cavernous malformation protein pathway. Nat. Med *15*, 169–176.

Knöll, R., Postel, R., Wang, J., Krätzner, R., Hennecke, G., Vacaru, A.M., Vakeel, P., Schubert, C., Murthy, K., Rana, B.K., et al. (2007). Laminin-α4 and Integrin-Linked Kinase Mutations Cause Human Cardiomyopathy Via Simultaneous Defects in Cardiomyocytes and Endothelial Cells. Circulation *116*, 515 –525.

Knopf, F., Schnabel, K., Haase, C., Pfeifer, K., Anastassiadis, K., and Weidinger, G.
(2010). Dually inducible TetON systems for tissue-specific conditional gene
expression in zebrafish. Proc. Natl. Acad. Sci. U.S.A. *107*, 19933–19938.

Kopp, R., Schwerte, T., and Pelster, B. (2005). Cardiac performance in the zebrafish
breakdance mutant. J. Exp. Biol *208*, 2123–2134.

Kupperman, E., An, S., Osborne, N., Waldron, S., and Stainier, D.Y. (2000). A
sphingosine-1-phosphate receptor regulates cell migration during vertebrate heart
development. Nature *406*, 192–195.

Labauge, P., Denier, C., Bergametti, F., and Tournier-Lasserve, E. (2007). Genetics of
cavernous angiomas. Lancet Neurol *6*, 237–244.

Lawson, N.D., and Weinstein, B.M. (2002). In vivo imaging of embryonic vascular
development using transgenic zebrafish. Dev. Biol. *248*, 307–318.

Lazic, S., and Scott, I.C. (2011). Mef2cb regulates late myocardial cell addition from a
second heart field-like population of progenitors in zebrafish. Dev Biol.

Lee, R.K., Stainier, D.Y., Weinstein, B.M., and Fishman, M.C. (1994). Cardiovascular
development in the zebrafish. II. Endocardial progenitors are sequestered within the
heart field. Development *120*, 3361–3366.

Lin, Y.-F., Swinburne, I., and Yelon, D. (2012). Multiple influences of blood flow on
cardiomyocyte hypertrophy in the embryonic zebrafish heart. Developmental Biology
362, 242–253.

Liu, J., Bressan, M., Hassel, D., Huisken, J., Staudt, D., Kikuchi, K., Poss, K.D., Mikawa,
T., and Stainier, D.Y.R. (2010). A dual role for ErbB2 signaling in cardiac
trabeculation. Development *137*, 3867–3875.

Lou, X., Deshwar, A.R., Crump, J.G., and Scott, I.C. (2011). Smarcd3b and Gata5 promote a cardiac progenitor fate in the zebrafish embryo. Development *138*, 3113–3123.

Mably, J.D., Mohideen, M.-A.P.., Burns, C.G., Chen, J.-N., and Fishman, M.C. (2003). heart of glass Regulates the Concentric Growth of the Heart in Zebrafish. Current Biology *13*, 2138–2147.

Mably, J.D., Chuang, L.P., Serluca, F.C., Mohideen, M.-A.P.K., Chen, J.-N., and Fishman, M.C. (2006). santa and valentine pattern concentric growth of cardiac myocardium in the zebrafish. Development *133*, 3139–3146.

Marques, S.R., and Yelon, D. (2009). Differential requirement for BMP signaling in atrial and ventricular lineages establishes cardiac chamber proportionality. Dev. Biol *328*, 472–482.

Marques, S.R., Lee, Y., Poss, K.D., and Yelon, D. (2008). Reiterative roles for FGF signaling in the establishment of size and proportion of the zebrafish heart. Dev. Biol *321*, 397–406.

Meder, B., Laufer, C., Hassel, D., Just, S., Marquart, S., Vogel, B., Hess, A., Fishman, M.C., Katus, H.A., and Rottbauer, W. (2009). A Single Serine in the Carboxyl Terminus of Cardiac Essential Myosin Light Chain-1 Controls Cardiomyocyte Contractility In Vivo. Circ Res *104*, 650–659.

Milan, D.J., Jones, I.L., Ellinor, P.T., and MacRae, C.A. (2006a). In vivo recording of adult zebrafish electrocardiogram and assessment of drug-induced QT prolongation. American Journal of Physiology - Heart and Circulatory Physiology *291*, H269 – H273.

Milan, D.J., Giokas, A.C., Serluca, F.C., Peterson, R.T., and MacRae, C.A. (2006b). Notch1b and neuregulin are required for specification of central cardiac conduction tissue. Development *133*, 1125–1132.

Milan, D.J., Kim, A.M., Winterfield, J.R., Jones, I.L., Pfeufer, A., Sanna, S., Arking, D.E., Amsterdam, A.H., Sabeh, K.M., Mably, J.D., et al. (2009). Drug-sensitized zebrafish screen identifies multiple genes, including GINS3, as regulators of myocardial repolarization. Circulation *120*, 553–559.

Moens, C.B., Donn, T.M., Wolf-Saxon, E.R., and Ma, T.P. (2008). Reverse genetics in zebrafish by TILLING. Brief Funct Genomic Proteomic *7*, 454–459.

Munson, C., Huisken, J., Bit-Avragim, N., Kuo, T., Dong, P.D., Ober, E.A., Verkade, H., Abdelilah-Seyfried, S., and Stainier, D.Y.R. (2008). Regulation of neurocoel morphogenesis by Pard6[gamma]b. Developmental Biology *324*, 41–54.

Ohn, J., Tsai, H.-J., and Liebling, M. (2009). Joint dynamic imaging of morphogenesis and function in the developing heart. Organogenesis *5*, 166–173.

Omori, Y., and Malicki, J. (2006). Oko meduzy and related crumbs genes are determinants of apical cell features in the vertebrate embryo. Current Biology *16*, 945–957.

Osborne, N., Brand-Arzamendi, K., Ober, E.A., Jin, S.-W., Verkade, H., Holtzman, N.G., Yelon, D., and Stainier, D.Y.R. (2008). The spinster homolog, two of hearts, is required for sphingosine 1-phosphate signaling in zebrafish. Curr. Biol *18*, 1882–1888.

Palencia-Desai, S., Kohli, V., Kang, J., Chi, N.C., Black, B.L., and Sumanas, S. (2011). Vascular endothelial and endocardial progenitors differentiate as cardiomyocytes in the absence of Etsrp/Etv2 function. Development *138*, 4721–4732.

Panáková, D., Werdich, A.A., and Macrae, C.A. (2010). Wnt11 patterns a myocardial electrical gradient through regulation of the L-type Ca(2+) channel. Nature *466*, 874–878.

Pardo-Martin, C., Chang, T.-Y., Koo, B.K., Gilleland, C.L., Wasserman, S.C., and Yanik, M.F. (2010). High-throughput in vivo vertebrate screening. Nat Meth *7*, 634–636.

De Pater, E., Clijsters, L., Marques, S.R., Lin, Y.-F., Garavito-Aguilar, Z.V., Yelon, D., and Bakkers, J. (2009). Distinct phases of cardiomyocyte differentiation regulate growth of the zebrafish heart. Development *136*, 1633–1641.

Patra, C., Diehl, F., Ferrazzi, F., van Amerongen, M.J., Novoyatleva, T., Schaefer, L., Mühlfeld, C., Jungblut, B., and Engel, F.B. (2011). Nephronectin regulates atrioventricular canal differentiation via Bmp4-Has2 signaling in zebrafish. Development *138*, 4499–4509.

Peshkovsky, C., Totong, R., and Yelon, D. (2011). Dependence of cardiac trabeculation on neuregulin signaling and blood flow in zebrafish. Dev Dyn.

Peterkin, T., Gibson, A., and Patient, R. (2007). Redundancy and evolution of GATA factor requirements in development of the myocardium. Dev. Biol *311*, 623–635.

Peterson, R.T., Mably, J.D., Chen, J.N., and Fishman, M.C. (2001). Convergence of distinct pathways to heart patterning revealed by the small molecule concentramide and the mutation heart-and-soul. Curr. Biol *11*, 1481–1491.

Poss, K.D. (2007). Getting to the heart of regeneration in zebrafish. Semin. Cell Dev. Biol *18*, 36–45.

Poss, K.D., Wilson, L.G., and Keating, M.T. (2002). Heart regeneration in zebrafish. Science *298*, 2188–2190.

Reiter, J.F., Alexander, J., Rodaway, A., Yelon, D., Patient, R., Holder, N., and Stainier, D.Y. (1999). Gata5 is required for the development of the heart and endoderm in zebrafish. Genes Dev *13*, 2983–2995.

Reiter, J.F., Verkade, H., and Stainier, D.Y. (2001). Bmp2b and Oep promote early myocardial differentiation through their regulation of gata5. Dev. Biol *234*, 330–338.

Rentschler, S., Vaidya, D.M., Tamaddon, H., Degenhardt, K., Sassoon, D., Morley, G.E., Jalife, J., and Fishman, G.I. (2001). Visualization and functional characterization of the developing murine cardiac conduction system. Development *128*, 1785–1792.

Rohr, S. (2006). Heart and soul/PRKCi and nagie oko/Mpp5 regulate myocardial coherence and remodeling during cardiac morphogenesis. Development *133*, 107–115.

Rohr, S., Otten, C., and Abdelilah-Seyfried, S. (2008). Asymmetric Involution of the Myocardial Field Drives Heart Tube Formation in Zebrafish. Circ Res *102*, e12–19.

Rottbauer, W., Baker, K., Wo, Z.G., Mohideen, M.A., Cantiello, H.F., and Fishman, M.C. (2001). Growth and function of the embryonic heart depend upon the cardiac-specific L-type calcium channel alpha1 subunit. Dev. Cell *1*, 265–275.

Rottbauer, W., Saurin, A.J., Lickert, H., Shen, X., Burns, C.G., Wo, Z.G., Kemler, R., Kingston, R., Wu, C., and Fishman, M. (2002). Reptin and Pontin Antagonistically Regulate Heart Growth in Zebrafish Embryos. Cell *111*, 661–672.

Rottbauer, W., Just, S., Wessels, G., Trano, N., Most, P., Katus, H.A., and Fishman, M.C. (2005). VEGF–PLCγ1 pathway controls cardiac contractility in the embryonic heart. Genes & Development *19*, 1624–1634.

Rottbauer, W., Wessels, G., Dahme, T., Just, S., Trano, N., Hassel, D., Burns, C.G., Katus, H.A., and Fishman, M.C. (2006). Cardiac Myosin Light Chain-2: A Novel Essential Component of Thick-Myofilament Assembly and Contractility of the Heart. Circ Res *99*, 323–331.

Sakaguchi, T., Kikuchi, Y., Kuroiwa, A., Takeda, H., and Stainier, D.Y.R. (2006). The yolk syncytial layer regulates myocardial migration by influencing extracellular matrix assembly in zebrafish. Development *133*, 4063–4072.

Sander, J.D., Cade, L., Khayter, C., Reyon, D., Peterson, R.T., Joung, J.K., and Yeh, J.-R.J. (2011). Targeted gene disruption in somatic zebrafish cells using engineered TALENs. Nat Biotech *29*, 697–698.

Scherz, P.J., Huisken, J., Sahai-Hernandez, P., and Stainier, D.Y.R. (2008). High-speed imaging of developing heart valves reveals interplay of morphogenesis and function. Development *135*, 1179–1187.

Schnabel, K., Wu, C.-C., Kurth, T., and Weidinger, G. (2011). Regeneration of cryoinjury induced necrotic heart lesions in zebrafish is associated with epicardial activation and cardiomyocyte proliferation. PLoS ONE *6*, e18503.

Schoenebeck, J.J., and Yelon, D. (2007). Illuminating cardiac development: Advances in imaging add new dimensions to the utility of zebrafish genetics. In Seminars in Cell & Developmental Biology, pp. 27–35.

Schoenebeck, J.J., Keegan, B.R., and Yelon, D. (2007). Vessel and Blood Specification

Override Cardiac Potential in Anterior Mesoderm. Developmental Cell *13*, 254–267.

Scott, I.C., Masri, B., D'Amico, L.A., Jin, S.-W., Jungblut, B., Wehman, A.M., Baier, H.,

Audigier, Y., and Stainier, D.Y.R. (2007). The G Protein-Coupled Receptor Agtrl1b

Regulates Early Development of Myocardial Progenitors. Developmental Cell *12*,

403–413.

Sedmera, D., Reckova, M., deAlmeida, A., Sedmerova, M., Biermann, M., Volejnik, J.,

Sarre, A., Raddatz, E., McCarthy, R.A., Gourdie, R.G., et al. (2003). Functional and

morphological evidence for a ventricular conduction system in zebrafish and Xenopus

hearts. Am J Physiol Heart Circ Physiol *284*, H1152–1160.

Sedmera, D., Reckova, M., Bigelow, M.R., Dealmeida, A., Stanley, C.P., Mikawa, T.,

Gourdie, R.G., and Thompson, R.P. (2004). Developmental transitions in electrical

activation patterns in chick embryonic heart. The Anatomical Record Part A:

Discoveries in Molecular, Cellular, and Evolutionary Biology *280*, 1001–1009.

Sehnert, A.J., Huq, A., Weinstein, B.M., Walker, C., Fishman, M., and Stainier, D.Y.R.

(2002). Cardiac troponin T is essential in sarcomere assembly and cardiac

contractility. Nat Genet *31*, 106–110.

Smith, K.A., Chocron, S., Hardt, S. von der, Pater, E. de, Alex, Soufan, er, Bussmann, J.,

Schulte-Merker, S., Hammerschmidt, M., and Bakkers, J. (2008). Rotation and

Asymmetric Development of the Zebrafish Heart Requires Directed Migration of

Cardiac Progenitor Cells. Developmental Cell *14*, 287–297.

Smith, K.A., Joziasse, I.C., Chocron, S., van Dinther, M., Guryev, V., Verhoeven, M.C.,

Rehmann, H., van der Smagt, J.J., Doevendans, P.A., Cuppen, E., et al. (2009).

Dominant-negative ALK2 allele associates with congenital heart defects. Circulation *119*, 3062–3069.

Smith, K.A., Lagendijk, A.K., Courtney, A.D., Chen, H., Paterson, S., Hogan, B.M., Wicking, C., and Bakkers, J. (2011). Transmembrane protein 2 (Tmem2) is required to regionally restrict atrioventricular canal boundary and endocardial cushion development. Development *138*, 4193 –4198.

Sorrell, M.R.J., and Waxman, J.S. (2011). Restraint of Fgf8 signaling by retinoic acid signaling is required for proper heart and forelimb formation. Dev. Biol. *358*, 44–55.

Srivastava, D. (2006). Making or breaking the heart: from lineage determination to morphogenesis. Cell *126*, 1037–1048.

Stainier, D.Y., and Fishman, M.C. (1992). Patterning the zebrafish heart tube: acquisition of anteroposterior polarity. Dev. Biol *153*, 91–101.

Stainier, D., Fouquet, B., Chen, J., Warren, K., Weinstein, B., Meiler, S., Mohideen, M., Neuhauss, S., Solnica-Krezel, L., Schier, A., et al. (1996). Mutations affecting the formation and function of the cardiovascular system in the zebrafish embryo. Development *123*, 285–292.

Stainier, D.Y., Lee, R.K., and Fishman, M.C. (1993). Cardiovascular development in the zebrafish. I. Myocardial fate map and heart tube formation. Development *119*, 31–40.

Stainier, D.Y., Weinstein, B.M., Detrich, H.W., Zon, L.I., and Fishman, M.C. (1995). Cloche, an early acting zebrafish gene, is required by both the endothelial and hematopoietic lineages. Development *121*, 3141–3150.

Steinbicker, A.U., Sachidanandan, C., Vonner, A.J., Yusuf, R.Z., Deng, D.Y., Lai, C.S., Rauwerdink, K.M., Winn, J.C., Saez, B., Cook, C.M., et al. (2011). Inhibition of bone

morphogenetic protein signaling attenuates anemia associated with inflammation. Blood *117*, 4915–4923.

Takeuchi, J.K., Lou, X., Alexander, J.M., Sugizaki, H., Delgado-Olguin, P., Holloway, A.K., Mori, A.D., Wylie, J.N., Munson, C., Zhu, Y., et al. (2011). Chromatin remodelling complex dosage modulates transcription factor function in heart development. Nat Commun *2*, 187.

Targoff, K.L., Schell, T., and Yelon, D. (2008). Nkx genes regulate heart tube extension and exert differential effects on ventricular and atrial cell number. Dev. Biol *322*, 314–321.

Thomas, N.A., Koudijs, M., van Eeden, F.J.M., Joyner, A.L., and Yelon, D. (2008). Hedgehog signaling plays a cell-autonomous role in maximizing cardiac developmental potential. Development *135*, 3789–3799.

Timmerman, L.A., Grego-Bessa, J., Raya, A., Bertrán, E., Pérez-Pomares, J.M., Díez, J., Aranda, S., Palomo, S., McCormick, F., Izpisúa-Belmonte, J.C., et al. (2004). Notch promotes epithelial-mesenchymal transition during cardiac development and oncogenic transformation. Genes Dev *18*, 99–115.

Totong, R., Schell, T., Lescroart, F., Ryckebüsch, L., Lin, Y.-F., Zygmunt, T., Herwig, L., Krudewig, A., Gershoony, D., Belting, H.-G., et al. (2011). The novel transmembrane protein Tmem2 is essential for coordination of myocardial and endocardial morphogenesis. Development *138*, 4199 –4205.

Trinh, L.A., and Stainier, D.Y.. (2004). Fibronectin Regulates Epithelial Organization during Myocardial Migration in Zebrafish. Developmental Cell *6*, 371–382.

Trinh, L.A., Yelon, D., and Stainier, D.Y.R. (2005). Hand2 Regulates Epithelial Formation during Myocardial Differentiation. Current Biology *15*, 441–446.

Tu, C.-T., Yang, T.-C., and Tsai, H.-J. (2009). Nkx2.7 and Nkx2.5 function redundantly and are required for cardiac morphogenesis of zebrafish embryos. PLoS ONE *4*, e4249.

Ueno, S., Weidinger, G., Osugi, T., Kohn, A.D., Golob, J.L., Pabon, L., Reinecke, H., Moon, R.T., and Murry, C.E. (2007). Biphasic role for Wnt/beta-catenin signaling in cardiac specification in zebrafish and embryonic stem cells. Proc. Natl. Acad. Sci. U.S.A *104*, 9685–9690.

Vermot, J., Forouhar, A.S., Liebling, M., Wu, D., Plummer, D., Gharib, M., and Fraser, S.E. (2009). Reversing blood flows act through klf2a to ensure normal valvulogenesis in the developing heart. PLoS Biol *7*, e1000246.

Vogel, B., Meder, B., Just, S., Laufer, C., Berger, I., Weber, S., Katus, H.A., and Rottbauer, W. (2009). In-vivo characterization of human dilated cardiomyopathy genes in zebrafish. Biochemical and Biophysical Research Communications *390*, 516–522.

Voss, K., Stahl, S., Hogan, B.M., Reinders, J., Schleider, E., Schulte-Merker, S., and Felbor, U. (2009). Functional analyses of human and zebrafish 18-amino acid in-frame deletion pave the way for domain mapping of the cerebral cavernous malformation 3 protein. Human Mutation *30*, 1003–1011.

Walsh, E.C., and Stainier, D.Y. (2001). UDP-glucose dehydrogenase required for cardiac valve formation in zebrafish. Science *293*, 1670–1673.

Wang, J., Panáková, D., Kikuchi, K., Holdway, J.E., Gemberling, M., Burris, J.S., Singh, S.P., Dickson, A.L., Lin, Y.-F., Sabeh, M.K., et al. (2011). The regenerative capacity of zebrafish reverses cardiac failure caused by genetic cardiomyocyte depletion. Development *138*, 3421–3430.

Waxman, J.S., Keegan, B.R., Roberts, R.W., Poss, K.D., and Yelon, D. (2008). Hoxb5b acts downstream of retinoic acid signaling in the forelimb field to restrict heart field potential in zebrafish. Dev. Cell *15*, 923–934.

Wei, X., and Malicki, J. (2002). nagie oko, encoding a MAGUK-family protein, is essential for cellular patterning of the retina. Nature Genetics *31*, 150–157.

Xu, X., Meiler, S.E., Zhong, T.P., Mohideen, M., Crossley, D.A., Burggren, W.W., and Fishman, M.C. (2002). Cardiomyopathy in zebrafish due to mutation in an alternatively spliced exon of titin. Nat Genet *30*, 205–209.

Yelon, D., Horne, S.A., and Stainier, D.Y. (1999). Restricted expression of cardiac myosin genes reveals regulated aspects of heart tube assembly in zebrafish. Dev. Biol *214*, 23–37.

Yelon, D., Ticho, B., Halpern, M.E., Ruvinsky, I., Ho, R.K., Silver, L.M., and Stainier, D.Y. (2000). The bHLH transcription factor hand2 plays parallel roles in zebrafish heart and pectoral fin development. Development *127*, 2573–2582.

Yoruk, B., Gillers, B.S., Chi, N.C., and Scott, I.C. (2011). Ccm3 functions in a manner distinct from Ccm1 and Ccm2 in a zebrafish model of CCM vascular disease. Developmental Biology.

Zeng, X.-X.I., Wilm, T.P., Sepich, D.S., and Solnica-Krezel, L. (2007). Apelin and its receptor control heart field formation during zebrafish gastrulation. Dev. Cell *12*, 391–402.

Zhang, P.-C., Llach, A., Sheng, X.Y., Hove-Madsen, L., and Tibbits, G.F. (2010). Calcium handling in zebrafish ventricular myocytes. Am J Physiol Regul Integr Comp Physiol.

Zheng, X., Xu, C., Di Lorenzo, A., Kleaveland, B., Zou, Z., Seiler, C., Chen, M., Cheng, L., Xiao, J., He, J., et al. (2010). CCM3 signaling through sterile 20–like kinases plays an essential role during zebrafish cardiovascular development and cerebral cavernous malformations. Journal of Clinical Investigation *120*, 2795–2804.

Zhou, Y., Cashman, T.J., Nevis, K.R., Obregon, P., Carney, S.A., Liu, Y., Gu, A., Mosimann, C., Sondalle, S., Peterson, R.E., et al. (2011). Latent TGF-[bgr] binding protein 3 identifies a second heart field in zebrafish. Nature *474*, 645–648.

CHAPTER 2: High Resolution Imaging of Cardiomyocyte Behavior Reveals Two

Separable Steps in Ventricular Trabeculation

This work was performed by:

Staudt, D.W., Liu, J.L., Thorn, K.S., Stuurman, N., Liebling, M., Stainier, D.Y.

<u>Abstract</u>

Over the course of development, the vertebrate heart undergoes a series of complex morphogenetic processes that transforms it from a simple myocardial epithelium to a complex 3D structure required for its function. One of these processes leads to the formation of trabeculae to optimize the internal structure of the ventricle for efficient conduction and contraction. However, despite the important role of trabeculae in the development and physiology of the heart, little is known about their mechanism of formation. Using 3D time-lapse imaging of beating zebrafish hearts, we determined that the initiation of cardiac trabeculation can be divided into two processes. Before any cell bodies have entered the trabeculae, cardiomyocytes extend processes that invade luminally along neighboring cell-cell junctions. These processes can interact within the trabecular layer to form new cell-cell contacts. Subsequently, myocytes constrict their abluminal surface, moving their cell bodies into the trabecular layer while elaborating more processes. We further examined trabecular mutants and found that while both *erbb2* and *tnnt2a* deficient animals do form processes, only the *erbb2* deficient ones maintain them, thereby providing novel insight into the cause of their trabecular defects. By detailed 4D imaging of beating hearts, we have identified novel cell biological mechanisms underlying cardiac trabeculation.

Introduction

The adult heart is composed of a number of sub-structures optimized for pumping blood. In order to create this efficient pump, the heart undergoes a number of morphogenetic changes during development, all while continuing to beat and maintain blood flow to the developing animal. One early morphogenetic process is the development of the ventricular trabeculae. Ventricular trabeculae are ridge-like myocardial structures within the walls of the ventricles that form a complex network early in development (Liu et al., 2010; Peshkovsky et al., 2011; Sedmera et al., 2000; Stankunas et al., 2008; Staudt and Stainier, 2012). Trabeculae are crucial for heart function, as mutations that abrogate trabecular formation are embryonic lethal (Gassmann et al., 1995; Lee et al., 1995; Liu et al., 2010; Meyer and Birchmeier, 1995; Morris et al., 1999; Suri, 1996; Tidcombe et al., 2003), while human patients with hypertrabeculation exhibit a form of heart failure (Jenni et al., 1999). The trabeculae serve to increase myocardial mass before the formation of coronary vessels and as such have been shown to contribute to ventricular contractility; they are also necessary for the formation of the conduction system (Liu et al., 2010; Sedmera et al., 2003). While studies in mouse have revealed the genetic basis of cardiac trabeculation, how cardiomyocytes form these important structures while continuously contracting remains relatively unknown. Most challenging for these *in vivo* studies is the fact that the heart is constantly moving, and so obtaining high-resolution images over time required novel image processing techniques. The zebrafish is an organism amenable to long-term imaging of the developing heart (Beis and Stainier, 2006), thereby providing

an ideal model system in which to study cardiac trabeculation with cellular resolution in real time.

A number of factors are known to play a role in trabeculation. Several signaling pathways, including the Angiopoietin/Tie2 pathway (Suri, 1996), Semaphorin/Plexin pathway (Toyofuku et al., 2004a, 2004b), and the Neuregulin/ErbB2/ErbB4 pathway (Gassmann et al., 1995; Lee et al., 1995; Liu et al., 2010; Morris et al., 1999; Tidcombe et al., 2003) have been implicated in the process. Among these regulators of trabeculation, the ErbB2 pathway has been implicated to be important cell-autonomously in cardiomyocytes. (Liu et al., 2010; Morris et al., 1999; Tidcombe et al., 2003). Additionally, mechanical factors such as blood flow and/or cardiac contractility contribute to trabeculation. Zebrafish embryos with completely disrupted cardiac contractility due to disrupted sarcomeres fail to form trabeculae (Chi et al., 2008). Meanwhile, disrupting blood flow through the ventricle by disrupting atrial contractility leads to impaired trabeculation (Peshkovsky et al., 2011). Similarly, disrupting flow into the left ventricle of embryonic chick hearts by left atrial ligation decreases left ventricular trabecular volume (Sedmera et al., 1999). It is currently unknown how ErbB2 signaling or mechanical forces regulate trabeculation.

Most of what we know about trabeculation comes from endpoint analyses of mutants, which can reveal whether or not embryos develop trabeculae. However, no studies have addressed how cardiomyocytes form trabeculae at the cellular level. Previous studies have reported the location of cardiomyocytes in the trabecular layer starting at 55 hpf

(Chi et al., 2008; Liu et al., 2010; Peshkovsky et al., 2011). Additionally, although trabecular cardiomyocytes are clonally related to myocytes in the outer, compact layer (Liu et al., 2010; Meilhac et al., 2003, 2004a, 2004b; Mikawa et al., 1992), our recent cell lineage tracing data indicate that trabeculation occurs via a process of delamination, rather than asymmetric division (Liu et al., 2010). However, how cardiomyocytes delaminate from the compact layer remains unclear. Here, using a combination of clonal analysis and live cell imaging of beating hearts, we show that trabeculae are formed by a two-step delamination process. Cells first extend fine processes over their neighbors, and then gradually constrict their abluminal surfaces to move their cell bodies into the trabecular layer. Further, we show that mutations disrupt ventricular trabeculation at different steps in the process. In hearts that do not contract, cardiomyocytes extend short-lived processes that do not result in trabeculation, while *erbb2* mutant cardiomyocytes form processes, but their hearts fail to fully trabeculate.

Materials and Methods

Zebrafish and Morpholino Injections

Embryonic and adult zebrafish were maintained according to standard laboratory conditions (Westerfield, 2000) and IACUC license. We used the following transgenic and mutant lines: *Tg(myl7:ras-eGFP)^{s883}* (D'Amico et al., 2007), *erbb2^{st61}* (Liu et al., 2010; Lyons et al., 2005). To make *tnnt2a* morphants, 1.2 ng of *tnnt2a* morpholino (sequence 5-CATGTTTGCTCTGATCTGACACGCA-3) was injected in 1nL total volume into the yolk of single-cell stage embryos.

Mosaic Analysis

DNA constructs based on the miniTol2 construct (Balciunas et al., 2006), harboring a *myl7* promoter (Huang et al., 2003) upstream of TagRFP-T (Shaner et al., 2008), TagBFP (Subach et al., 2008), IRFP (Filonov et al., 2011) were constructed using the Cold Fusion cloning kit (SBI cat# MC100B-1). For single-color mosaic analysis, 1nL of a mixture of *myl7:TagRFP-T* plasmid at a concentration of 5-10 ng/μL and Tol2 RNA at a concentration of 25 ng/μL was injected into *Tg(myl7:ras-eGFP)^{s883}* embryos. For multi-colored analysis, three different DNA constructs at an individual concentration between 5-10 ng/μL were co-injected with 25 ng/μL Tol2 RNA. Embryos were screened for fluorescence and normal morphology at 55 hpf before being selected for imaging.

Imaging

Live Imaging of Heart Development

55-60 hpf embryos were mounted in 1% low-melting agarose supplemented with 0.015% (w/v) tricaine on glass bottomed dishes (MatTek cat#P35G-0-20-C). Movies of live zebrafish hearts were acquired using a Nikon Ti-E inverted microscope with a Yokagawa CSU-22 spinning disk head using either a 20X/0.75 air objective (Nikon), or a 40X/1.15 water immersion objective. For movies taken with the 20X lens, a 1.5X multiplier lens was added to the light path. Movies were recorded using an Evolve EMCCD camera (Photometrics). To achieve the acquisition rate of 60 fps, the camera was binned 2x2, yielding a calculated pixel resolution of 0.61 (20X objective/1.5X multiplier) or 0.455 (40X/1.15 objective) microns/pixel. We used the following laser lines: 405 nm (100 mW Coherent Cube Diode), 491 nm (100 mW Cobolt Calypso DPSS), 561 nm (100 mW Coherent Sapphire DPSS) and 640 nm (100 mW Coherent Cube Diode). Emission filters used were TagBFP (460±25 nm), GFP (525±25 nm), TagRFP-T (610±30 nm) and IRFP (700±38 nm). To reduce laser exposure and motion blur, lasers were pulsed for 2-5 ms/frame using an Acousto-Optic Tunable Filter (Neos) gated on the camera trigger. Multiple embryos were imaged using a motorized stage (Prior). The microscope was controlled using μManager (Edelstein et al., 2010), and Z translation of the heart was corrected live using a custom script. To increase the rate of development, the imaging environment was heated to 31°C using a thermally-controlled enclosure (In Vivo

Scientific). Generally, movies of 90 frames each were collected at 50 z positions 1 μm apart for each developmental time point. Developmental time points were collected every 15-30 minutes for 12-19 hours, depending on the experiment. The assembled datasets were then temporally aligned using previously published Matlab software (Liebling et al., 2005, 2006; Ohn et al., 2009), and the aligned files were viewed and analyzed in Fiji (Schindelin et al., 2012).

Quantitation of Processes

Cells were mosaically labeled as described above in WT, *erbb2* mutants, or *tnnt2a* morphants, and imaged live for 12 hours. Z projections of the resulting movies were generated and subsequently blinded. Readily separable cells were scored for presence or absence of processes. Each process was scored as stable throughout the whole 12 hour movie, or unstable if it collapsed. Data from cells and processes was summed individually for WT, *erbb2* mutants, and *tnnt2a* morphants, and then compared pairwise with a chi-square test.

Periodic Stopped Heart Imaging

Embryos were mounted in agarose as above, then anaesthetized to the point of cardioplegia with tricaine. A z-stack was then acquired on the microscope described above using a 40X/1.15 water immersion objective (Nikon). In this case, the camera was not binned, yielding a calculated pixel resolution of 227.5 nm/pixel. The anesthetic was

then washed out, and embryos were monitored until the heart resumed normal beating. To increase the rate of development, embryos were then incubated at 31°C for 3 hours, at which time anesthetic was reapplied to induce cardioplegia, and the process was repeated. Each dataset consisted of four separate time points. Cardiac health of the embryos was visually assessed after imaging to ensure normal function.

Imaging of Stopped Hearts

Embryos were mounted in 1% agarose containing 0.2% (w/v) Tricaine. Embryos were then imaged using a Zeiss confocal microscope.

Image Processing

Most 3D datasets were rendered in Fiji using the Z projection tool or the 3D Viewer plugin. When noted, surface renderings were created in Imaris (Bitplane). When noticeable drift in X, Y, or Z dimensions was noticed, it was corrected using the Correct 3D Drift plugin in Fiji. Occasionally, XY rotation of the entire heart was noted after Z projections were created. In some instances, the StackReg plugin was used on the time lapse of Z projections to allow for better analysis of individual cells.

Results

Cardiomyocytes extend long processes before the first trabeculae appear

In seeking to understand how cardiomyocytes first form trabeculation, we examined *Tg(myl7:ras-GFP)* fish, which express a membrane-bound GFP in cardiomyocytes, at the start of trabeculation between 50-60 hpf. We focused on the outer curvature (OC, Fig. 1A), and looked for the first trabeculation, which we define as cardiomyocytes located on the luminal side of the myocardial epithelium. Interestingly, we observed small myocardial structures on the luminal side of the epithelium even before the first trabeculae appeared (Fig. 1B, B'). In order to more closely examine these structures, we created embryos mosaically expressing a random combination of fluorescent proteins in the cytoplasm of *Tg(myl7:ras-GFP)* cardiomyocytes by Tol2-mediated transgenesis (Kawakami, 2007). Plasmids were generated where the myocardial *myl7* promoter drives expression of either the red TagRFP-T (Shaner et al., 2008), blue TagBFP (Subach et al., 2008), or near-infrared IRFP (Filonov et al., 2011). Co-injection of these three plasmids generated numerous, multi-colored cells that could be uniquely tracked. The cytoplasmic fluorescent proteins allowed us to unambiguously identify cells throughout the 3D structure of the heart, while the membrane GFP allowed us to relate marked cells to their unmarked neighbors, as well as the overall structure of the myocardium. This approach allowed us to identify these invading membrane-bound structures as processes from cells that remained in contact with the abluminal surface of the myocardial epithelium (Fig.

1C,D). Interestingly, these processes tended to invade above cell-cell junctions of neighboring cardiomyocytes (Fig. 1B,C).

In order to study the dynamics of these processes, we employed a combination of high-speed spinning disk confocal microscopy and post-acquisition temporal alignment to acquire 3D time-lapse movies of the beating hearts (Liebling et al., 2005; Ohn et al., 2009) (Fig. 2A-D, Supplemental Movie S1). In brief, we used a spinning disk microscope run by a custom script to obtain confocal movies of beating zebrafish hearts at sequential z levels. The script allowed for repeated imaging of multiple positions corrected for z-drift. Z-stacks of movies were obtained at multiple developmental time points between 55 and 76 hpf. These movies were triggered without regard to the stage of the cardiac contraction cycle, and so were unsynchronized (Fig. 2B). Using previously published image alignment algorithms (Liebling et al., 2005, 2006; Ohn et al., 2009), these stacks of movies were re-synchronized post-acquisition, yielding 3D movies of hearts from regularly spaced intervals within the cardiac cycle, allowing us to focus on the heart at ventricular diastole, when the ventricle is most expanded (Fig. 2C-D). We could then examine cellular behaviors over the course of development without the complicating motion of normal contraction. Live imaging of *Tg(myl7:ras-GFP)* embryos revealed that a large proportion of cells extended processes (Supplemental Movie S2). Live imaging of mosaically marked cardiomyocytes revealed that approximately 81% of cells extended processes (Fig. 5F, n=16 cells from 3 embryos). These processes extended slowly, taking 8-10 hours to reach their full length of 10-20 microns (Fig. 2E,

Supplemental movie S3). Occasionally, processes from different cells extended towards one another and formed cell-cell junctions (Fig. 2F, Supplemental Movie S4).

Cardiomyocytes constrict their abluminal surfaces while extending processes to enter the trabecular layer

These data suggest that cells start to extend processes before cardiomyocytes begin entering the trabeculae, but it is not clear how cells actually translocate into the forming trabecular layer. To address this question, we obtained high-resolution time-lapse images using a different technique to image developing hearts. In brief, *Tg(myl7:ras-GFP)* fish mosaically labeled as above were anaesthetized to the point that their heart stopped beating. After acquiring Z-stacks of the stopped ventricles, we washed out the anesthetic, at which time the hearts began to beat again. Hearts were then allowed to develop 3-4 hours before being stopped again. The high-resolution images obtained allowed us to unambiguously identify individual cells as they entered the trabecular layer. We found that cells progressively constricted their abluminal surfaces, eventually exiting the compact layer (Fig. 3C-E). Interestingly, we observed cells extending new processes as they constricted their abluminal surface (Fig. 3C-K). The total volume of the cell remained relatively constant, suggesting that cells redistributed their abluminal volume into the new expanding projection (Fig. 3F-K).

To examine this process further, we returned to imaging beating hearts. As mentioned above, cells entering the trabecular layer concurrently extended processes into the

trabecular layer while constricting their abluminal surface (green cell in Fig. 4A,B; arrow in Fig. 4B; Supplemental Movie S5). Notably, although we could identify occasional cell divisions within our time-lapse movies (Supplemental Fig. S1; Supplemental Movie S6), all cells observed entering the trabeculae did so without undergoing cell division. Interestingly, in several cases, cells neighboring trabeculating cells exhibited dramatic cell shape changes, allowing them to fill the space vacated by the exiting cell (purple cell in Fig. 4A,B; Supplemental Movie S5).

Trabecular Mutants Exhibit Different Modes of Trabecular Failure

A number of mutants have been identified that lead to defects in trabeculation (Gassmann et al., 1995; Jones et al., 2003; Kramer et al., 1996; Lee et al., 1995; Liu et al., 2010; Meyer and Birchmeier, 1995; Peshkovsky et al., 2011; Suri, 1996). However, the affected cellular behaviors underlying trabecular defects remain undefined. To determine how changes in cell behaviors lead to defects in trabeculation, we examined two models of trabecular failure in zebrafish: hearts with defective contractility, and *erbb2* mutant hearts. We began by examining embryos with impaired contractility. Contractility and/or blood flow play an important role in cardiac development (Bartman et al., 2004; Berdougo et al., 2003; Chi et al., 2008, 2010; Peshkovsky et al., 2011; Vermot et al., 2009), and specifically have been implicated in trabecular development (Chi et al., 2008; Peshkovsky et al., 2011). Notably, *tnnt2a* mutant embryos, which fail to form sarcomeres and thus fail to contract (Sehnert et al., 2002), do not form trabeculae (Chi et al., 2008). Other contractile mutants, such as *weak atrium* (*wea*), which has disrupted

atrial contraction, and thus reduced blood flow through the ventricle, also have defects in trabeculation (Peshkovsky et al., 2011). To study the cellular mechanisms underlying trabecular failure when contractility is disrupted, we examined cell morphology and behavior in embryos injected with *tnnt2a* morpholino (MO), which phenocopy the *tnnt2a* mutant (Sehnert et al., 2002). Despite the lack of trabeculation in MO-injected (morphant) animals (Fig. 5B), live imaging of mosaically marked cells revealed that a similar proportion of cells sent out processes over the course of 12 hours of imaging (8/8 cells in 3 *tnnt2a* morphant embryos vs. 13/16 cells in 4 wild-type embryos, Fig. 5F). Notably, these processes were unstable, collapsing over the course of several hours (Fig. 5E,G). While only a few processes collapsed over the time period examined in wild-types (3/13 processes examined), the majority of processes were unstable in *tnnt2a* morphants (9/10 processes examined) (Fig. 5H). Thus, *tnnt2a* morphants appear to have an early defect in the stability of cardiomyocyte processes.

To determine whether or not unstable processes are a common underpinning to trabecular failure, we examined an unrelated model of trabecular failure, the *erbb2* mutant. We and others have previously shown that the ErbB2 receptor tyrosine kinase is necessary for trabecular development in both mouse and zebrafish (Gassmann et al., 1995; Jones et al., 2003; Kramer et al., 1996; Lai et al., 2010; Lee et al., 1995; Liu et al., 2010; Meyer and Birchmeier, 1995; Peshkovsky et al., 2011). We have also shown that *erbb2* cardiomyocytes exhibit a cell-autonomous defect in trabeculation (Liu et al., 2010). However, the cellular mechanisms that cause this defect remain unknown. To determine whether there was a defect in initial process formation, we first looked at high-resolution

confocal images of *erbb2* mutant embryos. Though trabeculation was impaired,

processes within the trabeculae could still be detected at 70 hpf (Fig. 5B). To further

analyze this defect, we performed live-imaging of mosaically marked cells within *erbb2*

mutant and WT embryos. In contrast to their behavior in *tnnt2a* morphants, *erbb2*

cardiomyocytes extended processes at a similar rate to wild-type (15/27 cells from 6

erbb2 mutant embryos vs. 13/16 cells in 4 wild-type embryos, p=0.087, Fig. 5F), and

showed similar stability of processes (2/20 processes retracted in *erbb2* mutant hearts vs.

3/13 in WT, Fig. 5G). Despite this similarity, trabeculae failed to elaborate by 100 hpf in

erbb2 mutants (Supplemental Fig. S2). Thus, *erbb2* mutant hearts have a later defect in

trabeculation, one that interferes with the process after the extension of cellular processes

into the luminal side of neighboring cardiomyocytes.

Discussion

In this study, we combined clonal analysis with powerful live imaging techniques to identify myocardial cell behaviors leading to trabeculation. We identified a previously unknown capability for actively contracting cardiomyocytes to extend long processes invading into the trabecular layer, even before cells translocate to form the trabeculae. Further, our data show that cells enter the trabecular layer through abluminal constriction, extending processes as they enter. While cells constrict their abluminal surface and enter the trabecular layer, neighboring cells actively move into the space left behind to maintain a separate compact layer. Finally, we found that non-contractile hearts fail to stabilize trabecular processes, which likely contributes to their failure to form trabeculae, while *erbb2* mutants fail to form trabeculae despite forming stable processes.

Previous studies in zebrafish have shown that cardiomyocytes change their shape depending on their location within the heart (Auman et al., 2007; Chi et al., 2010; Lin et al., 2012). However, given the necessity to maintain the integrity of the myocardial epithelium, it has been generally assumed that it was a very stable and static structure. Thus, it was surprising to find such a dynamic behavior of these cells. The combination of live imaging, clonal analysis, and image processing allowed us to reveal this fascinating process for the first time. The identification of myocardial processes that invade luminally to the compact layer before cells translocate into the trabeculae raises a number of interesting hypotheses about their function. How trabecular and compact layer cells are specified remains unknown. The early extension of processes could allow

cardiomyocytes to sample their surrounding environment, seeking limiting supplies of fate-determining morphogens. In addition, these processes could provide the cell extra space to redistribute its volume once it translocates into the trabecular layer. Interestingly, we noted that cardiomyocyte processes preferentially extend over cell-cell junctions of the compact layer. This arrangement could provide a mechanism for strengthening weak attachments or aligning cytoskeletons amongst multiple cells. Further studies looking at the distribution of growth signals known to be important for trabeculation, as well as further studies to identify the molecular underpinnings for cardiomyocyte processes, will shed light on their role in the maturation of the heart as a contractile machine.

The ventricular trabeculae form an intricate, interconnected network in zebrafish (Chi et al., 2008; Peshkovsky et al., 2011; Sedmera et al., 2003), as well as in chick, mouse and human (Sedmera et al., 2000). How cells interact to form this network is poorly understood. In theory, the trabecular network organization could form in two broad ways. Trabecular ridges could be specified in the compact layer, and multiple neighboring cells could translocate to the trabecular layer to form an already-assembled ridge. Alternatively, trabecular cells could be specified intermittently throughout the compact layer, and form new connections with other trabecular cells to create the trabecular network. Our live imaging identified instances where processes from two non-neighboring cardiomyocytes came together to form a new cell-cell junction between the two cells. Though the role of these new connections remains to be explored, this

observation provides a clue that the trabecular network could form through the assembly of new cell-cell connections within the forming trabecular layer.

Our previous work had suggested that trabeculation involves cardiomyocyte migration, rather than oriented cell division (Liu et al., 2010). However, the exact mechanism of migration remained unknown. Our live imaging of cardiomyocyte delamination reveals that cardiomyocytes enter the trabecular layer via constriction of their abluminal surface, coupled to a redistribution of their cell volume into processes in the trabecular layer. Importantly, cell divisions were never seen accompanying this migration, confirming that delamination is independent of cardiomyocyte proliferation. The abluminal constriction of cardiomyocytes resembles the process of apical constriction, which is involved in a number of important morphogenic events (Sawyer et al., 2010). Indeed, if the apical domain of the cardiomyocytes remains unchanged from the 20 somite stage, where it faces away from the endocardium (Trinh, Le A. and Stainier, 2004; Trinh, Le A. et al., 2005), this process may represent apical constriction.

Delamination following apical constriction has been noted in a number of different systems. Generally, there are two non-exclusive mechanisms that can drive cellular constriction and delamination. First, delaminating cells can constrict their own apical surfaces through actin rearrangements and myosin-mediated contraction as is seen in *c. elegans* gastrulation (Lee et al., 2006). Second, their neighbors could coordinate to form an actin ring to extrude the delaminating cell out of the compact layer, as is seen in crowding-induced delamination from the fly notum (Marinari et al., 2012). The

combination of these two mechanisms has also been observed in the extrusion of apoptotic cells from epithelial layers (Gu et al., 2011; Rosenblatt et al., 2001; Slattum et al., 2009). Our study cannot distinguish between these three possibilities. Our previous study has shown that trabeculation can be inhibited cell-autonomously (Liu et al., 2010), though this cannot rule out a mechanism in which delaminating cells signal to their neighbors to form a contractile ring. Further studies are needed to clarify the precise roles of future trabecular cells and their neighbors during delamination.

In conclusion, our study demonstrates the power of combining clonal analysis and live imaging to probe cardiac development in the zebrafish. Expanding this approach will provide a unique tool to address other *in vivo* cell biological questions in the development of the heart and other fast moving tissues.

Acknowledgements:

Contributions:

D.W.S. designed and performed the experiments, analyzed data, and wrote the paper. J.L. designed experiments, analyzed data, and wrote the paper. D.Y.S. designed experiments and wrote the paper. D.W.S., K.S.T. and N.S. set up the live microscopy platform. M.L. wrote the post-acquisition alignment program. All authors commented on the paper.
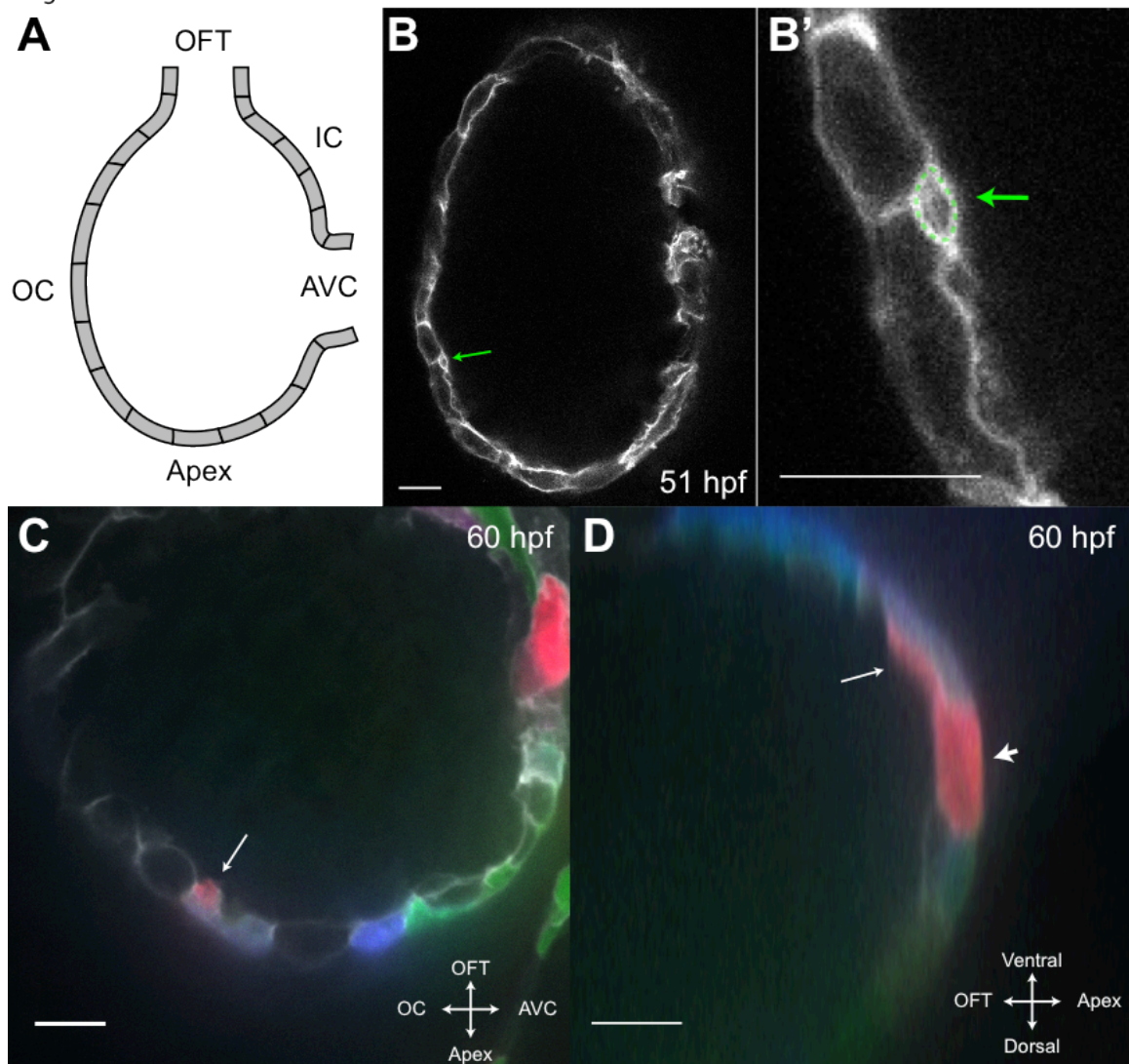
Figure 1

A — OFT, IC, OC, AVC, Apex

B — 51 hpf

B' —

C — 60 hpf — OC ↔ AVC, OFT ↕ Apex

D — 60 hpf — OFT ↔ Apex, Ventral ↕ Dorsal

Figure 1.

Figure 1. Cardiomyocytes extend cellular processes luminally while still in the compact

layer. (A) Cartoon showing the orientation of the myocardium in (B) and (C). (B)

Optical slice of 51 hpf *Tg(myl7:ras-GFP)* ventricle. Arrow points to a myocardial

cellular process extending above the myocardial epithelium. (B') Close-up of process

(outlined by green dotted line). (C) Optical slice of a 60 hpf *Tg(myl7:ras-GFP)* heart

with cells marked with multiple fluorescent proteins. Arrow points to a marked cellular

process (red), extending over another marked cell (purple). (D) Reslice of (C) showing

that this process extends from a cell still mostly contained within the compact layer.
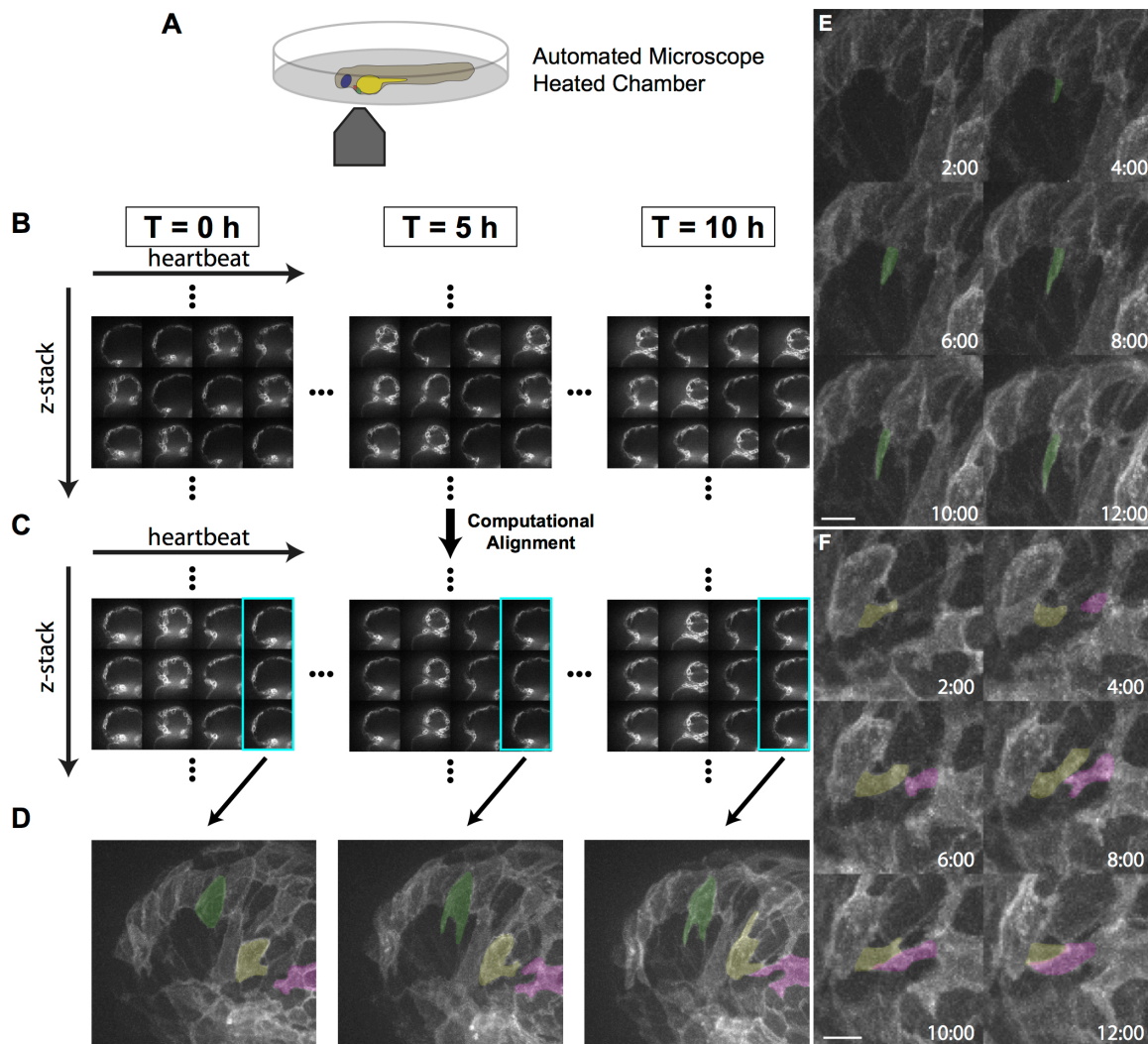
Scale bars, 10μm.

Figure 2

Figure 2.

Figure 2. Live imaging reveals the dynamics of cardiomyocyte processes. (A) 55-60 hpf zebrafish embryos were imaged in glass plates on an automated, inverted microscope equipped with a spinning disk. (B-D) Steps in the data processing pipeline. The 3 columns show datasets acquired from the same embryo at the indicated time points after the start of imaging. (B) Data are initially acquired as unsynchronized z-stacks of movies. Frames from 3 sequential z-slices are shown. Note that the rows (z-slices) are unsynchronized. (C) Frames from the same sequential z-slices are shown after post-acquisition alignment. Note that the movies are synchronized after the alignment. Turquoise box indicates the frame during ventricular relaxation that will be used for further comparison. (D) Maximum intensity z projections of the relaxed ventricle from the 3 developmental time points. Individual cells are pseudocolored in green, magenta, and yellow. Note the dramatic cell shape changes that can be observed after computational alignment. (E) Time lapse images of cellular process. Emerging process marked in green. (F) Time lapse images of two cells extending processes, highlighted in yellow and purple. The two processes form a cell-cell junction by 12 hours of imaging. Scale bars, 10μm.
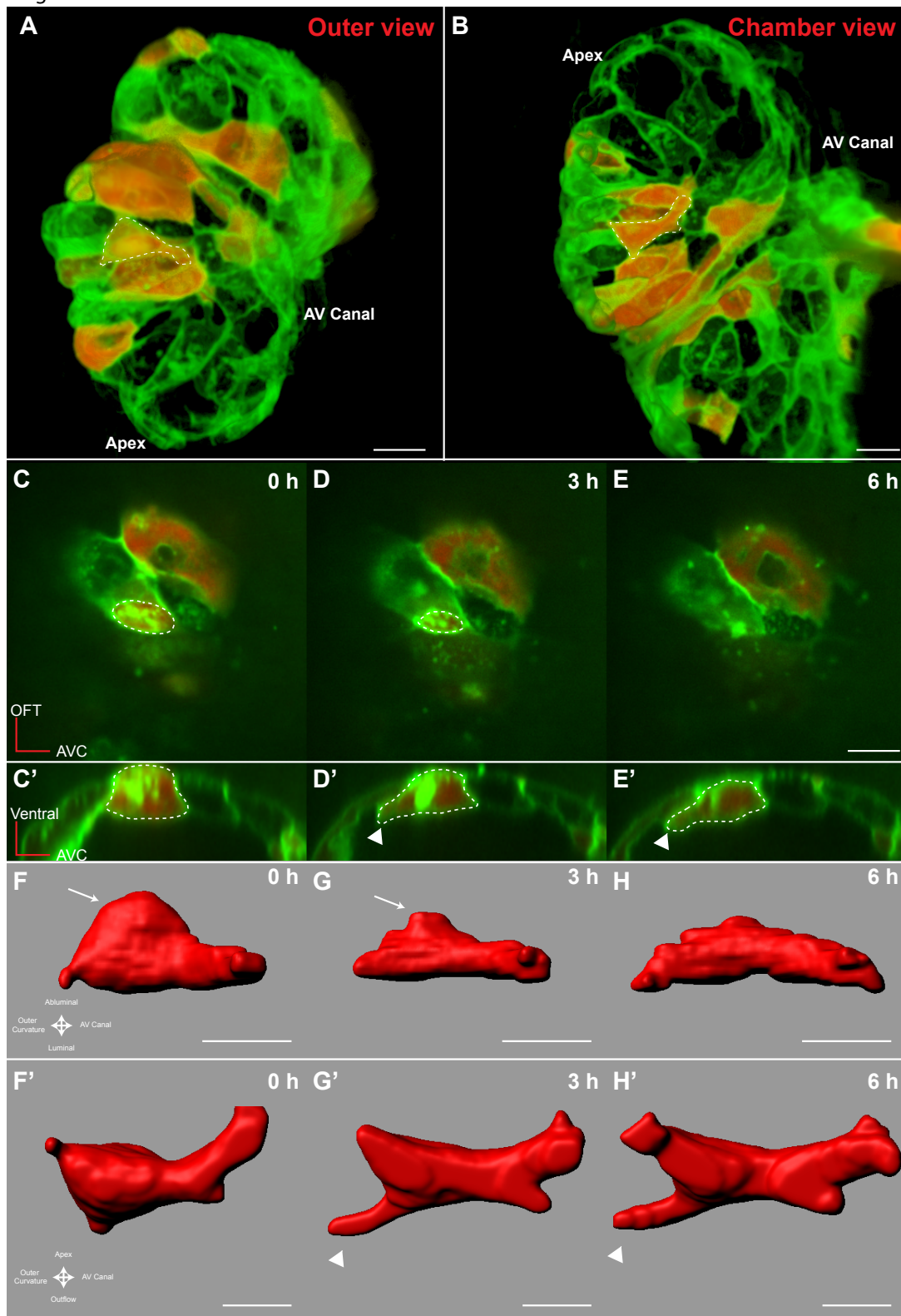
Figure 3

Figure 3.

Figure 3. Cardiomyocytes show evidence of abluminal constriction. (A) 3D exterior view of 72 hpf *Tg(myl7:ras-GFP)* heart with a subset of cardiomyocytes randomly labeled with RFP. Cell of interest is outlined in white. (B) Interior chamber view of the same heart. Cell of interest in outlined in white. Scale bars, 10 μm. (C-E) Time-lapse of single cell. A single XY plane is shown at (C) the start of imaging, (D) +3 hours of imaging, and (E) +6 hours of imaging. Orientation is as in (A). Dotted lines outline gradually constricting cell contact with the abluminal surface. In (E), the cell has lost contact with the abluminal surface, and thus can no longer be seen. (C'-E') Re-slice of the confocal stack showing the same cell rotated 90°. Cell is outlined. The cell can be seen extending a process (arrowhead) as it exits the compact layer. Scale bars, 10μm. (F-H) 3D volume rendering of the highlighted cell. Arrow points to contracting contact with abluminal surface. Arrowhead points to extending process. (F'-H') 90° rotation of (F-H) showing luminal view of the cell. Scale bars, 5μm.
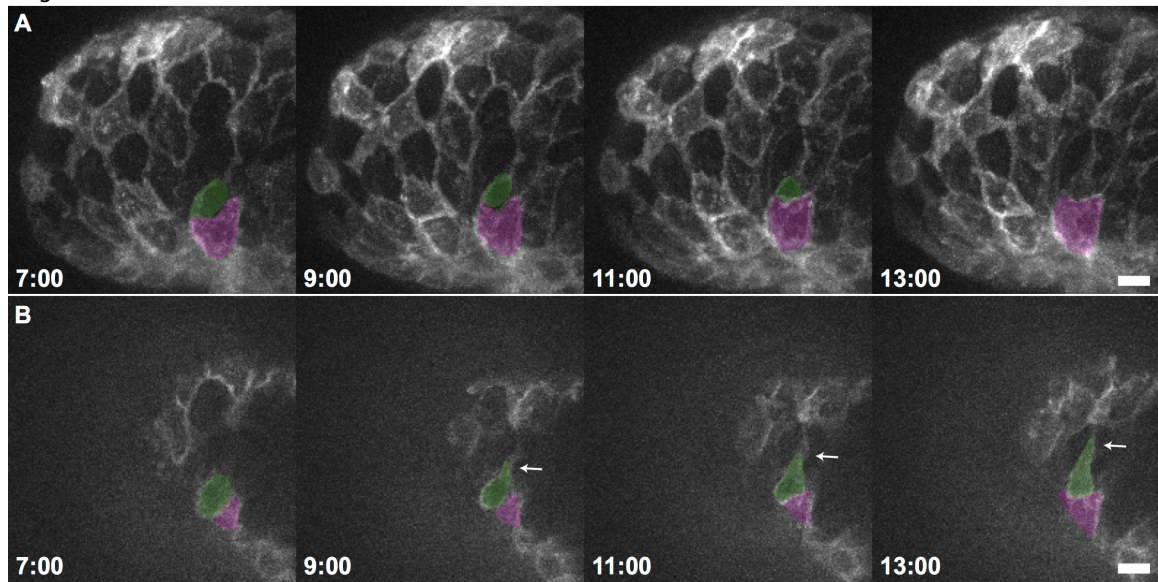
Figure 4

Figure 4.

Figure 4. Cardiomyocytes extend processes while constricting their abluminal surface.

(A) 3D projection of a *Tg(myl7:ras-GFP)* heart imaged starting at 59 hpf. Time from start of imaging is given in the lower left . The cell marked in green constricts its abluminal surface. This cell completely exits the compact layer by 13 hours of imaging. The cell marked in purple changes shape to take up the space vacated by the green cell. (B) Drift-corrected (see methods) optical slice 15 microns from the abluminal surface of the heart in (A). Green and purple cells from (A) are marked accordingly. The green cell extends a process luminally (arrow). Scale bars, 10μm.
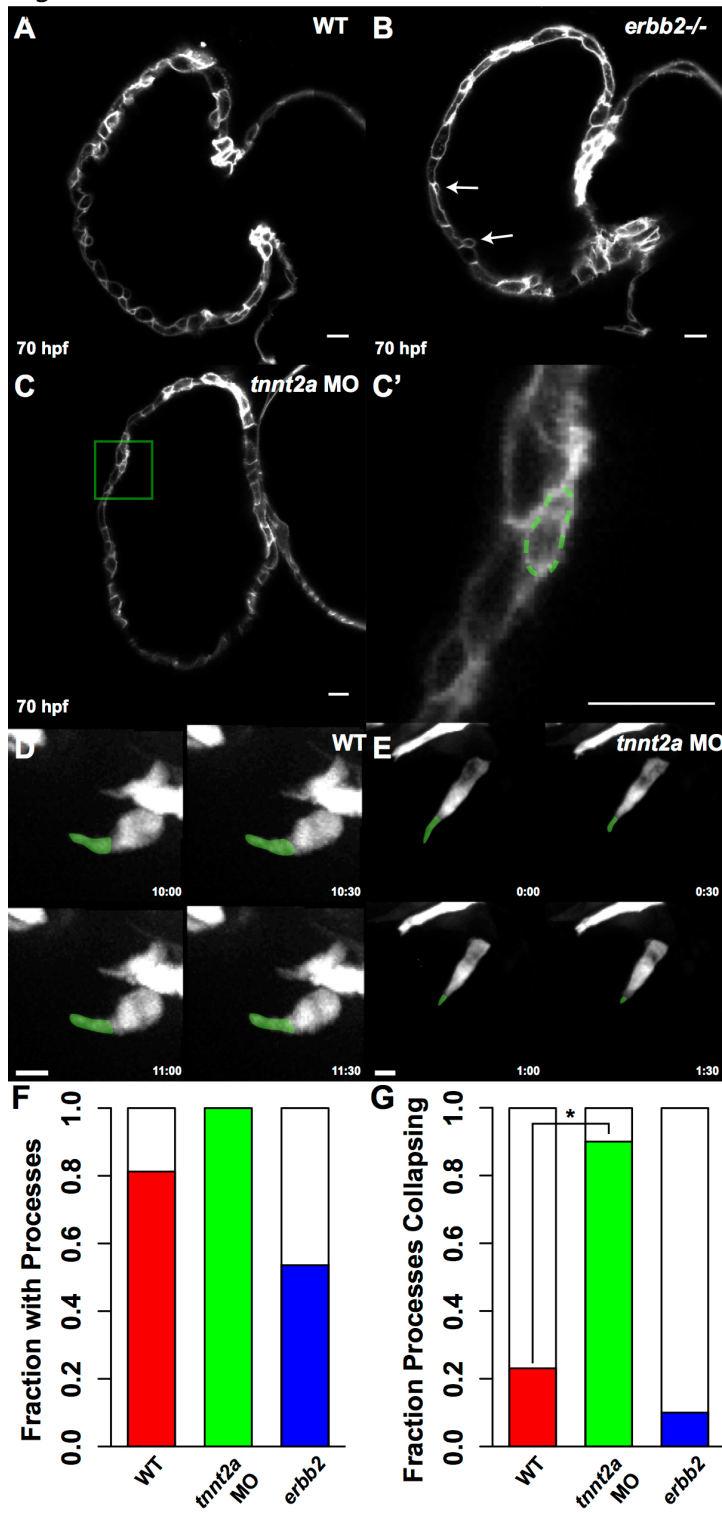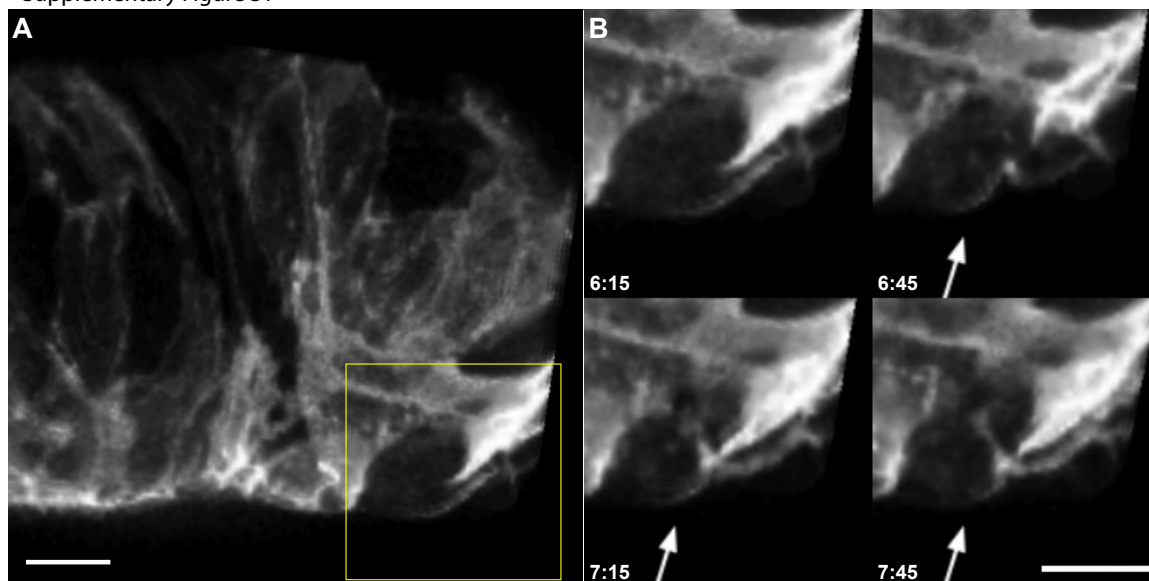
Figure 5

Figure 5.

Figure 5. Trabecular mutants exhibit different modes of trabecular failure. (A-C) Confocal sections through (A) wild-type, (B) *erbb2* mutant, and (C) *tnnt2a* morphant 70 hpf embryos. Arrows in (B) point towards cellular processes in the *erbb2* mutant. Box in (C) highlights a cellular process in the *tnnt2a* morphant. (C') Close-up of *tnnt2a* morphant process (outlined in green) (D-E) Time lapse of individual TagRFP-T expressing cells in (D) wild-type and (E) *tnnt2a* morphant embryos. Cellular processes are highlighted in green. Note that the process in (E) collapses over 2 hours, while the wild-type process in (D) remains stable over a similar time period. Scale bars, 10μm. (F) Graph showing fraction of cells that extend processes in WT, *tnnt2a* morphant, and *erbb2* mutant hearts. No statistically significant differences were observed. (G) Graph showing fraction of processes that retract over 12 hours. Processes in *tnnt2a* morphant hearts show significant instability. * p=0.001.

Supplemental Figure S1.

Supplemental Figure S1. Visualization of cardiomyocyte divisions. (A) 3D view of a

78 hpf *Tg(myl7:ras-GFP)* heart. Yellow box marks area of interest in (B). (B) Zoom in

on dividing cell. Arrow points to cleavage furrow. Time into the movie indicated in

hours:minutes. Scale bars, 10μm.
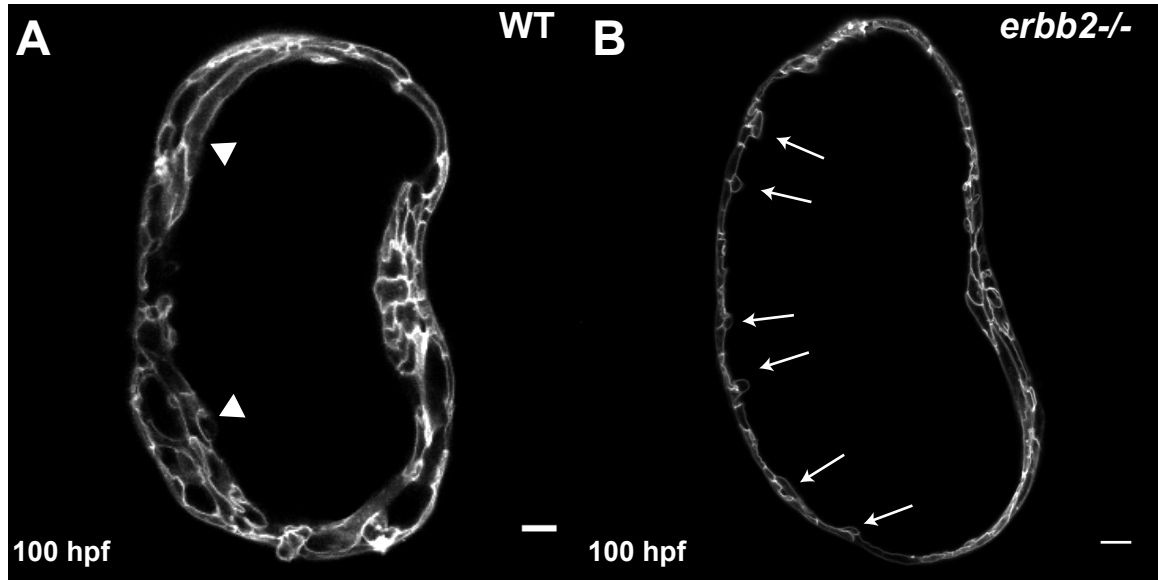
Supplemental Figure S2.

Supplemental Figure S2. *erbb2* mutants fail to form mature trabeculae by 100 hpf. (A)

WT heart at 100 hpf shows clear trabeculae (arrowheads). (B) 100 hpf *erbb2* mutant

heart shows clear cellular processes in the trabecular layer (arrows). Scale bars 10 μm.

Supplemental Movies

Supplemental Movie S1. Example of pre- and post-alignment data. The data are the same as shown in Figure 2. The left 3 columns show raw movies from each of those developmental time points representing one heartbeat. The right 3 columns show the same datasets after post-acquisition alignment. Rows show position in the z-stack in microns from the heart surface. The last row shows a z-projection of each dataset. Note that the z projection of the raw data is uninterpretable, while the aligned datasets can be easily analyzed. Movies were acquired at 60 fps (approximately 16 ms/frame).

Supplemental Movie S2. *Tg(myl7:ras-GFP)* embryo shown in Figure 2. Arrows point to locations where processes clearly extend. Arrowheads point to two processes extending towards each other, which is shown in more detail in Figure 2C and Supplemental Movie 3. Frames taken every 30 minutes.

Supplemental Movie S3. Zoom in of Supplemental Movie S2 focusing on the process shown in Figure 2B. Arrow points to location of emerging process. Frames were taken every 30 minutes.

Supplemental Movie S4. Zoom in of Supplemental Movie S2 focusing on the two processes shown in Figure 2C. Arrowheads point to the two processes that form a cellular contact by the end of the movie. Frames taken every 30 minutes.

Supplemental Movie S5. 59 hpf *Tg(myl7:ras-GFP)* embryo shown in Figure 4. Green and purple cells marked as in Figure 4. The green cell constricts its abluminal surface over the course of the movie, while the purple cell expands to take its place. Frames taken every 30 minutes.

Supplemental Movie S6. 78 hpf *Tg(myl7:ras-GFP)* embryo as shown in Supplemental Figure S1. One cell (marked in purple at the beginning) undergoes a cell division (arrows). Frames taken every 15 minutes.

References

Auman, H.J., Coleman, H., Riley, H.E., Olale, F., Tsai, H.J., and Yelon, D. (2007). Functional modulation of cardiac form through regionally confined cell shape changes. PLoS Biol *5*, e53.

Balciunas, D., Wangensteen, K.J., Wilber, A., Bell, J., Geurts, A., Sivasubbu, S., Wang, X., Hackett, P.B., Largaespada, D.A., McIvor, R.S., et al. (2006). Harnessing a high cargo-capacity transposon for genetic applications in vertebrates. PLoS Genet. *2*, e169.

Bartman, T., Walsh, E.C., Wen, K.K., McKane, M., Ren, J., Alexander, J., Rubenstein, P.A., and Stainier, D.Y.R. (2004). Early myocardial function affects endocardial cushion development in zebrafish. PLoS Biology *2*, 673–681.

Beis, D., and Stainier, D.Y.R. (2006). In vivo cell biology: following the zebrafish trend. Trends Cell Biol. *16*, 105–112.

Berdougo, E., Coleman, H., Lee, D.H., Stainier, D.Y.R., and Yelon, D. (2003). Mutation of weak atrium/atrial myosin heavy chain disrupts atrial function and influences ventricular morphogenesis in zebrafish. Development *130*, 6121–6129.

Chi, N.C., Shaw, R.M., Jungblut, B., Huisken, J., Ferrer, T., Arnaout, R., Scott, I., Beis, D., Xiao, T., Baier, H., et al. (2008). Genetic and Physiologic Dissection of the Vertebrate Cardiac Conduction System. PLoS Biol *6*, e109.

Chi, N.C., Bussen, M., Brand-Arzamendi, K., Ding, C., Olgin, J.E., Shaw, R.M., Martin, G.R., and Stainier, D.Y.R. (2010). Cardiac conduction is required to preserve cardiac chamber morphology. Proc. Natl. Acad. Sci. U.S.A *107*, 14662–14667.

D'Amico, L., Scott, I.C., Jungblut, B., and Stainier, D.Y.R. (2007). A mutation in zebrafish hmgcr1b reveals a role for isoprenoids in vertebrate heart-tube formation. Curr. Biol *17*, 252–259.

Edelstein, A., Amodaj, N., Hoover, K., Vale, R., and Stuurman, N. (2010). Computer control of microscopes using µManager. Curr Protoc Mol Biol *Chapter 14*, Unit14.20.

Filonov, G.S., Piatkevich, K.D., Ting, L.-M., Zhang, J., Kim, K., and Verkhusha, V.V. (2011). Bright and stable near-infrared fluorescent protein for in vivo imaging. Nat Biotech *29*, 757–761.

Gassmann, M., Casagranda, F., Orioli, D., Simon, H., Lai, C., Klein, R., and Lemke, G. (1995). Aberrant neural and cardiac development in mice lacking the ErbB4 neuregulin receptor. Nature *378*, 390–394.

Gu, Y., Forostyan, T., Sabbadini, R., and Rosenblatt, J. (2011). Epithelial cell extrusion requires the sphingosine-1-phosphate receptor 2 pathway. The Journal of Cell Biology *193*, 667–676.

Huang, C.-J., Tu, C.-T., Hsiao, C.-D., Hsieh, F.-J., and Tsai, H.-J. (2003). Germ-line transmission of a myocardium-specific GFP transgene reveals critical regulatory elements in the cardiac myosin light chain 2 promoter of zebrafish. Developmental Dynamics *228*, 30–40.

Jenni, R., Rojas, J., and Oechslin, E. (1999). Isolated Noncompaction of the Myocardium. New England Journal of Medicine *340*, 966–967.

Jones, F.E., Golding, J.P., and Gassmann, M. (2003). ErbB4 signaling during breast and

neural development: novel genetic models reveal unique ErbB4 activities. Cell Cycle

2, 555–559.

Kawakami, K. (2007). Tol2: a versatile gene transfer vector in vertebrates. Genome Biol.

8 Suppl 1, S7.

Kramer, R., Bucay, N., Kane, D.J., Martin, L.E., Tarpley, J.E., and Theill, L.E. (1996).

Neuregulins with an Ig-like domain are essential for mouse myocardial and neuronal

development. Proceedings of the National Academy of Sciences of the United States

of America *93*, 4833 –4838.

Lai, D., Liu, X., Forrai, A., Wolstein, O., Michalicek, J., Ahmed, I., Garratt, A.N.,

Birchmeier, C., Zhou, M., Hartley, L., et al. (2010). Neuregulin 1 sustains the gene

regulatory network in both trabecular and nontrabecular myocardium. Circ. Res. *107*,

715–727.

Lee, J.-Y., Marston, D.J., Walston, T., Hardin, J., Halberstadt, A., and Goldstein, B.

(2006). Wnt/Frizzled signaling controls C. elegans gastrulation by activating

actomyosin contractility. Curr. Biol. *16*, 1986–1997.

Lee, K.-F., Simon, H., Chen, H., Bates, B., Hung, M.-C., and Hauser, C. (1995).

Requirement for neuregulin receptor erbB2 in neural and cardiac development.

Nature *378*, 394–398.

Liebling, M., Forouhar, A.S., Gharib, M., Fraser, S.E., and Dickinson, M.E. (2005). Four-

dimensional cardiac imaging in living embryos via postacquisition synchronization of

nongated slice sequences. J Biomed Opt *10*, 054001.

Liebling, M., Forouhar, A.S., Wolleschensky, R., Zimmermann, B., Ankerhold, R., Fraser, S.E., Gharib, M., and Dickinson, M.E. (2006). Rapid three-dimensional imaging and analysis of the beating embryonic heart reveals functional changes during development. Dev. Dyn. *235*, 2940–2948.

Lin, Y.-F., Swinburne, I., and Yelon, D. (2012). Multiple influences of blood flow on cardiomyocyte hypertrophy in the embryonic zebrafish heart. Developmental Biology *362*, 242–253.

Liu, J., Bressan, M., Hassel, D., Huisken, J., Staudt, D., Kikuchi, K., Poss, K.D., Mikawa, T., and Stainier, D.Y.R. (2010). A dual role for ErbB2 signaling in cardiac trabeculation. Development *137*, 3867–3875.

Lyons, D.A., Pogoda, H.-M., Voas, M.G., Woods, I.G., Diamond, B., Nix, R., Arana, N., Jacobs, J., and Talbot, W.S. (2005). erbb3 and erbb2 Are Essential for Schwann Cell Migration and Myelination in Zebrafish. Current Biology *15*, 513–524.

Marinari, E., Mehonic, A., Curran, S., Gale, J., Duke, T., and Baum, B. (2012). Live-cell delamination counterbalances epithelial growth to limit tissue overcrowding. Nature *484*, 542–545.

Meilhac, S.M., Kelly, R.G., Rocancourt, D., Eloy-Trinquet, S., Nicolas, J.-F., and Buckingham, M.E. (2003). A retrospective clonal analysis of the myocardium reveals two phases of clonal growth in the developing mouse heart. Development *130*, 3877–3889.

Meilhac, S.M., Esner, M., Kelly, R.G., Nicolas, J.-F., and Buckingham, M.E. (2004a). The Clonal Origin of Myocardial Cells in Different Regions of the Embryonic Mouse Heart. Developmental Cell *6*, 685–698.

Meilhac, S.M., Esner, M., Kerszberg, M., Moss, J.E., and Buckingham, M.E. (2004b). Oriented clonal cell growth in the developing mouse myocardium underlies cardiac morphogenesis. J. Cell Biol. *164*, 97–109.

Meyer, D., and Birchmeier, C. (1995). Multiple essential functions of neuregulin in development. Nature *378*, 386–390.

Mikawa, T., Borisov, A., Brown, A.M., and Fischman, D.A. (1992). Clonal analysis of cardiac morphogenesis in the chicken embryo using a replication-defective retrovirus: I. Formation of the ventricular myocardium. Dev. Dyn *193*, 11–23.

Morris, J., Lin, W., Hauser, C., Marchuk, Y., Getman, D., and Lee, K. (1999). Rescue of the Cardiac Defect in ErbB2 Mutant Mice Reveals Essential Roles of ErbB2 in Peripheral Nervous System Development. Neuron *23*, 273–283.

Ohn, J., Tsai, H.-J., and Liebling, M. (2009). Joint dynamic imaging of morphogenesis and function in the developing heart. Organogenesis *5*, 166–173.

Peshkovsky, C., Totong, R., and Yelon, D. (2011). Dependence of cardiac trabeculation on neuregulin signaling and blood flow in zebrafish. Dev Dyn.

Rosenblatt, J., Raff, M.C., and Cramer, L.P. (2001). An epithelial cell destined for apoptosis signals its neighbors to extrude it by an actin- and myosin-dependent mechanism. Current Biology *11*, 1847–1857.

Sawyer, J.M., Harrell, J.R., Shemer, G., Sullivan-Brown, J., Roh-Johnson, M., and Goldstein, B. (2010). Apical constriction: a cell shape change that can drive morphogenesis. Dev. Biol *341*, 5–19.

Schindelin, J., Arganda-Carreras, I., Frise, E., Kaynig, V., Longair, M., Pietzsch, T.,
Preibisch, S., Rueden, C., Saalfeld, S., Schmid, B., et al. (2012). Fiji: an open-source
platform for biological-image analysis. Nat Meth *9*, 676–682.

Sedmera, D., Pexieder, T., Rychterova, V., Hu, N., and Clark, E.B. (1999). Remodeling
of chick embryonic ventricular myoarchitecture under experimentally changed
loading conditions. Anat. Rec. *254*, 238–252.

Sedmera, D., Pexieder, T., Vuillemin, M., Thompson, R.P., and Anderson, R.H. (2000).
Developmental patterning of the myocardium. The Anatomical Record *258*, 319–337.

Sedmera, D., Reckova, M., deAlmeida, A., Sedmerova, M., Biermann, M., Volejnik, J.,
Sarre, A., Raddatz, E., McCarthy, R.A., Gourdie, R.G., et al. (2003). Functional and
morphological evidence for a ventricular conduction system in zebrafish and Xenopus
hearts. Am J Physiol Heart Circ Physiol *284*, H1152–1160.

Sehnert, A.J., Huq, A., Weinstein, B.M., Walker, C., Fishman, M., and Stainier, D.Y.R.
(2002). Cardiac troponin T is essential in sarcomere assembly and cardiac
contractility. Nat Genet *31*, 106–110.

Shaner, N.C., Lin, M.Z., McKeown, M.R., Steinbach, P.A., Hazelwood, K.L., Davidson,
M.W., and Tsien, R.Y. (2008). Improving the photostability of bright monomeric
orange and red fluorescent proteins. Nature Methods *5*, 545–551.

Slattum, G., McGee, K.M., and Rosenblatt, J. (2009). P115 RhoGEF and microtubules
decide the direction apoptotic cells extrude from an epithelium. The Journal of Cell
Biology *186*, 693–702.

Stankunas, K., Hang, C.T., Tsun, Z.Y., Chen, H., Lee, N.V., Wu, J.I., Shang, C., Bayle,
J.H., Shou, W., and Iruela-Arispe, M.L. (2008). Endocardial Brg1 represses

ADAMTS1 to maintain the microenvironment for myocardial morphogenesis. Developmental Cell *14*, 298–311.

Staudt, D., and Stainier, D. (2012). Uncovering the molecular and cellular mechanisms of heart development using the zebrafish. Annu. Rev. Genet. *46*, 397–418.

Subach, O.M., Gundorov, I.S., Yoshimura, M., Subach, F.V., Zhang, J., Grüenwald, D., Souslova, E.A., Chudakov, D.M., and Verkhusha, V.V. (2008). Conversion of red fluorescent protein into a bright blue probe. Chem. Biol. *15*, 1116–1124.

Suri, C. (1996). Requisite Role of Angiopoietin-1, a Ligand for the TIE2 Receptor, during Embryonic Angiogenesis. Cell *87*, 1171–1180.

Tidcombe, H., Jackson-Fisher, A., Mathers, K., Stern, D.F., Gassmann, M., and Golding, J.P. (2003). Neural and mammary gland defects in ErbB4 knockout mice genetically rescued from embryonic lethality. PNAS *100*, 8281–8286.

Toyofuku, T., Zhang, H., Kumanogoh, A., Takegahara, N., Suto, F., Kamei, J., Aoki, K., Yabuki, M., Hori, M., Fujisawa, H., et al. (2004a). Dual roles of Sema6D in cardiac morphogenesis through region-specific association of its receptor, Plexin-A1, with off-track and vascular endothelial growth factor receptor type 2. Genes & Development *18*, 435–447.

Toyofuku, T., Zhang, H., Kumanogoh, A., Takegahara, N., Yabuki, M., Harada, K., Hori, M., and Kikutani, H. (2004b). Guidance of myocardial patterning in cardiac development by Sema6D reverse signalling. Nat Cell Biol *6*, 1204–1211.

Trinh, Le A., and Stainier, D.Y.. (2004). Fibronectin Regulates Epithelial Organization during Myocardial Migration in Zebrafish. Developmental Cell *6*, 371–382.

Trinh, Le A., Yelon, D., and Stainier, D.Y.R. (2005). Hand2 Regulates Epithelial
Formation during Myocardial Differentiation. Current Biology *15*, 441–446.

Vermot, J., Forouhar, A.S., Liebling, M., Wu, D., Plummer, D., Gharib, M., and Fraser,
S.E. (2009). Reversing blood flows act through klf2a to ensure normal valvulogenesis
in the developing heart. PLoS Biol *7*, e1000246.

Westerfield, M. (2000). The Zebrafish Book: a Guide for the Laboratory Use of Zebrafish
(Danio rerio) (Eugene: University of Oregon Press).

CHAPTER 3: Early Notch Responsive Cardiomyocytes Contribute to the

Trabecular and Cortical Layers

<u>Introduction</u>

One of the many interesting unanswered questions in heart development is why some cardiomyocytes contribute to the trabeculae while some stay in the compact layer. Recent work has shown that trabecular fate can be influenced cell-autonomously (Liu et al., 2010; Toyofuku et al., 2004), and that specifically reverse signaling through Semaphorin 6D may drive trabecular fate in the chick. Additionally, some studies theorize that that mechanical forces could act to specify the location of the trabecular ridges (Taber and Zahalak, 2001). However, it remains unclear what asymmetric signals may initially specify trabecular cells.

A well-known player in the development of many systems is the Notch pathway (High and Epstein, 2008). Notch is well known to play a role in the differentiation of myocardium from progenitors both *in vitro* and *in vivo*, with Notch inhibition biasing towards cardiomyogenesis and Notch activation preventing differentiation (High and Epstein, 2008). The Notch pathway has previously been implicated in trabeculation, and its activation in the endocardium was shown to be necessary for the release of growth factors required for trabeculation (Grego-Bessa et al., 2007). However, though a differential activation within the endocardium was observed, it was unclear whether this differential activation contributed to the behavior of the underlying myocardium, or whether Notch was active in the myocardium at all during trabecular stages.

Recent work has revealed another myocardial fate decision during development of the ventricle. Multicolored clonal analysis within the heart of zebrafish over their lifetimes revealed that, in the fish, the compact layer remains a single layer of cardiomyocytes until 30 days post fertilization (dpf) (Gupta and Poss, 2012). However, by 6 weeks post fertilization (wpf), a new layer of cardiomyocytes begins to cover the existing compact layer. This layer, termed the cortical layer, expands to cover the entire surface of the heart by 90 dpf. Surprisingly, this layer can be attributed to an average of just 8 cells per ventricle that are set aside at 2 dpf. This layer is distinct from the compact layer, and seems to originate from the trabeculae at approximately 6 wpf. However, though this analysis identified that these large clones covering the heart are specified at 2 dpf, the retrospective nature of the study prevented the authors from prospectively labeling these cells and determining how their fate is set.

Here, we set out to determine whether Notch activity within the myocardium plays a role in these cell fate decisions. Using a number of transgenic tools based around a Notch-responsive promoter element, we analyze the 3D pattern of Notch activity within the developing zebrafish heart at trabecular stages and show that Notch activity is restricted to cells within the compact layer. Notch activity does not seem to affect trabecular development directly, as inhibition and activation of the Notch pathway do not perturb trabecular formation. Further, inhibition of trabeculation does not inhibit Notch activation in the compact layer. Lineage tracing of these cells reveals that this subpopulation migrates to the trabeculae starting as early as 16 dpf and eventually

contributes to the cortical layer of the adult heart. These cells represent a new and interesting sub-population of cardiomyocytes with specific roles in cardiac development.

Results

Notch reporter lines mark cardiomyocytes in the compact layer

In order to examine Notch activity in the myocardium, we took advantage of a number of transgenic zebrafish lines that act as reporters of the Notch pathway. These lines use 12 repeats of a region of the Tp1 promoter region, which is Notch-responsive, to mark Notch responsive cells (add a reference here). We first examined the *Tg(Tp1bglob:Venus-PEST)* line (Ninov et al., 2012), which expresses a destabilized YFP in cells with an active Notch pathway. Because the fluorescent protein has a short half life, this line allows us to determine which cells had recently activated the Notch pathway. Before 3 dpf, the reporter was strongly expressed in the endocardium, but we did not detect any reporter activity in the myocardium (data not shown). At 3 dpf, after trabeculation has begun, we started to observe a few compact layer cells expressing the reporter (Fig. 1A, arrows), while the endocardial expression began to fade (Fig. 1A, arrowheads). By 4 dpf, we observe patches of compact layer cells expressing the reporter, but no trabecular expression (Fig. 1B). This pattern continued through 5 dpf (Fig. 1C). At no point during these time points did we observe any trabecular expression.

To determine the extent of the cardiomyocytes that activated the Notch pathway during early development, we used the *Tg(Tp1bglob:CreERT2)* line, which expresses the

CreERT2 fusion protein in a Notch responsive manner. We crossed this line to a

Tg(myl7:lox-dsRed-stop-lox-EGFP) line, in which cardiomyocytes are labeled in red, and

turn green in the presence of Cre activity. Adding 4-hydroxytamoxifen (4-OHT) to these

fish selectively labeled cardiomyocytes experiencing Notch signaling. By growing the

larvae in 4OHT starting before trabeculation, we could mark all cardiomyocytes that

express Notch during trabecular stages. Interestingly, when we used this approach, we

found that only compact layer cardiomyocytes were labeled (Fig. 1D-F). However, not

all compact cells were labeled. Rather, stripes of cells stretching around the outer

curvature were marked (Fig 1G). These stripes seemed to be associated with the

underlying branching trabecular network (Fig. 1H). Crossing the same

Tg(Tp1bglob:CreERT2) line with a *Tg(actb2:lox-dsred-stop-lox-GFP)* line, which is

cardiomyocyte specific within the heart, and with the ubiquitous *Tg(ubb:lox-GFP-lox-*

stop-cherry) line yielded a similar striped pattern of lineage tracing, though the number of

marked cells varied between the different lines (Fig 1E,F).

Notch activity in cardiomyocytes is not linked to trabeculation

Because Notch reporter activity was observed exclusively in compact layer cells, we

hypothesized that Notch activity prevented cells from entering the trabecular layer. We

predicted that inhibiting the Notch pathway during trabecular stages would lead to more

trabeculation, and activating it would decrease trabeculation. To test this hypothesis, we

first manipulated Notch activity in the whole embryo. Inhibiting Notch activity using the

gamma-secretase inhibitor DAPT from x hpf to y hpf did not noticeably alter trabecular

formation as assessed at z hpf (Fig. 2A,B). Similarly, activating the Notch pathway at x

hpf by overexpressing the Notch Intracellular Domain (NICD) via a heat-shock inducible

system (Scheer et al., 2001) did not inhibit trabeculation as assessed at z hpf (Fig. 2C,D).

Therefore, we determined that Notch was neither necessary nor sufficient for specifying

cells to the compact layer. To test whether trabeculation affects the pattern of Notch

activity, we treated embryos with PD168393, an inhibitor of the ErbB receptor tyrosine

kinase family. Treatment with this drug inhibits trabeculation (Fig. 2F). After treatment

of *Tg(Tp1bglob:EGFP)* embryos with PD168393 starting at 55 hpf, we still observed

reporter activity in the compact layer as assessed at 4 dpf (Fig 2F,arrow).   Thus, Notch

activity in the compact layer does not seem to relate to trabeculation.

Early Notch+ cardiomyocytes contribute to the trabecular and cortical layers

Since the Notch reporter marked a subset of compact layer cardiomyocytes, we

endeavored to determine what those cells give rise to within the heart. We treated

Tg(Tp1bglob:CreERT2); Tg(myl7:lox-dsRed-lox-EGFP) embryos with 4-OHT from 2 5

dpf, then raised the animals and examined their hearts at various stages. At 16 dpf,

labeled cells were mostly confined to the compact layer (Fig. 3A). However, in a few

cases (3/11 larvae examined), cells were seen entering the trabeculae (Fig 3B). These

trabecular cells were always connected to cells in the compact layer. We raised similarly

traced fish to adulthood and analyzed the distribution of labeled cells in the adult heart.

Grossly, the cells covered about half of the outside of the adult heart, and were arranged

in continuous patches with long spindle-like extensions (Fig 3C). Analysis of sections

revealed that the majority of cells contributed to the newly described cortical layer (Fig 3D-F). We often observed clones at the base of the heart (Fig 3C-D). However, we also observed a number of cells in the trabeculae neighboring labeled cells in the cortical layer (Fig 3F,G). This finding is in accordance with data suggesting that cortical cells derive from trabecular myocytes (Gupta and Poss, 2012).

Discussion

In this study, we identified a population of cardiomyocytes within the early compact layer that activate the Notch pathway. These cells are generally found directly underlying the trabecular ridges, and the pattern of Notch activity early in development mirrors the branching structure of the trabeculae. Although Notch activity is confined to the compact layer, manipulating the Notch pathway during trabecular stages did not appear to affect trabeculation, and inhibiting trabeculation did not appear to perturb Notch expression. Finally, through long-term lineage tracing, we demonstrated that these Notch responsive cardiomyocytes contribute to a subset of the trabecular layer, and eventually go on to populate the cortical layer. Overall, this study identifies an interesting subpopulation of cardiomyocytes specified early in development.

An earlier study identified that the cortical layer of the heart in adult zebrafish was derived from, on average, 8 clones that were specified around 2 dpf. However, they traced these cells using retrospective clonal analysis, and could not mark these cells prospectively. The tools used in our study may allow for the prospective labeling of cells

in the cortical layer, allowing for a more detailed analysis of their fate. Live imaging of

Notch responsive lines will allow for examination of the dynamics of Notch activation,

and whether Notch activity correlates with trabeculation. It would, for instance, be

interesting if the immediate neighbors of delaminating trabecular cardiomyocytes turned

on Notch during delamination, or whether trabeculae need to be fully established before

their underlying compact layer neighbors turn on Notch. The lineage tracing line used

provides a powerful tool for examining the cortical layer. Though it is unclear whether

the incomplete labeling of the cortical layer is reflective of another population of cells

that contribute to the cortical layer, or whether the *Tg(Tp1bglob:CreERT2)* line does not

mark all Notch responsive cells in the developing myocardium, this line provides a

powerful tool for manipulating this myocardial subset. Combining the

Tg(Tp1bglob:CreERT2) line with Cre-responsive effector or ablation lines will allow for

manipulation of Notch responsive cardiomyocytes, enabling future studies to probe the

function of these cells within the myocardial wall, as well as the molecular basis behind

their specification, movement to the trabecular layer, and eventual migration into the

cortical layer.

Notch activity seems to mark cells that eventually contribute to the cortical layer.

However, it is unclear whether Notch is necessary for their specification, or whether it is

simply a marker of the eventual cortical cells. Further studies deactivating the Notch

pathway in the myocardium will be necessary to determine whether early Notch activity

is necessary for cortical layer development. Additionally, this study did not identify the

relevant Notch ligands and receptors that activate the pathway in cardiomyocytes, or the

location of the ligands. The mouse endocardium is known to express Notch1a, but it cannot be easily detected in the myocardium (Grego-Bessa et al., 2007). Additionally, the mouse endocardium expresses a number of Notch ligands (Grego-Bessa et al., 2007), opening up the possibility that endocardial ligands might be responsible for myocardial activation of the Notch pathway. Interestingly, a study in mouse identified preferential expression of Delta4 and Delta1 in the endocardium at the base of trabeculae (Grego-Bessa et al., 2007), which could explain preferential activation in the sub-trabecular myocardium. Further studies are necessary to identify the identity and location of the molecular players in myocardial Notch activation.

In conclusion, this study identifies a new sub-population of cardiomyocytes marked by Notch activation during early trabeculation stages, which contribute to both the trabeculae and cortical layers in the adult zebrafish. Further studies will help identify both the function and cell biological properties of this interesting subpopulation of the myocardium.

Materials and Methods

Zebrafish

Embryonic and adult zebrafish were maintained according to standard laboratory conditions (Westerfield, 2000) and IACUC license. We used the following transgenic and mutant lines: *Tg(Tp1bglob:CreERT2)*, *Tg(Tp1bglob:Venus-PEST)* (Ninov et al., 2012), *Tg(Tp1bglob:EGFP)* (Parsons et al., 2009), *Tg(cmlc2:lox-mcherry-stop-lox-*

EGFP), *Tg(actb2:lox-dsRed-stop-lox-EGFP)^{s928}*, *Tg(ubb:lox-EGFP-stop-lox-mcherry)^{cz1701}* (Mosimann et al., 2011), *Tg(myl7:ras-cherry)* (Yoruk et al., 2011), and *Tg(hsp70:Gal4); Tg(UAS:NICD-myc)* (Scheer et al., 2001).

Lineage Tracing

Tg(Tp1bglob:CreERT2) expressing embryos were treated with 5 μM 4-OHT (Sigma cat# H7904) from 2-5 dpf. The drug was then washed out and fish were then allowed to develop to the specified stages and imaged.

Drug Treatments and Heat Shock

Fish were treated with 5μM PD168393 (EMD Millipore cat# 513033), or 50μM DAPT (Sigma cat# D5942). For Notch pathway activation, embryos from a *Tg(hsp70:Gal4); Tg(UAS:NICD-myc)* incross were placed at 38°C for 7 minutes, then returned to 28.5°C embryo medium for recovery.
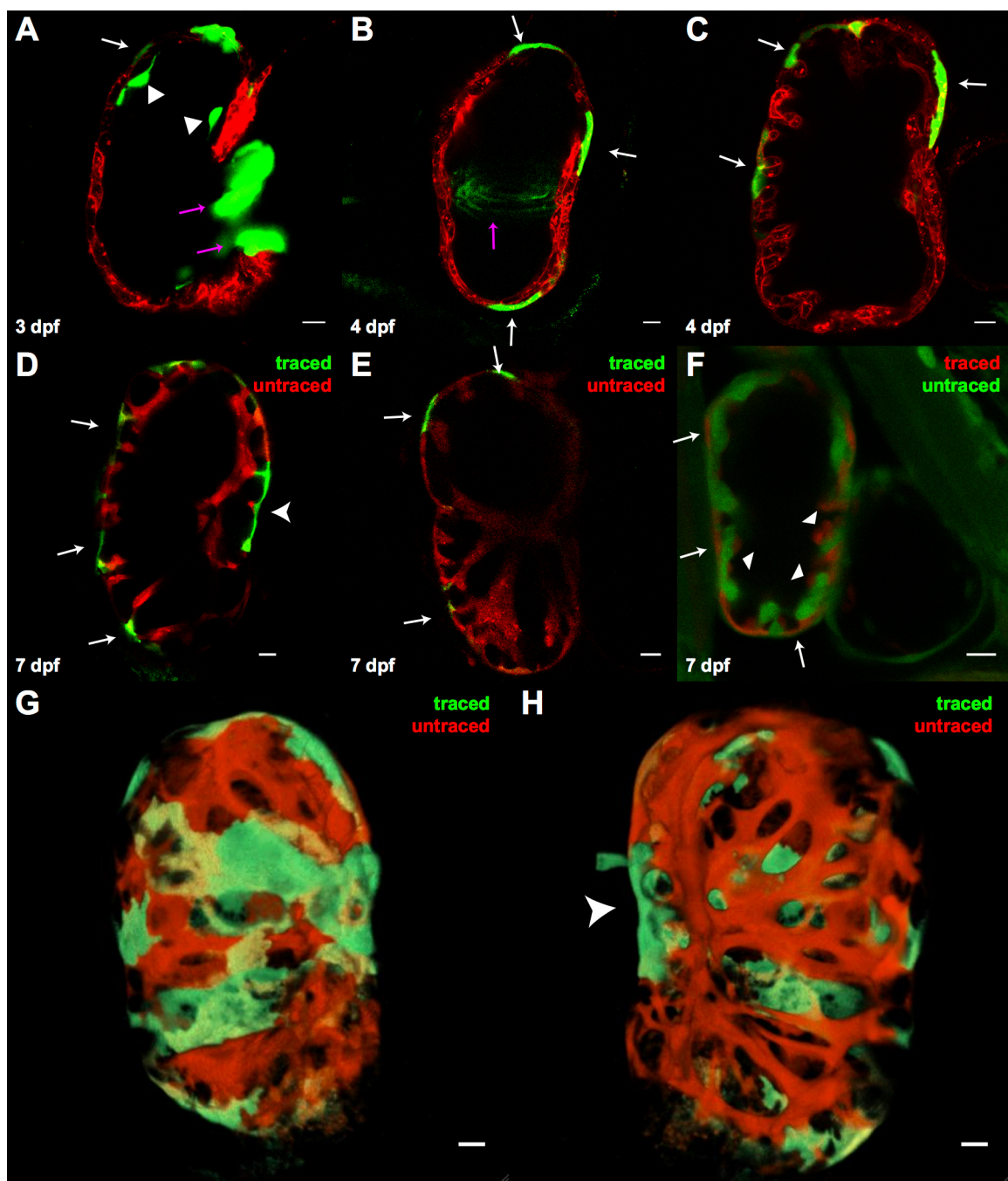
Figure 1.

Figure 1. Notch reporter lines reveal a Notch responsive subpopulation of cardiomyocytes. (A-C) Confocal sections of *Tg(Tp1bglob:Venus-PEST)*; *Tg(myl7:ras-cherry)* larvae at (A) 3 dpf, (B) 4 dpf, and (C) 5 dpf. Later stages were not examined. Arrows point to myocytes expressing the Notch-responsive reporter. Arrowheads in (A) point to fading expression in the endocardium. Purple arrows point to the developing AV valve in (A) and (B). (D-F) Confocal section of 7 dpf larval hearts derived from crossing the *Tg(Tp1bglob:CreERT2)* line to three different Cre-responsive reporters. In each case, embryos were treated treated with 4-OHT from 2-5 dpf. Arrows point to labeled cells in the compact layer. (D) Lineage traced *Tg(Tp1bglob:CreERT2); Tg(myl7:lox-mcherry-stop-lox-GFP)* embryo. Arrowhead points to cells neighboring the AV canal. (E) Lineage traced *Tg(Tp1bglob:CreERT2); Tg(actb2:lox-dsRed-stop-lox-GFP)* (F) Lineage traced *Tg(Tp1bglob:CreERT2); Tg(ubb:lox-GFP-stop-lox-cherry)*. Note that in this case lineage traced cells are red. Wide arrowheads point to labeled endocardial cells. (G) 3D rendering of the heart shown in (D) viewed externally showing the stripes of traced cells on the surface of the heart. (H) Chamber view of the same heart showing that trabeculae lie over the traced cells. Arrowhead points to traced cells near the AV canal. Scale bars 10μm.
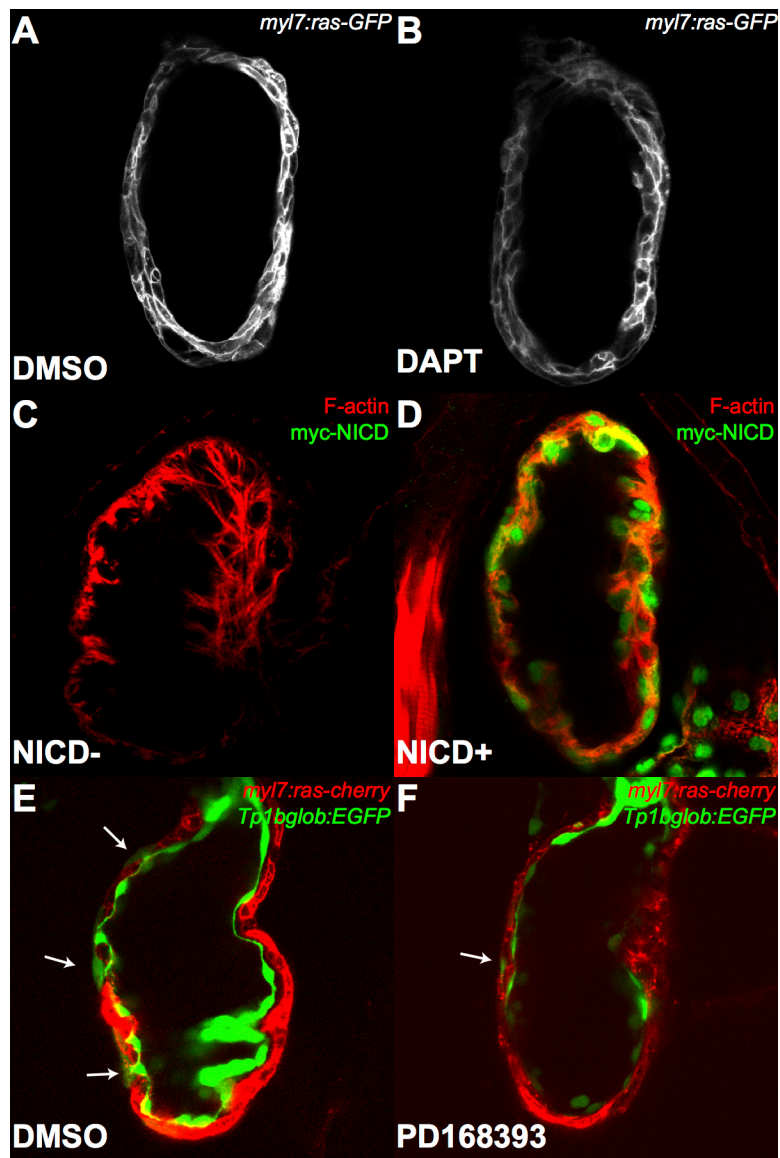
Figure 2.

Figure 2. Manipulation of Notch activity does not appear to affect trabeculation. (A-B)

4 dpf *Tg(myl7:ras-GFP)* embryos treated with (A) DMSO or (B) DAPT starting at 2 dpf.

Both show signs of trabeculation. (C-D) Activation of Notch does not appear to

compromise trabeculation. (C) Phalloidin stain of 3 dpf sibling control embryo heat

shocked at 2 dpf without NICD expression shows normal trabeculation. (D) 3 dpf

Tg(hsp70:Gal4); *Tg(UAS:NICD)* embryo heat shocked at 2 dpf also shows normal

trabeculation, despite expression of NICD-myc (green). (E) 4 dpf DMSO treated

Tg(Tp1bglob:EGFP); *Tg(myl7:ras-cherry)* embryos show normal activation of the Notch

reporter in the compact myocardium (arrows). (F) 4 dpf embryos treated with PD168393

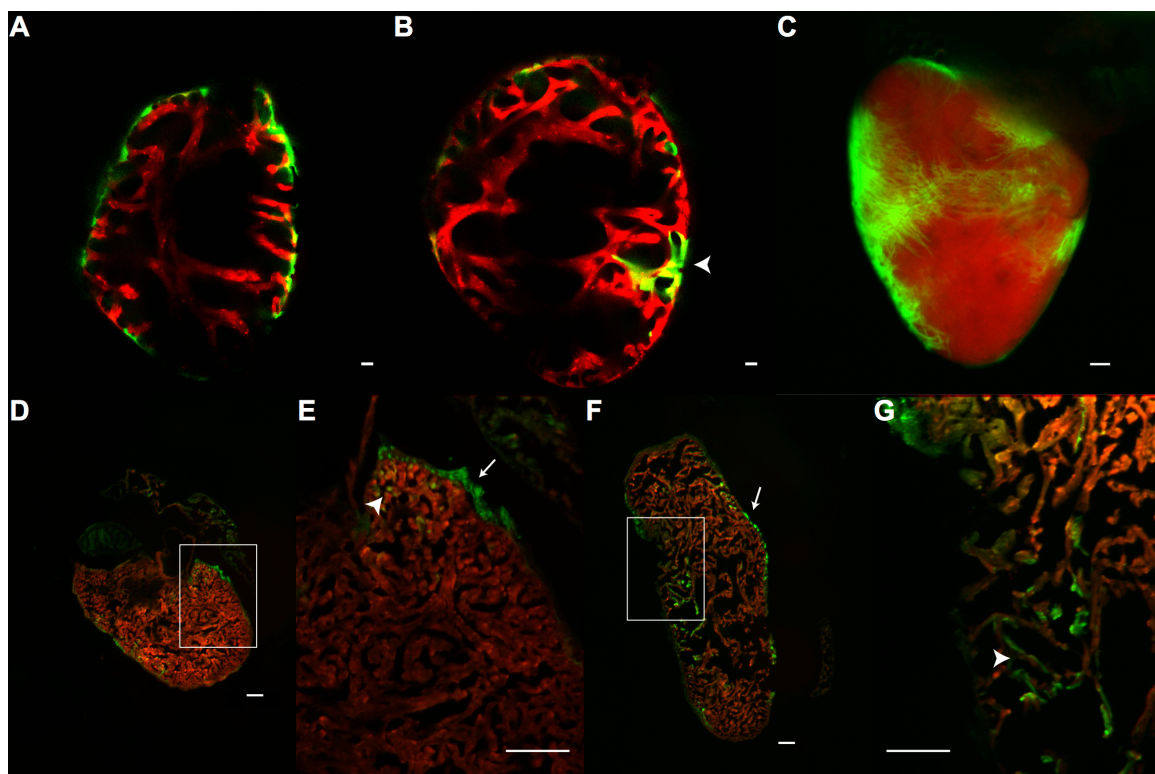starting at 3 dpf still have Notch activity in the myocardium (arrow). Scale bars 10 μm.

Figure 3.

Figure 3. Lineage tracing of Notch responsive cells reveals migration to trabeculae and cortical layer. (A-G) *Tg(Tp1bglob:CreERT2)*; *Tg(myl7:lox-cherry-stop-lox-EGFP)* animals treated with 4-OHT from 2-5 dpf and examined at various stages of life. (A) 16 dpf larva with only compact layer cells marked by the lineage trace. (B) In some cases, 16 dpf embryos exhibited traced cells in the trabeculae and compact layer (arrowhead). Scale bars 10μm. (C) Exterior view of 4 month old adult heart showing patches of lineage traced cells extending over its surface. Scale bar 100μm. (D-F) Sections of 4 month old lineage traced adult hearts. In each case, the sections are oriented with the base of the heart at the top, and the apex at the bottom of the image. (D) Section of adult 4 month old heart showing traced cells mostly in the cortical layer, but with some trabecular staining. (E) Close-up of the marked region in (D) showing traced cortical cells at the base of the heart adjacent to traced trabecular cells. (F) Section of adult heart with more trabecular tracing. (G) Close-up of marked region in (F) showing extensive trabecular contribution from the traced cells. Scale bars 10μm.

References

Grego-Bessa, J., Luna-Zurita, L., del Monte, G., Bolós, V., Melgar, P., Arandilla, A., Garratt, A.N., Zang, H., Mukouyama, Y.-S., Chen, H., et al. (2007). Notch signaling is essential for ventricular chamber development. Dev. Cell *12*, 415–429.

Gupta, V., and Poss, K.D. (2012). Clonally dominant cardiomyocytes direct heart morphogenesis. Nature *484*, 479–484.

High, F.A., and Epstein, J.A. (2008). The multifaceted role of Notch in cardiac development and disease. Nat. Rev. Genet. *9*, 49–61.

Liu, J., Bressan, M., Hassel, D., Huisken, J., Staudt, D., Kikuchi, K., Poss, K.D., Mikawa, T., and Stainier, D.Y.R. (2010). A dual role for ErbB2 signaling in cardiac trabeculation. Dev. Camb. Engl. *137*, 3867–3875.

Mosimann, C., Kaufman, C.K., Li, P., Pugach, E.K., Tamplin, O.J., and Zon, L.I. (2011). Ubiquitous transgene expression and Cre-based recombination driven by the ubiquitin promoter in zebrafish. Development. *138*, 169–177.

Ninov, N., Borius, M., and Stainier, D.Y.R. (2012). Different levels of Notch signaling regulate quiescence, renewal and differentiation in pancreatic endocrine progenitors. Development *139*, 1557–1567.

Parsons, M.J., Pisharath, H., Yusuff, S., Moore, J.C., Siekmann, A.F., Lawson, N., and Leach, S.D. (2009). Notch-responsive cells initiate the secondary transition in larval zebrafish pancreas. Mech. Dev. *126*, 898–912.

Scheer, N., Groth, A., Hans, S., and Campos-Ortega, J.A. (2001). An instructive function

    for Notch in promoting gliogenesis in the zebrafish retina. Development *128*, 1099–

    1107.

Taber, L.A., and Zahalak, G.I. (2001). Theoretical model for myocardial trabeculation.

    Dev. Dyn. *220*, 226–237.

Toyofuku, T., Zhang, H., Kumanogoh, A., Takegahara, N., Yabuki, M., Harada, K., Hori,

    M., and Kikutani, H. (2004). Guidance of myocardial patterning in cardiac

    development by Sema6D reverse signalling. Nat Cell Biol *6*, 1204–1211.

Westerfield, M. (2000). The Zebrafish Book: a Guide for the Laboratory Use of Zebrafish

    (Danio rerio) (Eugene: University of Oregon Press).

Yoruk, B., Gillers, B.S., Chi, N.C., and Scott, I.C. (2011). Ccm3 functions in a manner

    distinct from Ccm1 and Ccm2 in a zebrafish model of CCM vascular disease. Dev.

    Biol.

CHAPTER 4: Further Questions and Future Directions

<u>Introduction</u>

Despite years of progress in unraveling the genetic underpinnings of cardiac

morphogenesis, very little is known about how genetic defects lead to anatomical

abnormalities. Determining how cardiomyocytes create structures within the heart and

how previously identified genetic lesions modify myocardial behavior will deepen our

understanding of how congenital heart defects arise. Additionally, understanding the

cytoskeletal rearrangements and coordinated behavior of cardiomyocytes might one day

contribute to our ability to enhance cardiac regeneration by directing cardiomyocytes to

grow and integrate into damaged cardiac structures. However, studying myocardial

behaviors *in vivo* is complicated by the optical inaccessibility of the heart in most model

organisms, as well as the cyclical cardiac motion necessary to maintain embryo viability

and cardiac morphogenesis. The studies outlined in this dissertation demonstrate two

intriguing avenues for further research within the zebrafish heart, namely trabeculation

and the population of Notch reactive cells within the compact layer. The trabeculae are

evolutionarily conserved, complex myocardial structures whose formation depends on

myocardial intrinsic factors (Liu et al., 2010), myocardial-endocardial interactions

(Grego-Bessa et al., 2007; Peshkovsky et al., 2011), and intracardiac forces (Chi et al.,

2008; Peshkovsky et al., 2011), all of which probably contribute to the formation of other

cardiac structures. Because they are optically accessible in the early zebrafish embryo,

they are ideal model structures for studying how cardiomyocytes form structures *in vivo*.

The population of Notch responsive cardiomyocytes appears to be similar, if not

identical, to the progenitor population set aside to form the cortical layer in the adult

123

zebrafish heart (Gupta and Poss, 2012). This fascinating process provides a clear example of myocardial sub-specification, which is difficult to study in other systems. In this section, I will outline a number of outstanding questions relating to the cell biology of cardiac morphogenesis, and how techniques outlined in this dissertation and other recent technical advances can be expanded to further our understanding.

Specification

Not all cardiomyocytes are created equal. Besides the clear differences between ventricular and atrial cardiomyocytes, even within the ventricle different cardiomyocyte populations perform different tasks. For instance, the cells of the conduction system allow for apex to base contraction, while the papillary muscles help to stabilize the valves. How these different subsets of cardiomyocytes differentiate is unknown. The two systems studied in this dissertation, provide two different opportunities for studying how cardiomyocytes subspecialize. It remains unclear exactly what signals and intracellular factors act to specify trabecular cells. One key question is whether migration and specification can be de-coupled, or whether migration of trabecular cells, and their new location in the trabecular layer, leads to the known gene expression differences between the compact and trabecular layers. In order to probe this question, we must identify an early marker for trabeculation that comes on during, or even before obvious migration occurs. The known gene expression differences between the trabecular and compact layers suggest a number of interesting molecules to investigate, including *bmp10*, *nppa*, *connexin 40*, *cited1*, and *smpx* (Lai et al., 2010). Investigating whether

124

these markers are activated before migration begins, and whether mutants lacking trabeculae still express these markers, will reveal whether the trabecular fate is set before migration.

The Notch responsive cardiomyocytes described in this thesis present a unique opportunity for looking at specialization of cardiomyocytes. Our lineage tracing has revealed that these cells are among the cells set aside to form the cortical layer in the adult heart. In order to create the cortical layer, this unique population of cardiomyocytes undergoes a very specific and complex program of development, separate from other cells in the developing myocardium. Further, since these cells are marked by a Notch responsive element, it is likely that Notch plays a role in their specification. Further studies ablating Notch activity in the myocardium will be necessary to validate this hypothesis. It will be interesting to determine what transcriptional pathways Notch is activating in these cells that causes them to be set aside until the development of the cortical layer, and how these pathways differ from the rest of the myocardium that does not contribute to the cortical layer.

Myocardial Architecture

The cardiomyocytes within the heart are not arranged haphazardly – they form oriented sheets of contracting cells that coordinate to form an efficient pumping unit. How cardiomyocytes organize themselves in these functional patterns is unknown. The ventricular trabeculae provide an example of a complex, interconnected cardiac structure.

Examining the network in multiple species, it becomes clear that the trabecular ridges are not randomly arranged, but instead are arranged in a branching network extending from the AV canal (Sedmera et al., 2000). This network clearly forms in zebrafish hearts by 5 dpf, and the basic structure is clear even earlier (Peshkovsky et al., 2011). How is this network formed? Generally, we can predict two ways that cardiomyocytes could coordinate to form this branching network. First, trabecular cells could be specified in this branching pattern within the compact layer, and simply migrate luminally into the trabecular layer, forming the trabecular sheets. Second, trabecular cells could be specified randomly, move into the trabecular layer, and then spread out and migrate within the layer to contact their neighbors and form the network. Our studies so far suggest that cardiomyocytes spread out and create new contacts as they move into the trabecular layer, but have not identified whether trabecular cells are specified in sheets or not. Further studies using live imaging will shed further light on how the mature network forms. Interestingly, changes in blood flow seem to alter the pattern of trabeculation in both chick and zebrafish (Peshkovsky et al., 2011; Sedmera et al., 1999). Since the heart needs to form an efficient pumping unit, it makes sense that its structure should in part be determined by intracardiac forces during development. By building up myocyte mass in areas experiencing high wall stress or high shear stress, the developing heart could dynamically adjust its geometry to appropriately distribute the work of pumping blood. Manipulation of the cardiac hydrodynamics by drug treatments or other manipulations coupled with 4D imaging has the potential to shed light on how intracardiac forces can pattern the myocardium.

While the myocardium grows, it must coordinate proliferation in order to maintain and mature its internal structure. After the initial delamination described in this dissertation, the trabeculae must expand in mass and undergo further remodeling. Proliferation increases as trabeculation progresses (Liu et al., 2010), but it is unclear whether the trabecular mass comes from cell divisions within the trabecular layer, or through cell divisions in the compact layer followed by multiple rounds of delamination. Additionally, though oriented cell division does not seem to play a role in the initial trabecular delamination, it would be interesting to examine whether forming trabecular branches form via directed cell division or migration of trabecular cells. While expanding in mass, the trabeculae also remodel. Cross-sections of trabeculae reveal multiple overlapping cell contributions to trabecular sheets. How cardiomyocytes interweave to form the multilayered network remains unknown. Furthermore, between 96 and 120 hpf, the myocardial ridges partly separate from the compact layer (Peshkovsky et al., 2011). Future lineage tracing and imaging studies will reveal how cardiomyocytes form the mature the trabecular network.

Interacting Pathways

A number of signaling pathways have been identified that influence trabeculation. These include the Angiopoietin/Tie2 pathway (Suri, 1996), Semaphorin/Plexin pathway (Toyofuku et al., 2004a, 2004b), the Notch pathway (Grego-Bessa et al., 2007), and the Neuregulin/ErbB2/ErbB4 pathway (Gassmann et al., 1995; Lee et al., 1995; Liu et al., 2010; Morris et al., 1999; Tidcombe et al., 2003). Additionally, blood flow/intracardiac

forces play a role in trabeculation. Where each of these pathways acts in trabeculation is unclear, and it is mostly unknown how they interact with each other. Mosaic analysis in the zebrafish embryo will allow for a broader understanding of how these pathways interact. Previous studies have identified factors downstream of Semaphorin signaling, such as activated Abl, that can drive cells into trabeculae (Toyofuku et al., 2004b). However, these studies were carried out in the chick, which lacks the ability to manipulate mutants. Confirmation of these findings from chick in zebrafish will allow for an analysis of how the Semaphorin pathway interacts with other trabecular mutants. By mosaically overexpressing Abl or other drivers of trabeculation in a mutant background that lacks trabeculae, such as *erbb2* or *tnnt2a* mutants, interactions between the different pathways within trabeculae can be probed. Further identification of downstream drivers in the ErbB2 pathways or mechanosensation will permit similar analyses in *semaphorin* mutants. These analyses will be especially informative in the context of altered flow/intracardiac forces, where very little is known about downstream effectors of trabecular fate.

Subcellular dynamics

This dissertation focused on cell shape changes associated with cardiac trabeculation. To achieve these shape changes, cardiomyocytes must remodel their cell-cell junctions and cytoskeletons. The genetic tractability of zebrafish coupled with its optical clarity provides a unique system for looking into the dynamics of junctional and cytoskeletal remodeling. New lines marking the sarcomeres with actinin-GFP (Lin et al., 2012), or

the entire actin cytoskeleton with Lifeact-GFP (Stainier lab, unpublished data) will allow for the monitoring of sarcomeric and non-sarcomeric actin rearrangements during all the steps of trabeculation. Similar lines could be made to mark myocardial microtubules to determine their role in trabeculation, and also to monitor orientation of cell division. Gene trap screens using the FlipTrap vector (Trinh et al., 2011) have fluorescently labeled junctional components such as alpha-catenin, which will allow monitoring of cell-cell adhesions and apical-basal polarity during trabeculation. Expanding the techniques used in this dissertation to acquire multi-color images (Ohn et al., 2011), and combining these new transgenic tools with cardiac membrane lines will allow for an unprecedented view of the dynamic inter- and intracellular processes occurring during trabecular morphogenesis.

Conclusion

The studies outlined in this dissertation have examined two early events in cardiac morphogenesis: the initial migration of cardiomyocytes into the trabeculae, and the specification of Notch-responsive cardiomyocytes early on in development. These studies demonstrate the power of the zebrafish system for studying early cell biological events crucial for cardiac morphogenesis, and provide a way forward for uncovering more about cardiac cell biology.

References

Chi, N.C., Shaw, R.M., Jungblut, B., Huisken, J., Ferrer, T., Arnaout, R., Scott, I., Beis, D.,
Xiao, T., Baier, H., et al. (2008). Genetic and Physiologic Dissection of the
Vertebrate Cardiac Conduction System. Plos Biol. *6*, e109.

Gassmann, M., Casagranda, F., Orioli, D., Simon, H., Lai, C., Klein, R., and Lemke, G.
(1995). Aberrant neural and cardiac development in mice lacking the ErbB4
neuregulin receptor. Nature *378*, 390–394.

Grego-Bessa, J., Luna-Zurita, L., del Monte, G., Bolós, V., Melgar, P., Arandilla, A.,
Garratt, A.N., Zang, H., Mukouyama, Y.-S., Chen, H., et al. (2007). Notch signaling
is essential for ventricular chamber development. Dev. Cell *12*, 415–429.

Gupta, V., and Poss, K.D. (2012). Clonally dominant cardiomyocytes direct heart
morphogenesis. Nature *484*, 479–484.

Lai, D., Liu, X., Forrai, A., Wolstein, O., Michalicek, J., Ahmed, I., Garratt, A.N.,
Birchmeier, C., Zhou, M., Hartley, L., et al. (2010). Neuregulin 1 sustains the gene
regulatory network in both trabecular and nontrabecular myocardium. Circ. Res.
107, 715–727.

Lee, K.-F., Simon, H., Chen, H., Bates, B., Hung, M.-C., and Hauser, C. (1995).
Requirement for neuregulin receptor erbB2 in neural and cardiac development.
Nature *378*, 394–398.

Lin, Y.-F., Swinburne, I., and Yelon, D. (2012). Multiple influences of blood flow on
cardiomyocyte hypertrophy in the embryonic zebrafish heart. Dev. Biol. *362*,
242–253.

Liu, J., Bressan, M., Hassel, D., Huisken, J., Staudt, D., Kikuchi, K., Poss, K.D., Mikawa, T., and Stainier, D.Y.R. (2010). A dual role for ErbB2 signaling in cardiac trabeculation. Dev. Camb. Engl. *137*, 3867–3875.

Morris, J., Lin, W., Hauser, C., Marchuk, Y., Getman, D., and Lee, K. (1999). Rescue of the Cardiac Defect in ErbB2 Mutant Mice Reveals Essential Roles of ErbB2 in Peripheral Nervous System Development. Neuron *23*, 273–283.

Ohn, J., Yang, J., Fraser, S.E., Lansford, R., and Liebling, M. (2011). High-speed multicolor microscopy of repeating dynamic processes. Genes. New York N 2000 *49*, 514–521.

Peshkovsky, C., Totong, R., and Yelon, D. (2011). Dependence of cardiac trabeculation on neuregulin signaling and blood flow in zebrafish. Dev. Dyn. Off. Publ. Am. Assoc. Anat.

Sedmera, D., Pexieder, T., Rychterova, V., Hu, N., and Clark, E.B. (1999). Remodeling of chick embryonic ventricular myoarchitecture under experimentally changed loading conditions. Anat. Rec. *254*, 238–252.

Sedmera, D., Pexieder, T., Vuillemin, M., Thompson, R.P., and Anderson, R.H. (2000). Developmental patterning of the myocardium. Anat. Rec. *258*, 319–337.

Suri, C. (1996). Requisite Role of Angiopoietin-1, a Ligand for the TIE2 Receptor, during Embryonic Angiogenesis. Cell *87*, 1171–1180.

Tidcombe, H., Jackson-Fisher, A., Mathers, K., Stern, D.F., Gassmann, M., and Golding, J.P. (2003). Neural and mammary gland defects in ErbB4 knockout mice genetically rescued from embryonic lethality. Proc. Natl. Acad. Sci. *100*, 8281–8286.

Toyofuku, T., Zhang, H., Kumanogoh, A., Takegahara, N., Suto, F., Kamei, J., Aoki, K.,
Yabuki, M., Hori, M., Fujisawa, H., et al. (2004a). Dual roles of Sema6D in cardiac
morphogenesis through region-specific association of its receptor, Plexin-A1,
with off-track and vascular endothelial growth factor receptor type 2. Genes Dev.
18, 435–447.

Toyofuku, T., Zhang, H., Kumanogoh, A., Takegahara, N., Yabuki, M., Harada, K., Hori,
M., and Kikutani, H. (2004b). Guidance of myocardial patterning in cardiac
development by Sema6D reverse signalling. Nat Cell Biol *6*, 1204–1211.

Trinh, L.A., Hochgreb, T., Graham, M., Wu, D., Ruf-Zamojski, F., Jayasena, C.S., Saxena,
A., Hawk, R., Gonzalez-Serricchio, A., Dixson, A., et al. (2011). A versatile gene
trap to visualize and interrogate the function of the vertebrate proteome. Genes
Dev. *25*, 2306 –2320.

It is the policy of the University to encourage the distribution of all theses, dissertations, and manuscripts. Copies of all UCSF theses, dissertations, and manuscripts will be routed to the library via the Graduate Division. The library will make all theses, dissertations, and manuscripts accessible to the public and will preserve these to the best of their abilities, in perpetuity.

I hereby grant permission to the Graduate Division of the University of California, San Francisco to release copies of my thesis, dissertation, or manuscript to the Campus Library to provide access and preservation, in whole or in part, in perpetuity.

_____   ___June 3, 2013_____
Author Signature   Date